AD_____

Award Number: DAMD17-03-1-0531

TITLE: The Role of a Novel Topological Form of the Prion Protein in Prion Disease

PRINCIPAL INVESTIGATOR: Richard S. Stewart, Ph. D.

CONTRACTING ORGANIZATION: Washington University
St. Louis, MO 63110

REPORT DATE: July 2008

TYPE OF REPORT: Final

PREPARED FOR: U.S. Army Medical Research and Materiel Command
Fort Detrick, Maryland 21702-5012

REPORT DOCUMENTATION PAGE

Form Approved
OMB No. 0704-0188

1. REPORT DATE *(DD-MM-YYYY)*	**2. REPORT TYPE**	**3. DATES COVERED** *(From - To)*
01-07-2008	Final	1 JUL 2003 - 30 JUN 2008

4. TITLE AND SUBTITLE

The Role of a Novel Topological Form of the Prion Protein in Prion Disease

5a. CONTRACT NUMBER

5b. GRANT NUMBER
DAMD17-03-1-0531

5c. PROGRAM ELEMENT NUMBER

6. AUTHOR(S)
Richard S. Stewart, Ph. D.

E-Mail: rstewart@wustl.edu

5d. PROJECT NUMBER

5e. TASK NUMBER

5f. WORK UNIT NUMBER

7. PERFORMING ORGANIZATION NAME(S) AND ADDRESS(ES)

Washington University
St. Louis, MO 63110

8. PERFORMING ORGANIZATION REPORT NUMBER

9. SPONSORING / MONITORING AGENCY NAME(S) AND ADDRESS(ES)
U.S. Army Medical Research and Materiel Command
Fort Detrick, Maryland 21702-5012

10. SPONSOR/MONITOR'S ACRONYM(S)

11. SPONSOR/MONITOR'S REPORT NUMBER(S)

12. DISTRIBUTION / AVAILABILITY STATEMENT
Approved for Public Release; Distribution Unlimited

13. SUPPLEMENTARY NOTES

14. ABSTRACT
No abstract provided.

15. SUBJECT TERMS
No subject terms.

16. SECURITY CLASSIFICATION OF:			**17. LIMITATION OF ABSTRACT**	**18. NUMBER OF PAGES**	**19a. NAME OF RESPONSIBLE PERSON**
a. REPORT	**b. ABSTRACT**	**c. THIS PAGE**			USAMRMC
U	U	U	UU	51	**19b. TELEPHONE NUMBER** *(include area code)*

Table of Contents

INTRODUCTION

Prion diseases are commonly associated with the presence of a conformationally altered form of the prion protein (PrP^{Sc}). However, there is mounting evidence that PrP^{Sc} is not directly toxic to neurons; it may require interaction with other gene products to induce a neurotoxic pathway. One candidate alternate neurotoxic PrP species is CtmPrP, which results from an alternate topological decision when the prion protein is translocated into the endoplasmic reticulum. We have identified mutations in the prion protein sequence which dramatically favors the production of CtmPrP (which under normal conditions is not detectable). We have established lines of transgenic mice which express CtmPrP [designated Tg(L9R-3AV)], and these mice develop a spontaneous neurological illness similar to prion disease [Stewart et al. 2005]. We are characterizing the phenotype of these mice to further our understanding of CtmPrP–meditated neurotoxicity, which we believe will shed new light on the process of neurodegeneration in prion disease. We have also established cell lines expressing the L9R-3AV mutant PrP, which will allow us to develop *in vitro* models of CtmPrP-dependent cell toxicity.

BODY

Task 1: Generation of anti-signal peptide antisera. Months 1-24.

We have generated a specific antiserum to the signal peptide of PrP (amino acids 1-22), based on the observation that this amino acid sequence is not removed from CtmPrP, while it is efficiently removed form normal PrP. Therefore, an antibody specific for the signal peptide of PrP would be a highly specific tool for sensitive detection of CtmPrP in cells and tissues. A peptide corresponding to amino acids 14-27 of PrP was synthesized and injected into rabbits to generate a polyclonal serum. This antiserum was characterized for specificity using *in vitro* translated PrP and cell lysates expressing L9R-3AV PrP. We demonstrated that this serum (now called anti-SP) specifically recognized PrPs with uncleaved signal peptides, but did not recognize mature PrP. L9R-3AV PrP expressed in N2A cells was specifically immunoprecipitated from metabolically labeled cell lysates, while mature WT PrP was not [Stewart and Harris 2003, Fig. 7].

The sensitivity of the anti-SP antiserum was further demonstrated by the fact that a small amount of ~27 kDa PrP was immunoprecipitated from lysates expressing WT PrP [Stewart and Harris 2003, Fig. 7]. This PrP species (a small fraction of the total PrP in the cell at steady state) is derived from inefficient processing at the translocon. Treatment of cells with inhibitors of the proteasome permits this ~27 kDa PrP species to accumulate at much higher levels, indicating that it is normally very rapidly removed from the cell by the proteasome-dependent quality control pathway [Drisaldi et al. 2003, Fig. 7]. Immunostaining with the anti-SP antiserum showed that this PrP species accumulates at the endoplasmic reticulum (ER), and biochemical protease protection shows that it must reside in the cytosol, likely loosely attached to the ER [Drisaldi et al. 2003, Fig. 9].

It has been proposed that CtmPrP may be an obligate toxic intermediate species in the development of prion disease [Hegde et al. 1999]. This hypothesis suggests that

PrPSc itself is not toxic *per se*, but it causes disease by leading to the aberrant generation of CtmPrP. Therefore, it is of significant interest to determine if CtmPrP levels are increased in the brains of animals infected with prions. Previous data which attempted to demonstrate this phenomenon were problematic for technical reasons, and were not definitive. The generation of the anti-SP antiserum provides a much more sensitive tool to ask this particular question. We assayed uninfected and scrapie-infected N2a (ScN2a) cells for the presence of CtmPrP using the anti-SP antiserum, and found no evidence for CtmPrP production in ScN2a cells [Stewart and Harris 2003, Fig. 7]. The sensitivity of the assay was confirmed using L9R-3AV PrP expressing N2a cells, and also other PrP mutants which produce proportionally much less CtmPrP (such as A116V and 3AV). CtmPrP was easily detectable with anti-SP in A116V expressing cells, despite the fact that only ~2% of the total PrP in these cells is CtmPrP [Stewart and Harris 2001, Fig. 6].

We have also used the fact that CtmPrP retains this signal peptide to look for CtmPrP in brain homogenates from animals with prion disease. The anti-SP antiserum does not work efficiently on Western blots, so we took advantage of the size difference between mature PrP (25 kDa) and CtmPrP (27 kDa) after removal of N-linked sugars to look for CtmPrP in scrapie-infected mouse brains. Only 25 kDa PrP is detected in several different samples of scrapie-infected mouse brains, while both 25 and 27 kDa species are detected in brains from Tg(L9R-3AV) mice [Stewart and Harris 2003, Fig. 8]. We have found no evidence (using very sensitive assays) for CtmPrP in cells or brains of animals with prion disease. Therefore it seems unlikely that CtmPrP is an obligate intermediate in the neuronal toxicity pathway induced by prion disease. However, this does not rule out the separate hypothesis that CtmPrP and PrP^{Sc} may be separately activating a common neurodegenerative pathway.

Task 2: Characterization of the CtmPrP-induced neurotoxic pathway *in vivo* and *in vitro*. Months 12-36.

We have established two lines of transgenic mice expressing L9R-3AV PrP, and both of these lines develop a spontaneous neurological illness which is in many respects similar to authentic prion disease. The primary phenotype of these mice is a progressive ataxia, eventually resulting in severe impairment and death. The severity of the phenotype roughly correlates with the transgene expression level. The Tg(L9R-3AV) [A] line expressed the highest level (as determined by Western blot and RT-PCR) and died at weaning (20 days). The two lines which bred robustly developed spontaneous illness at ~90 days (Tg[L9R-3AV] C/ PrnP +/+) and ~180 days (Tg[L9R-3AV] B/ PrnP +/+). These mice show a progressive and severe cerebellar degeneration, specifically in the granule cell layer. Purkinje neurons of the cerebellum do not appear to degenerate. Milder degeneration is also detectable in the CA1 layer of the hippocampus. Pronounced gliosis also occurs in many regions of the brain, most obviously the cerebellar molecular layer.

The Tg(L9R-3AV) mice were generated on an endogenous PrP (PrnP +/+) genetic background. Surprisingly, elimination of endogenous PrP by outbreeding to PrnP o/o mice alleviated the phenotype considerably. The onset of illness in the Tg (L9R-3AV) [C]/PrnP o/o line was increased to ~150 days compared to ~85 days for Tg(L9R-3AV) [C]/PrnP +/+ mice, and the progression to fatal disease was dramatically lengthened

(~490 days versus ~160 days). The Tg (L9R-3AV) [B] line produced an even more dramatic result; these mice showed no clinical illness at all even out to 650 days, compared to terminal illness in ~390 days for Tg(L9R-3AV)[B]/PrnP +/+ mice. Careful histological examination of the Tg(L9R-3AV) [B]/PrnP o/o mice showed only a weak gliosis and very minor cerebellar granule neuronal cell death (by TUNEL staining), but this pathology was not significant enough to be observed at a gross anatomical level (data not shown).

One genetic cross was performed to attempt to determine the mechanism of cell death *in vivo*. The Bax protein is a well-characterized mitochondrial protein which plays a key role in many apoptotic pathways [Chiesa et al. 2005]. Several models of neurological illness have been shown to be alleviated or delayed in a Bax o/o genetic background. We crossed our Tg(L9R-3AV)[C]/(Bax +/+)/PrnP +/+ mice to Bax o/o mice to generate Tg(L9R-3AV)[C]/Bax o/o/PrnP +/+ mice. However, we did not observe any delay in clinical symptoms or alleviation of cerebellar granule cell loss in these mice compared to Tg(L9R-3AV)[C]/Bax +/+/PrnP +/+ controls (data not shown). Thus, we tentatively conclude that the cell death pathway induced by CtmPrP is Bax-independent.

Infection of mice with scrapie prions has been the “gold standard” for measuring infectivity and toxicity of prions for many years. While the animal bioassay has many strengths, it also has many weaknesses. The primary disadvantage is the long incubation time (~180 days) and expense of the assay. An *in vitro* cell-line based assay would be a significant advance in the prion field, both in terms of efficiency of resources and for the determination of specific molecular pathways involved in prion neurotoxicity. The scrapie cell model has allowed rapid testing of anti-prion agents, but this model is deficient in the toxicity aspect of prion disease. We (and others) have invested considerable effort into developing a robust cell-based scrapie or mutant-PrP dependent toxicity assay. Preliminary data suggests that such a model has now been established in our hands.

The basis of the cell assay is the fortuitous discovery that cells expressing mutant PrPs (which cause spontaneous prion-like disease in transgenic mice) are dramatically more sensitive to various classes of cell-killing drugs. Two different classes of drugs both show this effect in mutant PrP-expressing HEK293 cells. The first class are aminoglycoside antibiotics, such as geneticin and hygromycin. The second class are DNA damage agents, such as zeocin and bleomycin. Importantly, HEK293 cells transfected with empty vector or with wild-type PrP do not show this effect. The effect is robust, especially so in a mutant referred to as delta CR (Li et al. 2007). Other PrP mutants tested in this assay include delta 32-134 (Shmerling et al. 1998), and most relevant to this proposal, L9R-3AV [**Fig. 1**].

Additionally, co-expression of WT PrP with the mutant PrP abolishes the drug-dependent toxicity (data not shown). This observation is very important, as it recapitulates the phenotype seen in transgenic mice, strongly suggesting that the phenotype in cells is relevant to what is occurring in vivo.

While the exact mechanism of cell death has not yet been determined, preliminary data suggests that the mutant PrP is allowing much more rapid entry of the drug into cells, thus leading to rapid cell death. These drugs are known to normally enter cells relatively slowly, thus allowing their use as selection agents for establishment of

stable cell lines. Two observations support this hypothesis. 1) Addition of additional potassium (50mM) to the media in the presence of the drug completely abolishes the toxicity. This result strongly suggests that the drug is entering the cell through an electrochemical gradient. The fact these drugs are positively charged (and likely transported across the cell through protein –based permeases or ion channels) fits nicely with this data. Similar observations have been made in models of aminoglycoside toxicity in kidney cells and ear cells [Myrdal et al. 2005]. 2). Direct measurement of a marker for DNA damage by zeocin has been observed in mutant PrP cells using an assay for phosphorylation of H2AX (a well-characterized DNA damage assay). Importantly, the increase in DNA damage in Delta CR expressing cells can be detected within 30 min of drug application (long before toxicity can be detected), while control cells show little or no H2AX phosphorylation (data not shown).

This assay, while still indirect, is very robust, and will allow rapid characterization of the type of cell death occurring. Preliminary data shows the cell death is not caspase-dependent (data not shown).

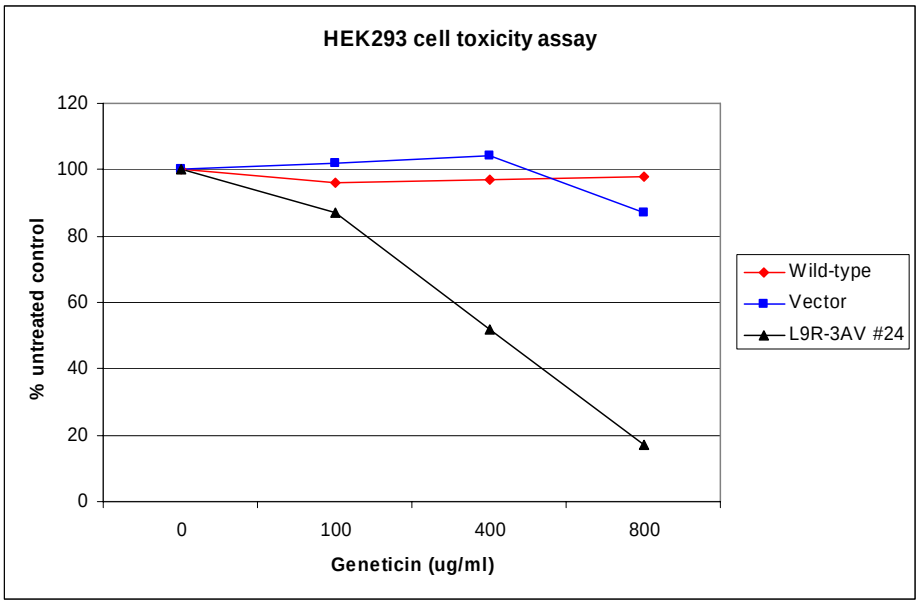

Fig. 1. HEK293 cell toxicity assay. HEK293 cells expressing the indicated PrP proteins were treated with Geneticin at the indicated concentration for 4 days at 37 C, then assayed for cell viability by MTT dye reduction assay. Data are normalized to untreated cells cultured simultaneously.

Task 3: Characterization of the cell biology of CtmPrP. Months 37-48.

Previously published data showed that L9R-3AV PrP expressed in CHO or BHK cells demonstrated a distinct localization in the cell, specifically in the ER, while WT PrP is mostly localized to the cell surface at steady-state. However, in cultured neurons from Tg(L9R-3AV) mice, L9R-3AV was prominently localized to the Golgi apparatus [Stewart and Harris 2005, Fig. 7]. We also demonstrated that the L9R-3AV PrP in the Golgi apparatus in cultured cerebellar granule neurons (the same cells which we know die *in vivo* in the transgenic mice) is in the CtmPrP conformation [Stewart and Harris 2005, Fig. 8].

We have now tested the localization of L9R-3AV PrP in HEK293 cells (the same cell line used in the cell-based toxicity assay described above). Surprisingly, L9R-3AV PrP is localized to the Golgi apparatus in these cells [**Fig. 2**]. Strong co-localization with a Golgi marker protein (giantin) is observed (data not shown). Using cell-surface staining of live cells, we showed that no L9R-3AV PrP reaches the cell surface at steady-state (data not shown). We have also observed Golgi localization of L9R-3AV PrP in another neuronal-derived cell line, HpL (data not shown). While HEK293 cells are reported to be kidney fibroblasts, recent data suggests they may in fact be derived from a neuronal precursor cell in the kidney, and are known to express many neuronal-specific proteins [Shaw et al. 2005]. Whether the localization of CtmPrP in the Golgi is a requirement for its pathogenicity is a potentially very interesting question, but the present data does not allow definitive conclusions to be drawn yet.

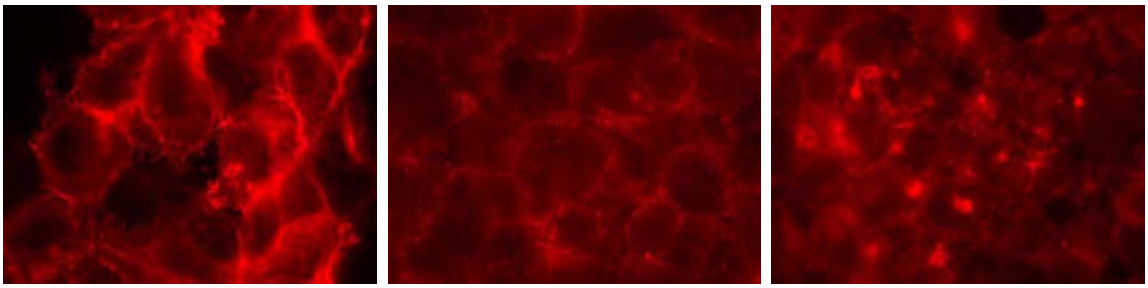

Fig. 2 Immunostaining of HEK293 cells. HEK293 cells expressing the indicated PrP proteins were fixed, stained with anti-PrP antibody 6D11, stained with fluorescent-coupled anti mouse IgG, then imaged by fluorescence microscopy. Note the prominent punctate staining in L9R-3AV PrP not present in wild-type.

Task 4: Structure-function analysis of CtmPrP using chimeric proteins. Months 42-60.

The assays proposed originally have not been performed yet, for several reasons. 1). Verification of the topology of the mutant constructs has not been confirmed yet. Topology of artificial proteins often do not turn out as predicted. 2) More importantly, the establishment of an in vitro assay to test these mutants was not established until very recently, and is still a somewhat preliminary (but very promising) assay. We believe these types of structure-function assays are now feasible.

We have attempted a different but related structure-function assay using presently available transgenic mice. These experiments are intended to answer a slightly different question: Which structural/sequence elements of endogenous PrP are required to interact with CtmPrP to induce spontaneous neurological illness? We have previously shown that the illness induced by CtmPrP expression is at least partially dependent on endogenous PrP expression (see above). When the Tg(L9R-3AV)B mouse line was bred onto a PrnP o/o genetic background, the spontaneous illness was abolished.. We have crossed these Tg(L9R-3AV)[B]/ PrnP o/o mice to two different mouse lines expressing altered PrP transgenes to determine if these altered PrPs are sufficient to restore illness.

The first mutant line is designated Tg(D11) [Shmerling et al.1998]; it expresses a PrP deleted from amino acids 32-80; thus it is missing most of the octapeptide repeat region of PrP. These Tg(L9R-3AV) B/Tg(D11)/ PrnP o/o mice do not show any spontaneous illness at greater than 365 days.

A second mouse line, Tg(GPIneg), express PrP , but abolish the GPI anchor addition site in PrP. Thus, they secrete PrP readily into the extracellular environment [Chesboro et al. 2005]. We have crossed Tg(L9R-3AV) B/PrnP o/o mice to these Tg(GPIneg) mice to determine if the WT PrP function requires PrP to be present on the cell surface of neurons in a membrane-anchored form. These mice also failed to develop any neurological illness, even at 600 days.

As a positive control, we crossed Tg(L9R-3AV)[B]/PrnP o/o mice to mice which express WT PrP from a similar transgene (designated WT-E1) to the above lines.

These experiments did not turn out as planned. None of the Tg(L9R-3AV) mice crossed to any of these transgenic mice restored the spontaneous illness. This includes the WT-E1 positive control line, even at 600 days. Therefore, we cannot draw any solid conclusion for the D11 or GPIneg transgenic mice in terms of their ability to restore the phenotype of L9R-3AV mice. The reasons for the failure of the positive control to restore the phenotype remain unclear.

KEY RESEARCH ACCOMPLISHMENTS

-Generation of anti-SP antiserum. Demonstration of its use as a sensitive marker for CtmPrP in vitro and in vivo, and that CtmPrP is not an obligate intermediate in scrapie-induced illness.

-Generation and characterization of Tg(L9R-3AV) mice. These mice are a unique spontaneous model for a prion-like disease. These mice prove that multiple forms of the prion protein are toxic, and suggest that many different alterations to PrP can lead to neurotoxicity.

-Localization of CtmPrP to the Golgi in cultured neurons and in HEK cells. Suggests a possible locus of action for CtmPrP.

-Preliminary development of an *in vitro* assay for prion protein -related toxicity.

This assay will allow genetic and/or pharmacological dissection of toxicity pathways, possibly leading to therapeutic interventions.

REPORTABLE OUTCOMES

See attached papers.

CONCLUSIONS

We have established a mouse model for spontaneous illness induced by an alternate topological isoform of the prion protein (PrP). We have employed these mice to further explore the cellular mechanisms of neuronal pathology induced by CtmPrP. We believe these mechanisms will yield new information on neurotoxic mechanisms in prion disease, a subject about which relatively little is known. With this information better therapeutic treatments can someday be developed.

REFERENCES

Chesboro, B., M. Trifilo, R. Race, K. Meade-White, C. Teng, R. LaCasse, L. Raymond, C. Favara, G. Baron, S. Priola, B. Caughey, E. Masliah, and M.Oldstone (2005). Anchorless Prion Protein Results in Infectious Amyloid Disease Without Clinical Scrapie. *Science* **308**:1435-1439.

Chiesa, R. P. Piccardo, S. Dossena, L. Nowoslawski, K. A. Roth, B. Ghetti, and D. A. Harris (2005). Bax deletion prevents neuronal loss but not neurological symptoms in a transgenic model of inherited prion disease. *Proc. Natl. Acad. Sci. USA* **102**:238-243.

Drisaldi, B., R. S. Stewart, C. Adles, L. R. Stewart, E. Quaglio, E. Biasini, L. Fioriti, R. Chiesa, And D. A. Harris. (2003). Mutant PrP Is Delayed in Its Exit from the Endoplasmic Reticulum, but Neither Wild-type nor Mutant PrP Undergoes Retrotranslocation Prior to Proteasomal Degradation. *J. Biol. Chem.* **278:** 21732-21743.

Hegde, R. S., P. Tremblay, D. Groth, S. J. DeArmond, S. B. Prusiner, and V. R. Lingappa. (1999).Transmissible and genetic prion diseases share a common pathway of neurodegeneration. *Nature* **402**: 822-826.

Li, A., H. M. Christensen, L. R. Stewart, K. A. Roth, R. Chiesa, and D. A. Harris. (2007). Neonatal lethality in transgenic mice expressing prion protein with a deletion of residues 105-125. *EMBO J* **26**:548-558.

Myrdal, S. E., and P. S. Steyger. (2005). TRPV1 regulators mediate gentamicin penetration of cultured kidney cells. *Hearing Research* **204**: 170-182.

Shaw, G., S. Morse, M. Ararat, and F. L. Graham. (2002). Preferential transformation of human neuronal cells by human adenoviruses and the origin of HEK 293 cells. *The FASEB Journal* express article 10.1096/fj.01-0995fje. Published online April 10, 2002.

Shmerling, D., I. Hegyi, M. Fischer, T. Blattler, S. Brandner, J. Gotz, T. Rulicke, E. Flechsig, A. Cozzio, C. von Mering, C. Hangartner, A. Aguzzi, and C. Weissmann

(1998). Expression of Amino-Terminally Truncated PrP in the Mouse Leading to Ataxia and Specific Cerebellar Lesions. *Cell* **93**:203-214.
Stewart, R. S., and D. A. Harris (2001). Most Pathogenic Mutations Do Not Alter the Membrane Topology of the Prion Protein. *J. Biol. Chem*. **276**: 2212-2220.
Stewart, R. S., and D. A. Harris (2003). Mutational Analysis of Topological Determinants in Prion Protein (PrP) and Measurement of Transmembrane and Cytosolic PrP during Prion Infection. *J. Biol. Chem*. **278**: 45960-45968.
Stewart, R. S., P. Piccardo, B. Ghetti, and D. A. Harris (2005). Neurodegenerative Illness in Transgenic Mice Expressing a Transmembrane Form of the Prion Protein. *J. Neurosci* **25**:3469-3477.
Stewart, R. S., and D. A. Harris (2005). A Transmembrane Form of the Prion Protein Is Localized in the Golgi Apparatus of Neurons. *J. Biol. Chem.* **280:** 15855-15864.

APPENDICES

THE JOURNAL OF BIOLOGICAL CHEMISTRY
Vol. 278, No. 46, Issue of November 14, pp. 45960–45968, 2003

Printed in U.S.A.

Mutational Analysis of Topological Determinants in Prion Protein (PrP) and Measurement of Transmembrane and Cytosolic PrP during Prion Infection*

Received for publication, July 20, 2003, and in revised form, August 15, 2003
Published, JBC Papers in Press, August 21, 2003, DOI 10.1074/jbc.M307833200

Richard S. Stewart‡ and David A. Harris§

From the Department of Cell Biology and Physiology, Washington University School of Medicine, St. Louis, Missouri 63110

The prion protein (PrP) can adopt multiple membrane topologies, including a fully translocated form (^{Sec}PrP), two transmembrane forms (^{Ntm}PrP and ^{Ctm}PrP), and a cytosolic form. It is important to understand the factors that influence production of these species, because two of them, ^{Ctm}PrP and cytosolic PrP, have been proposed to be key neurotoxic intermediates in certain prion diseases. In this paper, we perform a mutational analysis of PrP synthesized using an *in vitro* translation system in order to further define sequence elements that influence the formation of ^{Ctm}PrP. We find that substitution of charged residues in the hydrophobic core of the signal peptide increases synthesis of ^{Ctm}PrP and also reduces the efficiency of translocation into microsomes. Combining these mutations with substitutions in the transmembrane domain causes the protein to be synthesized exclusively with the ^{Ctm}PrP topology. Reducing the spacing between the signal peptide and the transmembrane domain also increases ^{Ctm}PrP. In contrast, topology is not altered by mutations that prevent signal peptide cleavage or by deletion of the C-terminal signal for glycosylphosphatidylinositol anchor addition. Removal of the signal peptide completely blocks translocation. Taken together, our results are consistent with a model in which the signal peptide and transmembrane domain function in distinct ways as determinants of PrP topology. We also present characterization of an antibody that selectively recognizes ^{Ctm}PrP and cytosolic PrP by virtue of their uncleaved signal peptides. By using this antibody, as well as the distinctive gel mobility of ^{Ctm}PrP and cytosolic PrP, we show that the amounts of these two forms in cultured cells and rodent brain are not altered by infection with scrapie prions. We conclude that ^{Ctm}PrP and cytosolic PrP are unlikely to be obligate neurotoxic intermediates in familial or infectiously acquired prion diseases.

Prion diseases are fatal neurological disorders of humans and animals that appear in sporadic, familial, and infectiously acquired forms. These disorders are caused by conversion of a normal neuronal glycoprotein (PrP^C)[1] into a conformationally altered isoform (PrP^{Sc}) that is infectious in the absence of nucleic acid (1, 2). PrP^C, which is soluble and protease-sensitive, consists of an α-helical, C-terminal domain and an unstructured N-terminal domain. In contrast, PrP^{Sc} is rich in β-sheets, aggregated, and protease-resistant. The physiological function of PrP^C is uncertain but may be related to transport of copper ions or protection from oxidative stress (3).

PrP^C is unusual because it can adopt multiple membrane topologies. Most PrP^C molecules are attached to the outer leaflet of the plasma membrane through a C-terminal glycosylphosphatidylinositol (GPI) anchor (this topology is designated ^{Sec}PrP) (4, 5). However, some PrP^C molecules assume a transmembrane orientation when synthesized *in vitro* or in cells (6–11). These forms, designated ^{Ntm}PrP and ^{Ctm}PrP, span the lipid bilayer once via a highly conserved hydrophobic region in the center of the molecule (amino acids 111–134), with either the N or C terminus, respectively, on the extracytoplasmic side of the membrane. It has been shown that these species are generated in small amounts (<10% of the total PrP) as part of the normal biosynthesis of wild-type PrP in the endoplasmic reticulum (ER). However, mutations within or near the transmembrane domain, including an A117V mutation linked to GSS as well as several "artificial" mutations not seen in human patients, increase the relative proportion of ^{Ctm}PrP to as much as 20–30% of the total (7, 12).

Recent studies have begun to define the mechanisms responsible for determining PrP topology during the translation process. We discovered that a non-conservative substitution (L9R) within the hydrophobic core of the signal sequence dramatically increased the proportion of ^{Ctm}PrP (13). Combining this mutation with a triple substitution (3AV) within the transmembrane domain resulted in a molecule that was synthesized exclusively as ^{Ctm}PrP. These results indicated that the signal sequence as well as the transmembrane domain were major determinants of PrP topology. Work by Hegde and colleagues (9–11) has demonstrated that these two determinants act in mechanistically distinct ways. The signal sequence serves a dual function, first targeting the nascent polypeptide chain to the translocon channel in the ER membrane via binding to the signal recognition particle, and subsequently gating the translocon to allow passage of the N terminus into the ER lumen. In contrast, the transmembrane domain acts primarily to trigger integration of the polypeptide into the lipid bilayer. The combined action of both domains operating during the transloca-

* This work was supported in part by Grant NS35496 (to D. A. H.) from the National Institutes of Health. The costs of publication of this article were defrayed in part by the payment of page charges. This article must therefore be hereby marked "*advertisement*" in accordance with 18 U.S.C. Section 1734 solely to indicate this fact.

‡ Supported by NRSA NS41500 from the National Institutes of Health.

§ To whom correspondence should be addressed: Dept. of Cell Biology and Physiology, Washington University School of Medicine, 660 S. Euclid Ave., St. Louis, MO 63110. Tel.: 314-362-4690; Fax: 314-747-0940; E-mail: dharris@cellbio.wustl.edu.

[1] The abbreviations used are: PrP^C, cellular isoform of PrP; PrP^{Sc}, scrapie isoform of PrP; CHO, Chinese hamster ovary; GPI, glycosylphosphatidylinositol; PK, proteinase K; PrP, prion protein; SP, signal peptide; WT, wild type; ER, endoplasmic reticulum; PNGase, peptide:*N*-glycosidase.

tion process serves to regulate the proportions of the three topological variants of PrP. Regulatory factors associated with the translocon, in addition to sequence determinants within the PrP molecule itself, have also been shown to influence the final topology achieved (14, 15).

Work from our laboratory has identified several novel cell biological features of ^{Ctm}PrP. First, ^{Ctm}PrP contains an uncleaved, N-terminal signal peptide (13). This characteristic makes ^{Ctm}PrP unusual among other type II transmembrane proteins, most of which have internal signal-anchor sequences. Second, ^{Ctm}PrP has a C-terminal GPI anchor in addition to a transmembrane domain, thus displaying an unusual, dual mode of membrane attachment (13, 16). Finally, by using the L9R/3AV mutant, we found that ^{Ctm}PrP expressed in cultured cells remains core-glycosylated and is retained completely in the ER (13). This result implies that the protein is recognized as abnormal by the ER quality control machinery that monitors folding of newly synthesized polypeptides.

A great deal of interest in the subject of PrP membrane topology derives from the possibility that topological variants of PrP may play an important pathogenic role in prion diseases. Although PrP^{Sc} is widely agreed to be the infectious form of PrP, there is considerable debate about whether it is the form responsible for neuronal loss in these disorders (17). The amount, anatomical distribution, and time course of accumulation of PrP^{Sc} often correlates with the development of neuropathology and clinical symptoms, but there are notable exceptions to this association. These discrepancies have led to the hypothesis that alternate forms of PrP, distinct from both PrP^{C} and PrP^{Sc}, are the proximate causes of neurodegeneration.

One candidate for such a neurotoxic intermediate is ^{Ctm}PrP. Two major pieces of evidence have been used to argue that ^{Ctm}PrP plays a key pathogenic role. First, transgenic mice have been generated that synthesize PrP molecules carrying the A117V mutation or one of the other ^{Ctm}PrP-favoring mutations (7, 12). Animals expressing the mutant proteins above a threshold level synthesize ^{Ctm}PrP in their brains and spontaneously develop a scrapie-like neurological illness, but without PrP^{Sc} detectable by Western blotting or infectivity assays. This result implies that certain familial forms of PrP may be due directly to increased levels of ^{Ctm}PrP. Second, mice have been constructed in which a wild-type hamster PrP transgene serves as a reporter of ^{Ctm}PrP formation (12). When these animals are inoculated with mouse prions, the amounts of ^{Ctm}PrP as well as PrP^{Sc} in the brain are found to increase during the course of the infection. This result has been interpreted to indicate that PrP^{Sc} induces formation of ^{Ctm}PrP, which is then the proximate cause of neurodegeneration during infectiously acquired prion diseases. In this view then, ^{Ctm}PrP is a key intermediate in both genetic and infectious prion diseases.

Another topological variant of PrP that has been proposed as a neurotoxic intermediate is cytosolic PrP. Expression of an artificial form of PrP lacking a signal sequence, which presumably favors accumulation of PrP in the cytoplasm, has been found to be toxic to cultured cells and transgenic mice (18). However, there is debate about whether PrP is found in the cytoplasm under normal circumstances and, if so, what mechanisms are responsible for delivering it there. Based on the observation that cytosolic PrP accumulates in cells that have been treated with proteasome inhibitors, it has been suggested that some molecules are retrotranslocated into the cytoplasm from the ER lumen as part of normal ER quality control mechanisms (19–21). In contrast, our experiments indicate that cytosolic PrP molecules represents untranslocated chains that have never entered the ER (22). These chains, which are observed primarily under conditions of protein overexpression, contain an uncleaved N-terminal signal peptide and lack a GPI anchor.

A key gap in the experimental evidence supporting roles for ^{Ctm}PrP and cytosolic PrP in prion-induced neurodegeneration is the lack of data demonstrating that the amounts of these forms increase during the course of a prion infection. In part, this difficulty is due to the absence of direct methods for detecting ^{Ctm}PrP and cytosolic PrP in infected cells and tissues. In this paper, we present characterization of an antibody that reacts with both ^{Ctm}PrP and cytosolic PrP by virtue of their uncleaved signal peptides and our use of this antibody to assay ^{Ctm}PrP and cytosolic PrP in infected samples. In addition, we carry out a mutational analysis of several sequence determinants in PrP to better understand the factors that influence the topology of the protein.

EXPERIMENTAL PROCEDURES

Plasmids—Synthetic oligonucleotides encoding point mutations in the PrP signal sequence (Fig. 1*A*) were used to amplify a portion of the PrP DNA sequence by PCR. DNA fragments carrying the mutation were digested with *Hin*dIII and PshA1 and cloned into a pcDNA3 plasmid (Invitrogen) containing the WT mouse PrP sequence from which the *Hin*dIII-PshA1 fragment had been removed. Plasmids encoding PrP molecules with a FLAG epitope (DYKDDDDK) inserted at position 22/23, and with altered numbers of octapeptide repeats (PG0, Δ51–90; PG1, Δ51–82; PG2, Δ67–90; PG14, +9 repeats) have been described previously (5, 13, 23). Other PrP mutants were constructed by PCR (16). All PrP coding regions carried an epitope tag for monoclonal antibody 3F4, created by changing residues 108 and 111 to methionine. Prior to *in vitro* transcription, plasmids were linearized with *Xba*I.

In Vitro Translation and PK Protection—mRNAs encoding WT and mutant PrP molecules were transcribed using the mMessage mMachine kit (Ambion, Austin, TX) and were translated using rabbit reticulocyte lysate (Promega, Madison, WI) containing [^{35}S]methionine as directed by the manufacturer, except that the final lysate concentration was 50%. Translation reactions were supplemented with microsomal membranes from mouse BW5174.3 cells (24) or from canine pancreas (Promega). After translation, 5-μl aliquots of lysate were incubated for 60 min at 4 °C in a final volume of 50 μl with or without 100 μg/ml PK (Roche Applied Science) in the presence or absence of 0.5% Triton X-100. PK was inactivated with phenylmethylsulfonyl fluoride for 5 min, and 12-μl aliquots were added to gel sample buffer containing phenylmethylsulfonyl fluoride for analysis by SDS-PAGE. In some cases, PrP was immunoprecipitated from translation reactions (as described below) prior to SDS-PAGE. For enzymatic deglycosylation, PrP was eluted from protein A-Sepharose beads with 1% SDS, 50 mM Tris-HCl (pH 7.5) and was then diluted 10-fold with 50 mM Tris-HCl (pH 7.5), 0.5% Triton X-100 containing 0.33 units/ml *N*-glycosidase F (New England Biolabs). After incubation at 37 °C for 1 h, proteins were precipitated with methanol and analyzed by SDS-PAGE. Radioactive bands on gels were quantitated using a PhosphorImager SI (Amersham Biosciences).

Scrapie Infection of N2a Cells—Highly scrapie-susceptible sub-clones of N2a cells were prepared as described (25). Briefly, N2a cells from the ATCC (CCL131) were first sub-cloned by limiting dilution. Each subclone was then tested for scrapie susceptibility by incubation for 3 days with an extract of N2a cells that had been infected previously with the Chandler strain of scrapie (26). Cells were then passaged for 6 weeks and analyzed for PrP 27–30 by cell blotting or by Western blotting after PK digestion. The susceptible sub-clone used for the experiment shown in Fig. 7 was designated N2a.3. It was used in the infected state, as well as in the uninfected state as a matched control.

Transfection, Metabolic Labeling, and Immunoprecipitation—CHO and N2a cells were transiently transfected with PrP-encoding plasmids using LipofectAMINE or LipofectAMINE 2000 (Invitrogen) according to the manufacturer's directions. Twenty-four hours after transfection, cells were labeled for 6 h in methionine- and cysteine-free medium containing 100–200 μCi/ml of [^{35}S]methionine/cysteine (Promix; Amersham Biosciences). Cultures were then lysed in 0.5% SDS, 50 mM Tris-HCl (pH 7.5), heated at 95 °C for 5 min, and diluted with 10 volumes of RIPA buffer (150 mM NaCl, 1% Triton X-100, 0.5% deoxycholate, 0.1% SDS, 50 mM Tris-HCl (pH 7.5)). Diluted lysates were incubated with anti-PrP antiserum for >1 h at 4 °C and then with 20 μl of protein A-Sepharose beads for 30 min at 4 °C. Beads were washed

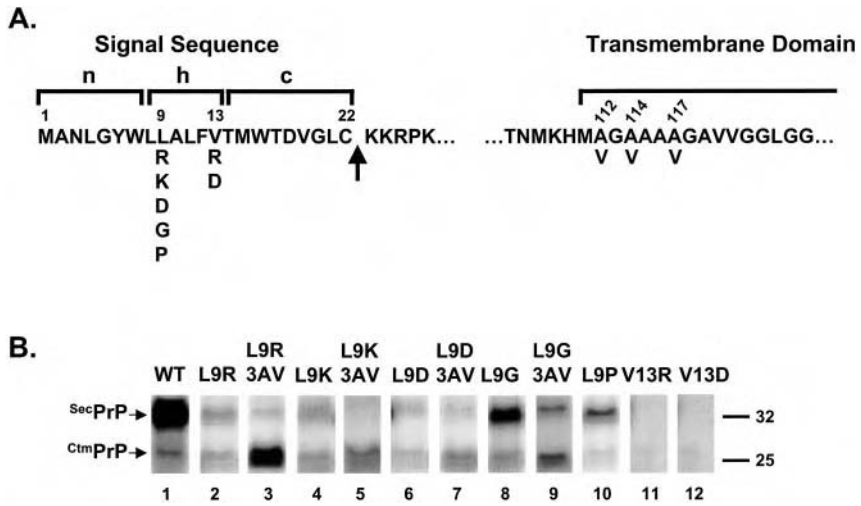

FIG. 1. **Mutations in the hydrophobic core of the signal sequence increase the proportion of ^{Ctm}PrP and reduce translocation efficiency.** *A,* amino acid sequence of the signal peptide and transmembrane domain of mouse PrP. The N-terminal (*n*), hydrophobic (*h*), and C-terminal (*c*) regions of the signal sequence, as defined by von Heijne (30), are indicated. The *upward arrow* indicates the site of signal peptide cleavage between residues 22 and 23. The amino acid substitutions that were made at positions 9 and 13 within the signal sequence are written *below* the wild-type residues at these positions. The 3AV triple mutation at positions 112, 114, and 117 in the transmembrane domain is also indicated. The wild-type sequence shows methionine residues at positions 108 and 111, which constitutes the 3F4 epitope present in all constructs. *B,* PrP mRNAs encoding the indicated constructs were translated using reticulocyte lysate supplemented with murine thymoma microsomes. Translation reactions were subjected to PK digestion, and then analyzed by SDS-PAGE and autoradiography. The positions of the PK-protected fragments corresponding to ^{Sec}PrP and ^{Ctm}PrP are indicated to the *left* of *lane 1.* Aliquots of each translation reaction were also incubated without PK to visualize total translation products or in the presence of PK plus Triton X-100 to demonstrate that all products were completely digested (not shown). Molecular size markers (to the *right* of *lane 12*) are in kilodaltons.

four times in RIPA buffer, and PrP was eluted by heating at 95 °C in gel sample buffer.

Scrapie Infection of Mice and Hamsters—Tg(WT)/*Prn-p*$^{0/0}$ mice (E1 line) expressing wild-type PrP carrying a 3F4 epitope have been described previously (27). Tg(L9R/3AV)/*Prn-p*$^{0/0}$ mice (B line) express mouse PrP carrying an L9R/3AV mutation and a 3F4 tag, a construct we have expressed previously in cultured cells (13). Full characterization of these mice will be provided elsewhere.[2] Scrapie inocula included the hamster 263K strain, the mouse RML strain, and the RML strain that had been passaged once in Tg(WT) mice to introduce the 3F4 epitope. To prepare inocula, infected brains were homogenized (10%, w/v) in phosphate-buffered saline using sterile, disposable tissue grinders. After clearing by centrifugation at 900 × *g* for 5 min, the homogenates were diluted to a final concentration of 1 or 2.5% in PBS, and 25 μl was injected intracerebrally into the right parietal lobe of 4–6-week-old recipient mice or hamsters using a 25-gauge needle.

Western Blots of Brain Homogenates—Brain lysates were prepared in 0.5% SDS, 50 mM Tris-HCl (pH 7.5). Samples were heated at 95 °C for 5 min and diluted 10-fold with 50 mM Tris-HCl (pH 7.5), 0.5% Triton X-100 containing 0.33 units/ml *N*-glycosidase F. After incubation at 37 °C for 2 h, proteins were precipitated with methanol, separated by SDS-PAGE, and subjected to Western blotting with 3F4 antibody.

Antibodies—An antibody (anti-SP) that selectively recognizes forms of murine PrP containing an uncleaved signal peptide was generated by immunizing rabbits with a synthetic peptide (TMWTDVGLCKKRPK; amino acids 14–27) that spans the signal peptide cleavage site at residues 22/23. The peptide was conjugated to keyhole limpet hemocyanin using both glutaraldehyde and 4-(*N*-maleimidomethyl)cyclohexane-1-carboxylic acid 3-sulfo-*N*-hydroxysuccinimide ester (Sigma).

Monoclonal antibodies 3F4 (28) and 8H4 (29) and polyclonal antibody P45-66 (5) against PrP have been described previously.

RESULTS

Mutations in the Hydrophobic Core of the Signal Peptide Increase the Proportion of ^{Ctm}PrP and Reduce Translocation Efficiency—For these experiments, we translated PrP mRNA in the presence of microsomes from murine thymoma cells, which are efficient at adding the C-terminal GPI anchor (16). Translation reactions were subsequently subjected to PK digestion to reveal protease-protected products corresponding to ^{Sec}PrP and ^{Ctm}PrP. ^{Ntm}PrP was not quantitated in these experiments, because negligible amounts of this form are produced in the presence of thymoma microsomes (16). We showed previously that substitution of arginine for leucine at position 9 (L9R) in the hydrophobic core (h-region) of the signal peptide had a dramatic effect on PrP membrane topology, with ~50% of the translocated protein assuming the ^{Ctm}PrP orientation, compared with ~10% for WT PrP (13). We then tested the effects of other amino acid substitutions at this site. The results are shown in Fig. 1 and summarized in Table I (lines 1–12). Substitution of either positively charged residues (Arg and Lys) or a negatively charged residue (Asp) for leucine at position 9 increased the proportion of ^{Ctm}PrP, with two non-polar residues (Pro and Gly) having very little effect. All of the substitutions also significantly reduced the efficiency of translocation (the total percentage of PK-protected chains) from ~25% for WT PrP to 5–15% for the mutants (data not shown). To examine the effect of substitutions at another residue in the h-region of the signal peptide, we analyzed V13R and V13D. Both of these mutations completely abolished translocation (Fig. 1).

Previous work demonstrated that certain mutations in the transmembrane segment also increased the amount of ^{Ctm}PrP. One mutation that has been studied extensively is the triple substitution designated 3AV (substitution of valine for alanine at positions 112, 114, and 117) (7, 13). When this mutation was combined with mutations in the signal sequence, an additive increase in the percentage of ^{Ctm}PrP was observed (Fig. 1; Table I, lines 1–12). PrP molecules carrying the 3AV mutation along with substitution of a charged amino acid (Arg, Lys, and Asp) at position 9 were synthesized almost exclusively as ^{Ctm}PrP.

Lack of Signal Peptide Cleavage Does Not Cause Production of ^{Ctm}PrP—We have shown previously (13) that ^{Ctm}PrP has an uncleaved signal peptide. However, it remained unknown whether the lack of signal peptide cleavage was a cause or a consequence of ^{Ctm}PrP formation. To address this question, we introduced mutations that prevent cleavage by signal peptidase, and we assayed their effect on synthesis of ^{Ctm}PrP. The −1 and −3 positions in the c-region of signal peptides have

[2] R. S. Stewart and D. A. Harris, manuscript in preparation.

TABLE I

Quantitation of ^{Ctm}Prp produced by the mutants used in this study

PrP mRNA was translated *in vitro* in the presence of either murine thymoma microsomes (constructs 1–18 and 23–28) or canine pancreatic microsomes (constructs 19–22 and 29–32). The ^{Ctm}PrP and ^{Sec}PrP fragments produced after PK digestion were quantitated by PhosphorImager analysis of SDS-PAGE gels. The percentage of ^{Ctm}PrP was expressed as ^{Ctm}Prp/(^{Ctm}PrP + ^{Sec}PrP) × 100. ^{Ntm}PrP was not included in this calculation because it is present in negligible amounts in translations performed with thymoma microsomes (16). Each value represents the mean of 2–8 replicates.

Construct	^{Ctm}PrP
	%
1. WT	12.4
2. L9R	30.1
3. L9R/3AV	87.6
4. L9K	62.6
5. L9K/3AV	87.7
6. L9D	43.0
7. L9D/3AV	77.5
8. L9G	22.3
9. L9G/3AV	67.8
10. L9P	11.0
11. V13R	[a]
12. V13D	[a]
13. WT	11.8
14. G20W	7.4
15. C22Y	13.7
16. C22Y/L9R/3AV	90.0
17. WT 23–254	[a]
18. 3AV 23–254	[a]
19. WT	31.3
20. FLAG/WT	58.7
21. 3AV	54.3
22. FLAG/3AV	89.6
23. PG0	21.3
24. PG1	14.7
25. PG2	14.3
26. PG5(WT)	11.2
27. PG14	5.5
28. 3AV	27.0
29. WT/GPI+	25.3
30. WT/GPI−	24.9
31. 3AV	46.1
32. 3AV/GPI−	39.5

[a] Neither ^{Ctm}PrP nor ^{Sec}PrP were present at detectable levels.

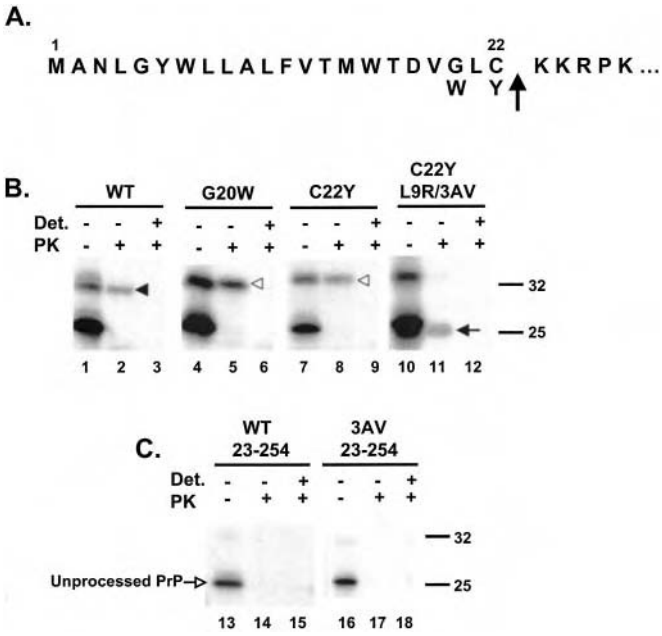

FIG. 2. **Lack of signal peptide cleavage does not cause production of ^{Ctm}PrP, and deletion of the signal peptide prevents translocation.** *A*, amino acid sequence of the N terminus of PrP. Substitutions made at positions 20 and 22 to block signal peptide cleavage are indicated *below* the corresponding wild-type residues. The *upward arrow* indicates the site of signal peptide cleavage. *B* and *C*, PrP mRNAs encoding the indicated constructs were translated in reticulocyte lysate supplemented with murine thymoma microsomes. Reactions were then incubated with (+ *PK lanes*) or without (− *PK lanes*) proteinase K in the presence (+ *Det. lanes*) or absence (− *Det. lanes*) of Triton X-100. Products were then analyzed by SDS-PAGE and autoradiography. The *arrowheads* indicate the positions of the protected fragments corresponding to ^{Sec}PrP. The ^{Sec}PrP fragments are slightly larger for G20W and C22Y PrP (*open arrowheads*, *lanes 5* and *8*) than for WT PrP (*filled arrowhead*, *lane 2*), confirming that the mutations prevent cleavage of the signal peptide. The *filled arrow* (*lane 11*) indicates the position of the ^{Ctm}PrP protected fragment. The *open arrow* (*lane 13*) indicates the position of unprocessed PrP that has not undergone signal peptide cleavage, GPI anchor addition, or glycosylation.

been shown to have the greatest influence on cleavage (30); small polar residues are strongly preferred. We therefore substituted large, hydrophobic residues at these positions to block the action of signal peptidase (Fig. 2*A*). Fig. 2*B* (*lanes 2*, *5*, and *8*) shows that these mutations had no effect on PrP topology. As in the WT molecule, PrP containing either G20W or C22Y substitutions produced primarily ^{Sec}PrP, with ~10% being synthesized as ^{Ctm}PrP (Table I, lines 13–15). This result was verified by assaying the topology of these mutants in transfected cells (data not shown). The mutant C22Y/L9R/3AV produced 90% ^{Ctm}PrP (Fig. 2*B*, *lane 11*; Table I, line 16), indicating that lack of signal peptide cleavage does not inhibit formation of ^{Ctm}PrP. We confirmed that the signal peptide remained uncleaved in the G20W and C22Y mutants by observing the slightly reduced mobility of the ^{Sec}PrP bands on SDS-PAGE (Fig. 2*B*, compare *lane 2* to *lanes 5* and *8*). We conclude from these results that lack of signal peptide cleavage is a consequence, and not a cause, of ^{Ctm}PrP formation.

Deletion of the Signal Peptide Prevents Translocation—^{Ctm}PrP has the topology of a type II transmembrane protein (N terminus in the cytoplasm). Most proteins of this type contain an internal signal-anchor sequence that initiates translocation by binding to the signal recognition particle, and also anchors the polypeptide chain in the lipid bilayer. To test whether the transmembrane segment of PrP could serve a membrane targeting function independent of the N-terminal signal sequence, we assayed PrP constructs in which the N-terminal sequence had been deleted. We observed that removal of the signal peptide completely abolished translocation of WT PrP, as evidenced by the failure to detect any protected fragments after PK digestion of translation reactions (Fig. 2*C*, *lane 14*). The same result was observed after introduction of the 3AV mutation, which normally increases ^{Ctm}PrP formation and might therefore be expected to enhance the ability of the transmembrane segment to function as a signal-anchor sequence (Fig. 2*C*, *lane 17*). Thus, the transmembrane segment cannot function independently to target PrP to the translocon to produce ^{Ctm}PrP but requires cooperation with the N-terminal signal sequence.

Residues on the C-terminal Side of the Signal Peptide Cleavage Site Influence PrP Topology—To demonstrate that ^{Ctm}PrP has an uncleaved signal, we had constructed previously a PrP molecule with a FLAG epitope inserted at the signal peptide cleavage site (amino acids 22/23) (Fig. 3*A*) (13). Insertion of this epitope (DYKDDDDK) changes the downstream amino acid context of the cleavage site from basic (KKRPKPGG) to acidic. We found that the presence of the FLAG epitope increases the proportion of ^{Ctm}PrP compared with untagged controls. This effect is relatively modest when microsomes from mouse thymoma cells are used (not shown) but more dramatic when

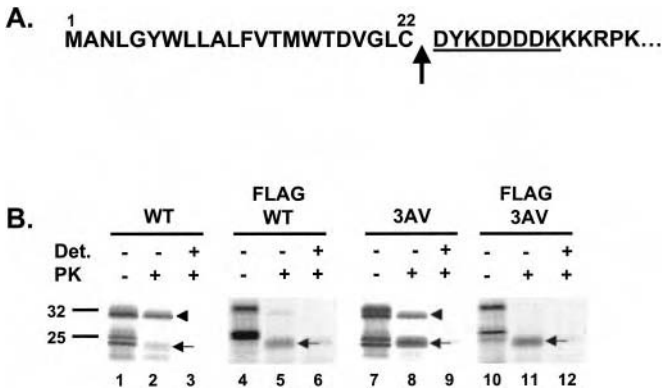

FIG. 3. **Insertion of a FLAG epitope at the signal peptide cleavage site influences PrP topology.** *A*, amino acid sequence of PrP with the FLAG epitope (*underline*) inserted at the signal peptide cleavage site (*upward arrow*). *B*, PrP mRNAs encoding the indicated constructs were translated in reticulocyte lysate supplemented with canine pancreatic microsomes. Reactions were then incubated with (+ *PK lanes*) or without (− *PK lanes*) proteinase K in the presence (+ *Det. lanes*) or absence (− *Det. lanes*) of Triton X-100. Products were then analyzed by SDS-PAGE and autoradiography. The *arrowheads* and *arrows* indicate the positions of ^{Sec}PrP and ^{Ctm}PrP, respectively.

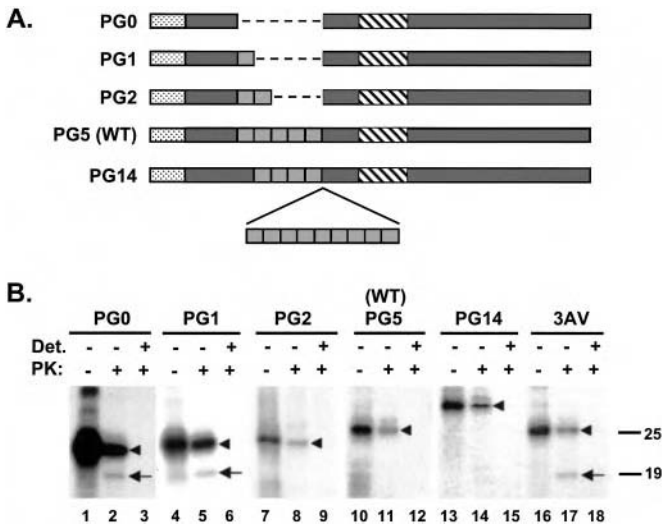

FIG. 4. **Changing the spacing between the signal peptide and the transmembrane domain affects membrane topology.** *A*, schematic of PrP molecules containing deletions or an insertion in the octapeptide repeat region. PG0, PG1, PG2, PG5, and PG14 refer to constructs having 0, 1, 2, 5, or 14 octapeptide repeats. WT PrP has 5 repeats. The *stippled region* represents the signal peptide, the *light-shaded boxes* represent the octapeptide repeats, and the *cross-hatched region* represents the transmembrane domain. *B*, PrP mRNAs encoding the indicated constructs were translated in reticulocyte lysate supplemented with murine thymoma microsomes. Reactions were then incubated with (+ *PK lanes*) or without (− *PK lanes*) proteinase K in the presence (+ *Det. lanes*) or absence (− *Det. lanes*) of Triton X-100. Products were immunoprecipitated with 3F4 antibody and deglycosylated with PNGase F prior to analysis by SDS-PAGE and autoradiography. *Arrowheads* and *arrows* indicate the positions of ^{Sec}PrP and ^{Ctm}PrP, respectively. On the autoradiographic exposures shown here, the ^{Ctm}PrP band is not visible for PG2, PG5, and PG14. However, small amounts of this form can be detected above background levels by PhosphorImager analysis (see Table I, lines 25–27).

canine pancreatic microsomes are used (Fig. 3*B*; Table I, lines 19–22). In this system, the percentage of ^{Ctm}PrP is doubled by introduction of the FLAG sequence into either WT or 3AV PrP. We have shown previously that, for all PrP constructs, pancreatic microsomes produce a higher ^{Ctm}PrP/^{Sec}PrP ratio than thymoma microsomes (16), possibly due to differences between these preparations in their content of translation accessory factors (14, 15). Insertion of the FLAG epitope does not alter the position of signal peptide cleavage, based on immunoreactivity with the monoclonal antibody M1, which is specific for the FLAG sequence containing a free N terminus (13).

Changing the Spacing between the Signal Peptide and the Transmembrane Domain Affects Membrane Topology—It has been proposed that the two topogenic determinants in PrP (the N-terminal signal peptide and the transmembrane domain) interact with other during the translocation process (9, 11). To test this idea, we determined whether altering the spacing between these determinants affected PrP membrane topology. The spacing was altered by deleting or inserting octapeptide repeat units (P(H/Q)GG(G/S/T)WGQ), five copies of which are normally found in the N-terminal region of PrP (Fig. 4*A*). As shown in Fig. 4*B* and Table I (lines 23–28), decreasing the number of octapeptide repeats to 2, 1, or 0 progressively increases the proportion of ^{Ctm}PrP, whereas increasing the number of repeats to 14 has the opposite effect. Similar results were obtained when translations were performed using canine pancreatic microsomes, in which the proportions of ^{Ctm}PrP were higher, and it was easier to appreciate the reduction in ^{Ctm}PrP produced by insertion of additional repeats (PG14 construct) (data not shown). These results demonstrate that PrP membrane topology is dependent upon the timing with which the two topological determinants are presented to the translocation machinery.

Deletion of the GPI Addition Signal Does Not Affect Membrane Topology—PrP has a hydrophobic segment at its C terminus (residues 231–254) which serves as a signal for attachment of the GPI anchor. This segment, which is normally cleaved off during addition of the anchor structure in the ER, is capable of inserting into the membrane post-translationally when the N-terminal signal sequence and transmembrane domains have been deleted (8). To test the effect of the GPI addition sequence on the membrane topology of PrP in the context of the full-length protein, we analyzed constructs in which this sequence was deleted. As shown in Fig. 5 and Table I (lines 29–32), deletion of the GPI addition signal had no effect on the proportion of ^{Ctm}PrP, either in the WT protein or in a protein carrying the 3AV mutation. We also observed that replacement of the GPI addition signal with an unrelated sequence (the KDEL ER retention signal) had no effect on membrane topology (data not shown).

An Antibody Directed against the PrP Signal Peptide Specifically Recognizes ^{Ctm}PrP and Untranslocated PrP—Because ^{Ctm}PrP, unlike ^{Ntm}PrP and ^{Sec}PrP, has an uncleaved signal peptide, we reasoned that an antibody raised against the signal peptide would be a useful tool for specifically assaying ^{Ctm}PrP in cells and tissues. Because of the hydrophobicity of the signal sequence made synthesis of synthetic peptides encompassing this region problematic, we chose as an immunogen a synthetic peptide that spanned the signal peptide cleavage site (Fig. 6*A*). This peptide included several positively charged residues on the C-terminal side of the cleavage site that facilitated synthesis of the peptide and improved antigenicity. This peptide was coupled to keyhole limpet hemocyanin via both amino and sulfhydryl groups and was used to raise a polyclonal antiserum (denoted anti-SP) in rabbits.

Initial characterization of the antiserum was performed using PrP synthesized by *in vitro* translation (Fig. 6*B*). When WT PrP was immunoprecipitated with an antibody (P45–66) that detects all forms of PrP, two bands were seen (Fig. 6*B*, *lane 1*): a 32-kDa species representing core-glycosylated ^{Sec}PrP chains, and a 27-kDa species representing unglycosylated, untranslocated chains that have not been processed at either their N or C termini (*i.e.* they retain both their signal and GPI addition peptides). The anti-SP antibody reacted only with the latter

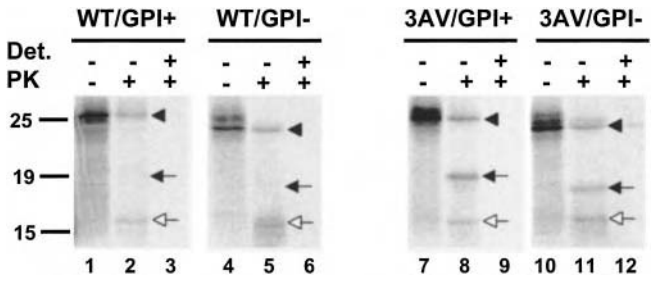

FIG. 5. **Deletion of the GPI addition signal does not affect membrane topology.** PrP mRNAs encoding the indicated constructs were translated in reticulocyte lysate supplemented with canine pancreatic microsomes. Reactions were then incubated with (+ *PK lanes*) or without (− *PK lanes*) proteinase K in the presence (+ *Det. lanes*) or absence (− *Det. lanes*) of Triton X-100. Products were immunoprecipitated with 3F4 antibody and deglycosylated with PNGase F prior to analysis by SDS-PAGE and autoradiography. The positions corresponding to ^{Sec}PrP, ^{Ctm}PrP, and ^{Ntm}PrP are indicated by the *filled arrowheads*, *filled arrows*, and *open arrows*, respectively. ^{Ctm}PrP is not clearly visible for the WT constructs on this autoradiographic exposure, but it is detectable above background levels by PhosphorImager analysis (Table I, lines 29–30).

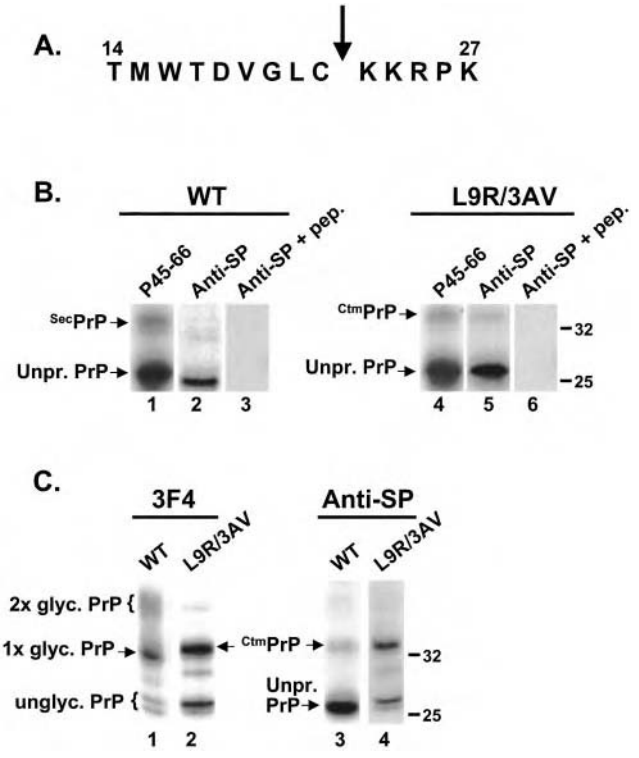

FIG. 6. **Characterization of anti-SP antibody.** *A*, sequence of the synthetic peptide used to raise anti-SP antibody. The *arrow* indicates the position of the signal peptide cleavage site. *B*, mRNAs encoding WT or L9R/3AV PrP were translated in reticulocyte lysate supplemented with murine thymoma microsomes. PrP was then immunoprecipitated from translation reactions with P45–66 antibody (*lanes 1* and *4*), anti-SP antibody (*lanes 2* and *5*), or anti-SP antibody pre-incubated with the peptide immunogen (*lanes 3* and *6*). *C*, transiently transfected CHO cells expressing WT or L9R/3AV PrP were labeled for 6 h with [^{35}S]methionine. PrP was then immunoprecipitated from cell lysates using either 3F4 antibody (*lanes 1* and *2*) or anti-SP antibody (*lanes 3* and *4*) and analyzed by SDS-PAGE and autoradiography. The positions of doubly and singly glycosylated forms of mature PrP, unglycosylated PrP, ^{Ctm}PrP, and unprocessed PrP are indicated.

form (Fig. 6*B*, lane 2), and this reactivity could be abolished by pre-incubation of the antibody with the peptide immunogen (Fig. 6*B*, *lane 3*). When L9R/3AV PrP was immunoprecipitated with P45–66, both core-glycosylated as well as unglycosylated, untranslocated forms were also observed, but the glycosylated form migrated at 33 kDa rather than 32 kDa because of the presence of an uncleaved signal peptide characteristic of ^{Ctm}PrP (Fig. 6*B*, *lane 4*) (13). Anti-SP recognized both the 33- and 27-kDa species (Fig. 6*B*, *lane 5*), and again reactivity could be blocked by pre-incubation with the peptide immunogen (*lane 6*). These results demonstrate that the anti-SP serum recognizes PrP translation products with a retained N-terminal signal peptide and does not react with molecules whose signal peptide has been cleaved.

We then tested the ability of the anti-SP serum to recognize PrP synthesized in transiently transfected CHO cells (Fig. 6*C*). Cells were metabolically labeled with [^{35}S]methionine, and PrP was immunoprecipitated from lysates using either anti-SP antibody or 3F4 antibody (which recognizes all forms of PrP). Cells expressing WT PrP produced two mature, glycosylated species recognized by 3F4 antibody: a doubly glycosylated form at 38 kDa and a singly glycosylated form at 32 kDa (Fig. 6*C*, *lane 1*). In addition, small amounts of unglycosylated PrP at 25–27 kDa were present. In contrast, cells expressing L9R/3AV PrP produced a 33-kDa glycosylated form that we have shown previously (13) represents an endoglycosidase H-sensitive form of ^{Ctm}PrP that has an uncleaved signal peptide (Fig. 6*C*, *lane 2*). Anti-SP antiserum immunoprecipitated the 33-kDa ^{Ctm}PrP species from cells expressing L9R/3AV PrP (Fig. 6*C*, *lane 4*), and trace amounts of the same band were detected in cells expressing WT PrP (*lane 3*). However, the doubly and singly glycosylated forms of WT PrP were not recognized by this antibody (Fig. 6*C*, *lane 3*), demonstrating its selectivity for signal peptide-bearing forms synthesized in cells. We noted that anti-SP also recognized an unglycosylated form of PrP (27 kDa), which we have shown represents untranslocated, unprocessed molecules that accumulate in the cytoplasm at high expression levels (22). These molecules are analogous to the untranslocated species observed after *in vitro* translation (Fig. 6*B*). Taken together, the results shown in Fig. 6, *B* and *C*, demonstrate that anti-SP antibody is capable of selectively recognizing PrP molecules that contain an uncleaved signal peptide, even in the presence of an excess of N-terminally processed forms. These signal peptide-bearing molecules, which are synthesized both *in vitro* and in cultured cells, are composed of ^{Ctm}PrP as well as untranslocated forms that remain on the cytoplasmic side of the ER membrane (13, 22).

The Amounts of ^{Ctm}PrP and Untranslocated PrP Are Not Altered by Scrapie Infection of Cultured Cells and Brain—^{Ctm}PrP has been proposed to be a neurotoxic intermediate whose levels are increased during infectiously acquired as well as familial prion diseases (7, 12). To test this hypothesis, we used the anti-SP antibody to assay the amount of ^{Ctm}PrP in scrapie-infected N2a cells. Infected and uninfected N2a cells were labeled to steady state with [^{35}S]methionine, and then PrP was immunoprecipitated with either anti-SP antibody or with an antibody (8H4) that recognizes all forms of PrP. Because the level of endogenous mouse PrP in N2a cells is relatively low, some cultures were transiently transfected to express high levels of WT PrP, with the idea that this might enhance the ability to detect small amounts of ^{Ctm}PrP. In addition, some cells were transfected with constructs encoding PrP mutants (A116V, 3AV, and L9R/3AV) that would serve as positive controls for synthesis of ^{Ctm}PrP. The transfection efficiency in these experiments, measured using a GFP-encoding plasmid, was sufficiently high (~30%) that we could be confident a substantial number of scrapie-infected cells in the culture expressed transfected PrP. The N2a cells used for these experiments represented a sub-clone (N2a.3) we had isolated that was highly susceptible to scrapie infection (see "Experimental Procedures"), so that the infected and uninfected versions could be directly compared without further cloning (25).

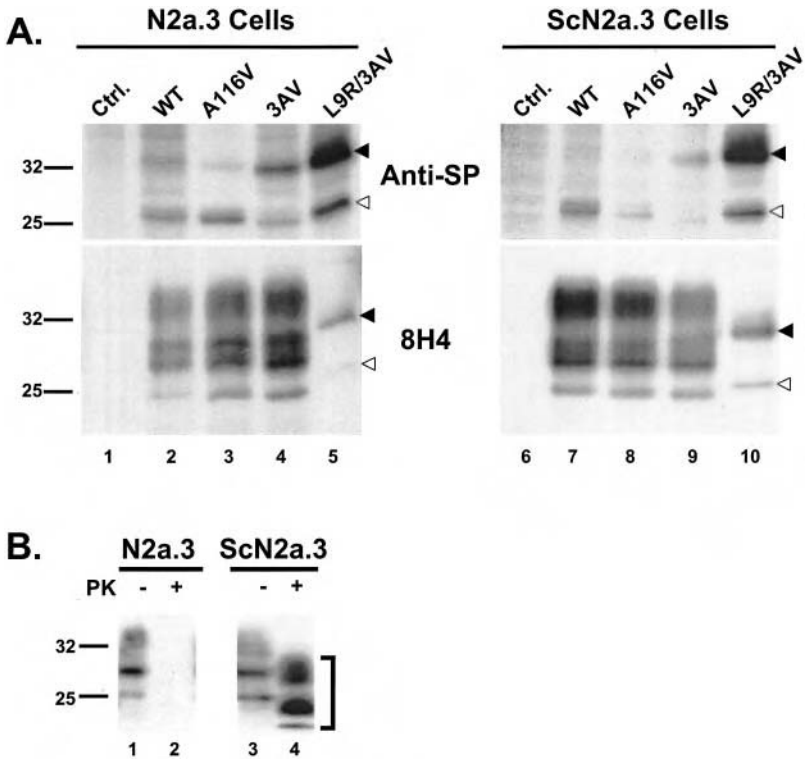

FIG. 7. **The amounts of ^{Ctm}PrP and untranslocated PrP are not altered by scrapie infection of N2a cells.** *A*, uninfected N2a.3 cells (*lanes 1–5*) and scrapie-infected N2a.3 cells (*lanes 6–10*) were untransfected (*lanes 1* and *6*) or were transiently transfected to express WT (*lanes 2* and *7*), A116V (*lanes 3* and *8*), 3AV (*lanes 4* and *9*), or L9R/3AV PrP (*lanes 5* and *10*). Cells were labeled for 6 h with [^{35}S]methionine and then lysed. PrP was immunoprecipitated from cell lysates using either anti-SP antibody (*upper panels*) or 8H4 antibody (*lower panels*) and analyzed by SDS-PAGE and autoradiography. The *filled* and *open arrowheads* indicate the positions of ^{Ctm}PrP and untranslocated PrP, respectively. *B*, lysates of uninfected N2a.3 cells (*lanes 1* and *2*) and scrapie-infected N2a.3 cells (*lanes 3* and *4*) were subjected to digestion with PK (20 μg/ml for 30 min at 37 °C), and analyzed by Western blotting using 3F4 antibody. The *bracket* indicates the position of PrP 27–30, the protease-resistant fragment of PrP^{Sc}.

Fig. 7*A* shows that there was no difference between infected and uninfected cells in the amounts of signal peptide-containing PrP they produced. Although untransfected cells synthesized low levels of PrP that required long autoradiographic exposures to visualize (data not shown), cells transfected with WT or mutant PrP plasmids expressed considerably higher levels of 8H4-reactive protein (*lower panels*). In cells transfected with the WT PrP plasmid, anti-SP antibody immunoprecipitated two bands of 27 and 33 kDa (*upper panels*, *lanes 2* and *7*). The 33-kDa species, which was sensitive to digestion with endoglycosidase H (not shown), was present in increased amounts in cells expressing A116V, 3AV, and L9R/3AV PrP (*upper panels*, *lanes 3–5* and *8–10*), confirming its identity as ^{Ctm}PrP (13). The unglycosylated 27-kDa band corresponds to untranslocated PrP, which we have shown to be present in increased amounts in transiently transfected cells (22). Importantly, the amounts of both the 33- and 27-kDa species did not differ between infected and uninfected cells. We conclude from these results that scrapie infection of N2a cells does not detectably increase the amount of either ^{Ctm}PrP or untranslocated PrP. Western blotting confirmed that that the scrapie-infected cells produced protease-resistant PrP^{Sc} (Fig. 7*B*). We note that the results shown in Fig. 7*A* are a further demonstration of the specificity of the anti-SP antibody for signal peptide-bearing forms of PrP, because ^{Ctm}PrP and untranslocated PrP are selectively immunoprecipitated in the presence of a large excess of processed PrP (compare anti-SP and 8H4 panels).

We also sought to measure the amounts of signal peptide-bearing PrP in scrapie-infected brain samples. Initial experiments failed to detect any proteins that reacted specifically with anti-SP antiserum on Western blots of lysates prepared from either infected or control brains, a result that is presumably due to the low levels of these proteins in brain and to the presence of bands that react non-specifically with the antibody on blots (data not shown). As an alternative assay, we used SDS-PAGE to detect the small (~2 kDa) difference in size between PrP molecules with and without a signal peptide. Proteins were enzymatically deglycosylated prior to SDS-PAGE to eliminate size differences due to differential glycosylation. When the gels were run long enough, we found we could reliably detect the difference in migration between PrP molecules containing a cleaved signal peptide (25 kDa) and an uncleaved signal peptide (27 kDa), as demonstrated by visualization of two bands in brain samples from Tg(L9R/3AV) mice (Fig. 8, *lane 5*). These mice, which spontaneously develop a severe neurodegenerative illness, synthesize ^{Ctm}PrP as well as signal peptide-cleaved forms.[3] The identity of the 27-kDa form as a signal peptide-bearing form was confirmed by immunoprecipitating it with anti-SP antibody from [^{35}S]methionine-labeled neurons cultured from Tg(L9R/3AV) mice (not shown). Importantly, we did not detect any of the 27-kDa band in brain samples from uninfected mice or from mice and hamsters infected with several different scrapie inocula (Fig. 8, *lanes 1–4*). Because samples were deglycosylated prior to SDS-PAGE, this analysis would not distinguish ^{Ctm}PrP from untranslocated PrP. We conclude from these data that scrapie infection of mice and hamsters does not increase the amount of either ^{Ctm}PrP or untranslocated PrP in the brain to detectable levels.

DISCUSSION

In this work, we have analyzed several structural features of the PrP molecule that influence its membrane topology. In addition, we have developed an antibody that selectively recognizes ^{Ctm}PrP and cytosolic PrP, topological variants of PrP implicated in prion-related neurodegeneration. We have used this antibody, as well as the distinctive gel mobility of ^{Ctm}PrP and cytosolic PrP, to measure the amounts of these forms in scrapie-infected cells and brain. Our results have implications for the mechanisms of protein translocation in the ER and for the role of transmembrane and cytosolic PrP in neurodegenerative disease.

Topological Determinants in PrP—Initial work on PrP membrane topology demonstrated that mutations within and adjacent to the hydrophobic transmembrane domain influenced the

[3] R. S. Stewart and D. A. Harris, manuscript in preparation.

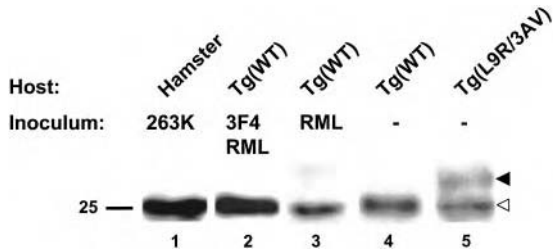

FIG. 8. **The amount of signal peptide-bearing PrP is not altered in scrapie-infected brain.** Brain homogenates were prepared from a Syrian hamster infected with 263K scrapie (*lane 1*), a Tg(WT) mouse infected with 3F4-tagged RML scrapie (*lane 2*), a Tg(WT) mouse infected with RML scrapie (*lane 3*), an uninfected Tg(WT) mouse (*lane 4*), and an uninfected Tg(L9R/3AV) mouse (*lane 5*). Infected animals were terminally ill at the time of sacrifice. Homogenates were treated with PNGase F, and proteins were then subjected to Western blotting with 3F4 antibody. The *filled* and *open arrowheads* indicate the positions of signal peptide-bearing PrP and signal peptide-cleaved PrP, respectively.

relative amount of ^{Ctm}PrP synthesized (7, 12). Some mutations (*e.g.* A116V, K109I/H110I, and 3AV) increased the proportion of ^{Ctm}PrP, whereas other mutations (*e.g.* G122P) decreased it. Subsequently, we found that a non-conservative substitution (L9R) within the hydrophobic core of the N-terminal signal sequence dramatically increased the amount of ^{Ctm}PrP (13). Combining this mutation with the 3AV mutation resulted in a molecule (L9R/3AV) that was synthesized exclusively as ^{Ctm}PrP both *in vitro* and in cultured cells. We also found that disease-associated mutations that lie outside the transmembrane region did not alter the membrane topology of PrP (16). Taken together, these results indicated that there were two major topogenic determinants in the PrP molecule: the N-terminal signal peptide and the hydrophobic transmembrane domain. Another potential topological determinant, the C-terminal, GPI addition signal, does not appear to play a significant role. Although the GPI signal can mediate post-translational translocation of PrP molecules lacking an N-terminal signal sequence (8), deletion or substitution of this segment has no effect on the membrane topology of the full-length protein (this paper and see Ref. 11).

To explore further the role of the signal peptide in determining PrP topology, we introduced several additional substitutions in the hydrophobic core (h-region) of the signal peptide. We found that introduction of either positively or negatively charged residues at position 9 significantly increased the proportion of ^{Ctm}PrP. These substitutions also decreased the overall efficiency of translocation. Introduction of either a positively or negatively charged residue at position 13 completely abolished translocation. These results are consistent with the suggestion (9) that the PrP signal sequence serves two distinct functions: 1) targeting the polypeptide chain to the translocon; and 2) determining the location of the N terminus with respect to the membrane (luminal or cytoplasmic). Introduction of charged residues in the h-region affects both of these functions, reducing the targeting activity of the signal sequence, as well as its ability to promote translocation of the N terminus to the luminal side of the membrane. Previous work has shown that mutations in the n-region of the signal peptide (the polar, N-terminal segment) can also influence the two functions of the signal sequence (9, 31).

Several other features of PrP topogenesis are also addressed by our results. First, we found that mutations in the c-region that block signal peptide cleavage do not alter the topology of PrP. Thus, the presence of an uncleaved signal peptide, which we have found is a characteristic of ^{Ctm}PrP, does not by itself favor formation of ^{Ctm}PrP. Rather, failure of signal peptide cleavage is likely to be a consequence of the fact that, in ^{Ctm}PrP, the N terminus of the protein remains in the cytoplasm and therefore does not come into contact with signal peptidase in the ER lumen.

We have also observed that deletion of the signal peptide prevents translocation, resulting in cytosolic molecules that are fully accessible to added protease. This result, which confirms other published reports (8, 10), indicates that the hydrophobic, transmembrane segment cannot by itself target the polypeptide chain to the translocon. Thus, in contrast to the case for other type II membrane-spanning proteins (whose N termini are cytoplasmic), the transmembrane domain of PrP is not capable of functioning as a signal-anchor sequence. These considerations are consistent with the proposal (9, 11) that the primary function of the PrP transmembrane domain is to determine whether polypeptide chains that have already been targeted to the translocon by the N-terminal signal sequence will integrate into the lipid bilayer. In the model of Hegde and colleagues (11), the signal sequence and transmembrane domain thus mediate two sequential events within the translocon channel that determine the partitioning of PrP chains among the possible topological variants. Consistent with such a model, decreasing the distance between the signal sequence and transmembrane domain increases synthesis of ^{Ctm}PrP (this paper and see Ref. 11).

We find that introduction of a FLAG epitope just C-terminal to the signal peptide cleavage site increases the proportion of ^{Ctm}PrP synthesized. This result indicates that, although the signal sequence and transmembrane domain are the primary determinants of PrP topology, other parts of the protein can also have an influence. This observation is reminiscent of experiments in which the translocation of chimeric proteins containing the same signal sequence but different mature domains was measured (31). These experiments indicated that signal sequences and mature domains cooperate in luminal gating of the translocon pore, a step that is correlated with synthesis of ^{Ntm}PrP and ^{Sec}PrP. In this light, introduction of the FLAG epitope would decrease the efficiency of luminal gating and thus increase the relative amount of ^{Ctm}PrP.

An Immunological Assay for ^{Ctm}PrP and Cytosolic PrP—Previously, the only method available for direct measurement of ^{Ctm}PrP has been the protease-protection assay using microsomal membranes, which relies upon the generation of a protected fragment representing the luminal domain of ^{Ctm}PrP (7–9, 11, 16). However, this assay can be cumbersome to perform and is problematic when applied to tissue samples because of the difficulty of preparing purified, ER-derived, microsomal membranes. The assay is also not applicable to scrapie-infected samples because of the intrinsic protease resistance of PrP^{Sc}. Another published method (7), which involves PK digestion of detergent extracts under "mild" conditions, has also been claimed to detect ^{Ctm}PrP, but there is no direct evidence that the PK-resistant fragment produced in this assay represents authentic ^{Ctm}PrP. Detection of cytosolic PrP has relied upon immunofluorescence staining and the use of proteasome inhibitors (19–21).

The presence of an uncleaved signal peptide on both ^{Ctm}PrP (13) and cytosolic PrP (22) provides a simple and direct method to detect these forms using an antibody directed against the signal sequence. We have prepared an antiserum against a synthetic peptide that spans the signal peptide cleavage site, and we have shown that this antiserum specifically immunoprecipitates ^{Ctm}PrP synthesized *in vitro* and in cells, even in the presence of a large excess of signal peptide-cleaved forms (^{Sec}PrP and ^{Ntm}PrP). The anti-SP antiserum also detects untranslocated forms of PrP that have not been processed at their N or C termini and that we have shown (22) remain on the

cytoplasmic side of the ER membrane. Thus, this antiserum is a useful reagent for specifically detecting untranslocated, cytosolic PrP as well as ^{Ctm}PrP.

Effect of Scrapie Infection on the Amounts of ^{Ctm}PrP and Cytosolic PrP—It has been proposed that ^{Ctm}PrP is a key pathogenic intermediate in both familial and infectiously acquired prion diseases (7, 12). In this scheme, certain pathogenic mutations in PrP are thought to increase directly the synthesis of ^{Ctm}PrP, whereas in cases of infectious origin PrP^{Sc} is hypothesized to indirectly cause accumulation of ^{Ctm}PrP. Although it is clear that ^{Ctm}PrP-favoring mutations cause a neurodegenerative phenotype when expressed in transgenic mice, there is a paucity of evidence that the amount of ^{Ctm}PrP actually increases during the course of a natural prion infection in either humans or animals. The only published experiment that supports this conclusion involved the use of a PrP reporter construct to monitor ^{Ctm}PrP levels in scrapie-infected mice (12). However, this assay did not directly quantitate ^{Ctm}PrP, and in addition, the maximal increase in ^{Ctm}PrP observed was only 3-fold, much smaller than the increase in PrP^{Sc}. Cytosolic PrP has also been proposed as a neurotoxic intermediate, but the only experiments to support this claim derive from expression of artificial forms of PrP that lack an N-terminal signal sequence (18).

We report here that scrapie infection of N2a cells and mouse brain does not alter the amount of signal peptide-bearing PrP, based on reactivity with anti-SP antibody, or on SDS-PAGE to detect the slightly larger molecular weight of this form. These results indicate that scrapie infection does not affect the levels of either ^{Ctm}PrP or untranslocated (presumably cytosolic) PrP, both of which have an uncleaved signal peptide. Of course, it is possible that these forms were present below the level of detectability of our assay methods. Arguing against this possibility is the fact that we can easily visualize signal peptide bearing forms of PrP in uninfected and scrapie-infected N2a cells that have been transfected to express WT molecules or molecules carrying ^{Ctm}PrP-favoring mutations. We estimate that ^{Ctm}PrP represents ~0.5–1% of total PrP in cells expressing the WT protein. In addition, we can detect ^{Ctm}PrP in brain extracts from Tg(L9R/3AV) mice that spontaneously develop a severe neurodegenerative illness (Fig. 8).[3] If the amount of ^{Ctm}PrP had been elevated in the brains of scrapie-infected mice to levels similar to those observed in the brains of Tg(L9R/3AV) mice, it is thus likely we would have been able to detect this change.

A growing body of evidence indicates that, although PrP^{Sc} is the infectious form of PrP, one or more alternate forms of the protein are responsible for the neurodegeneration observed in prion disorders (17). The results presented here, in conjunction with our previous work showing that levels of ^{Ctm}PrP and cytosolic PrP are not altered by disease-associated PrP mutations (16, 22), suggest that these two forms are unlikely to be obligate neurotoxic intermediates in familial or infectiously acquired prion diseases. It will be important now to identify other neurotoxic forms of PrP (32) and to develop specific and sensitive assays to detect these species during the course of prion diseases.

Acknowledgments—We thank Richard Kascsak for 3F4 antibody, Man-Sun Sy for 8H4 antibody, and Sylvain Lehmann for scrapie-infected N2a cells used as an inoculum. We also acknowledge Michael Green for isolating N2a.3 cells and Jiaxin Dong for testing them for PrP^{Sc}.

REFERENCES

1. Prusiner, S. B. (1998) *Proc. Natl. Acad. Sci. U. S. A.* **95,** 13363–13383
2. Collinge, J. (2001) *Annu. Rev. Neurosci.* **24,** 519–550
3. Brown, L. R., and Harris, D. A. (2002) in *Handbook of Copper Pharmacology and Toxicology* (Massaro, E. J., ed) pp. 103–113, Humana Press Inc., Totowa, NJ
4. Stahl, N., Borchelt, D. R., and Prusiner, S. B. (1990) *Biochemistry* **29,** 5405–5412
5. Lehmann, S., and Harris, D. A. (1995) *J. Biol. Chem.* **270,** 24589–24597
6. De Fea, K. A., Nakahara, D. H., Calayag, M. C., Yost, C. S., Mirels, L. F., Prusiner, S. B., and Lingappa, V. R. (1994) *J. Biol. Chem.* **269,** 16810–16820
7. Hegde, R. S., Mastrianni, J. A., Scott, M. R., Defea, K. A., Tremblay, P., Torchia, M., DeArmond, S. J., Prusiner, S. B., and Lingappa, V. R. (1998) *Science* **279,** 827–834
8. Hölscher, C., Bach, U. C., and Dobberstein, B. (2001) *J. Biol. Chem.* **276,** 13388–13394
9. Kim, S. J., Rahbar, R., and Hegde, R. S. (2001) *J. Biol. Chem.* **276,** 26132–26140
10. Rutkowski, D. T., Lingappa, V. R., and Hegde, R. S. (2001) *Proc. Natl. Acad. Sci. U. S. A.* **98,** 7823–7828
11. Kim, S. J., and Hegde, R. S. (2002) *Mol. Biol. Cell* **13,** 3775–3786
12. Hegde, R. S., Tremblay, P., Groth, D., DeArmond, S. J., Prusiner, S. B., and Lingappa, V. R. (1999) *Nature* **402,** 822–826
13. Stewart, R. S., Drisaldi, B., and Harris, D. A. (2001) *Mol. Biol. Cell* **12,** 881–889
14. Hegde, R. S., Voigt, S., and Lingappa, V. R. (1998) *Mol. Cell* **2,** 85–91
15. Fons, R. D., Bogert, B. A., and Hegde, R. S. (2003) *J. Cell Biol.* **160,** 529–539
16. Stewart, R. S., and Harris, D. A. (2001) *J. Biol. Chem.* **276,** 2212–2220
17. Chiesa, R., and Harris, D. A. (2001) *Neurobiol. Dis.* **8,** 743–763
18. Ma, J., Wollmann, R., and Lindquist, S. (2002) *Science* **298,** 1781–1785
19. Ma, J., and Lindquist, S. (2002) *Science* **298,** 1785–1788
20. Ma, J., and Lindquist, S. (2001) *Proc. Natl. Acad. Sci. U. S. A.* **98,** 14955–14960
21. Yedidia, Y., Horonchik, L., Tzaban, S., Yanai, A., and Taraboulos, A. (2001) *EMBO J.* **20,** 5383–5391
22. Drisaldi, B., Stewart, R. S., Adles, C., Stewart, L. R., Quaglio, E., Biasini, E., Fioriti, L., Chiesa, R., and Harris, D. A. (2003) *J. Biol. Chem.* **278,** 21732–21743
23. Quaglio, E., Chiesa, R., and Harris, D. A. (2001) *J. Biol. Chem.* **276,** 11432–11438
24. Vidugiriene, J., and Menon, A. K. (1995) *EMBO J.* **14,** 4686–4694
25. Bosque, P. J., and Prusiner, S. B. (2000) *J. Virol.* **74,** 4377–4386
26. Nishida, N., Harris, D. A., Vilette, D., Laude, H., Frobert, Y., Grassi, J., Casanova, D., Milhavet, O., and Lehmann, S. (2000) *J. Virol.* **74,** 320–325
27. Chiesa, R., Piccardo, P., Ghetti, B., and Harris, D. A. (1998) *Neuron* **21,** 1339–1351
28. Kascsak, R. J., Rubinstein, R., Merz, P. A., Tonna-DeMasi, M., Fersko, R., Carp, R. I., Wisniewski, H. M., and Diringer, H. (1987) *J. Virol.* **61,** 3688–3693
29. Zanusso, G., Liu, D., Ferrari, S., Hegyi, I., Yin, X., Aguzzi, A., Hornemann, S., Liemann, S., Glockshuber, R., Manson, J. C., Brown, P., Petersen, R. B., Gambetti, P., and Sy, M. S. (1998) *Proc. Natl. Acad. Sci. U. S. A.* **95,** 8812–8816
30. von Heijne, G. (1990) *J. Membr. Biol.* **115,** 195–201
31. Kim, S. J., Mitra, D., Salerno, J. R., and Hegde, R. S. (2002) *Dev. Cell* **2,** 207–217
32. Chiesa, R., Piccardo, P., Quaglio, E., Drisaldi, B., Si-Hoe, S. L., Takao, M., Ghetti, B., and Harris, D. A. (2003) *J. Virol.* **77,** 7611–7622

THE JOURNAL OF BIOLOGICAL CHEMISTRY
Vol. 278, No. 24, Issue of June 13, pp. 21732–21743, 2003
Printed in U.S.A.

Mutant PrP Is Delayed in Its Exit from the Endoplasmic Reticulum, but Neither Wild-type nor Mutant PrP Undergoes Retrotranslocation Prior to Proteasomal Degradation*

Received for publication, December 30, 2002, and in revised form, March 20, 2003
Published, JBC Papers in Press, March 26, 2003, DOI 10.1074/jbc.M213247200

Bettina Drisaldi‡§¶, Richard S. Stewart‡§, Cheryl Adles‡, Leanne R. Stewart‡, Elena Quaglio‡‖, Emiliano Biasini‖, Luana Fioriti‖, Roberto Chiesa‖‡‡, and David A. Harris‡§§**

From the ‡Department of Cell Biology and Physiology, Washington University School of Medicine, St. Louis, Missouri 63110 and the ‖Dulbecco Telethon Institute (DTI) and Department of Neuroscience, Istituto di Ricerche Farmacologiche "Mario Negri," Milano 20157, Italy

The cellular mechanisms by which prions cause neurological dysfunction are poorly understood. To address this issue, we have been using cultured cells to analyze the localization, biosynthesis, and metabolism of PrP molecules carrying mutations associated with familial prion diseases. We report here that mutant PrP molecules are delayed in their maturation to an endoglycosidase H-resistant form after biosynthetic labeling, suggesting that they are impaired in their exit from the endoplasmic reticulum (ER). However, we find that proteasome inhibitors have no effect on the maturation or turnover of either mutant or wild-type PrP molecules. Thus, in contrast to recent studies from other laboratories, our work indicates that PrP is not subject to retrotranslocation from the ER into the cytoplasm prior to degradation by the proteasome. We find that in transfected cells, but not in cultured neurons, proteasome inhibitors cause accumulation of an unglycosylated, signal peptide-bearing form of PrP on the cytoplasmic face of the ER membrane. Thus, under conditions of elevated expression, a small fraction of PrP chains is not translocated into the ER lumen during synthesis, and is rapidly degraded in the cytoplasm by the proteasome. Finally, we report a previously unappreciated artifact caused by treatment of cells with proteasome inhibitors: an increase in PrP mRNA level and synthetic rate when the protein is expressed from a vector containing a viral promoter. We suggest that this phenomenon may explain some of the dramatic effects of proteasome inhibitors observed in other studies. Our results clarify the role of the proteasome in the cell biology of PrP, and suggest reasonable hypotheses for the molecular pathology of inherited prion diseases.

Prion diseases, also called transmissible spongiform encephalopathies, are fatal neurodegenerative disorders that have attracted enormous scientific attention because they exemplify a novel mechanism of biological information transfer based on the transmission of protein conformation rather than on the inheritance of nucleic acid (1, 2). There is now considerable evidence that these diseases are caused by conformational conversion of PrP^{C},[1] a cell surface glycoprotein of uncertain function, into PrP^{Sc}, a β-rich and protease-resistant isoform that appears to be infectious in the absence of nucleic acid. This conversion can be catalyzed by exogenous PrP^{Sc} during infectious transmission, or can occur spontaneously in familial cases as a result of dominantly inherited, germline mutations in the gene encoding PrP (3). Point mutations in the C-terminal half of the PrP molecule are associated with Gerstmann-Sträussler syndrome, fatal familial insomnia, or familial forms of Creutzfeldt-Jakob disease. Insertional mutations, which produce a variable phenotype that can include features of both Creutzfeldt-Jakob disease and Gerstmann-Sträussler syndrome, consist of 1–9 additional copies of a peptide repeat that is normally present in 5 copies in the N-terminal half of the protein.

To understand how mutant PrP molecules cause neurological dysfunction in familial prion diseases, we have been analyzing the biochemical properties, metabolism, and cellular localization of these proteins in cultured cells. We and others have found that mutant PrPs expressed in several different cell types acquire biochemical properties that are reminiscent of PrP^{Sc} (4–10). These properties include partial resistance to protease digestion, insolubility in non-denaturing detergents, and resistance of the C-terminal glycolipid anchor to cleavage by phospholipase. Although the protease resistance of the mutant PrPs synthesized in cultured cells is quantitatively less than that of many strains of PrP^{Sc} from infected brain, it is likely that the cultured cells are reproducing key steps in the metabolism of mutant proteins that are relevant to the pathogenesis of familial prion diseases. Indeed, transgenic mice expressing a similar, weakly protease-resistant form of mutant PrP in their brains develop a fatal neurological illness with many similarities to human familial prion disorders (11, 12).

Several key results from our laboratory have identified the

* This work was supported by National Institutes of Health Grant NS35496 (to D. A. H.), National Research Service Award NS41500 (to R. S. S.), Telethon-Italy Grant TCP00083 (to R. C.), and European Community Grant QLG-CT-2001-2353 (to R. C.). The costs of publication of this article were defrayed in part by the payment of page charges. This article must therefore be hereby marked "*advertisement*" in accordance with 18 U.S.C. Section 1734 solely to indicate this fact.

§ Both authors contributed equally to this work.
¶ Current address: University of Toronto, Center for Research in Neurodegenerative Diseases, Tanz Neuroscience Bldg., 6 Queen's Park Crescent West, Toronto, Ontario M5S 3H2, Canada.
** Current address: Istituto di Ricerche Farmacologiche "Mario Negri," Via Eritrea 62, 20157 Milano, Italy.
‡‡ Assistant Telethon Scientist (DTI, Fondazione Telethon).
§§ To whom correspondence should be addressed: Dept. of Cell Biology and Physiology, Washington University School of Medicine, 660 S. Euclid Ave., St. Louis, MO 63110. Tel.: 314-362-4690; Fax: 314-747-0940; E-mail: dharris@cellbio.wustl.edu.

[1] The abbreviations used are: PrP^{C}, cellular isoform of PrP; PrP, prion protein; CHO, Chinese hamster ovary; endo H, endoglycosidase H; ER, endoplasmic reticulum; GPI, glycosylphosphatidylinositol; PBS, phosphate-buffered saline; PDI, protein-disulfide isomerase; PrP^{Sc}, scrapie isoform of PrP; PSI 1, proteasome inhibitor 1 (Z-Ile-Glu(OtBu)-Ala-Leu-al); RT, reverse transcriptase; SP, signal peptide; WT, wild-type; CMV, cytomegalovirus; BHK, baby hamster kidney.

endoplasmic reticulum (ER) as a critical cellular compartment in the metabolism of mutant PrP molecules. First, pulse-chase labeling experiments indicate that PrP molecules carrying pathogenic mutations first become phospholipase-resistant early in the secretory pathway, probably as a result of misfolding of the polypeptide chains during their synthesis in the ER (13, 14). Second, subcellular localization studies indicate that these same mutant PrP molecules accumulate in the ER and are expressed at reduced levels on the cell surface (15). Third, a mutant form of PrP, L9R/3AV, that is synthesized exclusively with a transmembrane topology is retained completely in the ER of cultured cells and is not detectably transported to the cell surface (16).

Interest in the role of the ER in PrP metabolism has been heightened recently by reports that both wild-type and mutant PrP molecules are recognized by the ER quality control machinery (17–19). It is well known that some membrane and secretory proteins, including several that are mutated in inherited human diseases, are recognized as abnormal soon after their synthesis as a result of misfolding of the polypeptide chain in the ER (20–22). These proteins are then transported backwards (retrotranslocated) through the translocon channel of the ER membrane into the cytoplasm, where they are degraded by the proteasome, often following conjugation to ubiquitin. The primary evidence for involvement of this pathway in the metabolism of PrP is the observation that treatment of cultured cells with proteasome inhibitors causes accumulation of an aggregated, unglycosylated form of PrP in the cytoplasm (17–19). It has also been reported that the cytosolic PrP found in inhibitor-treated cells displays properties of PrP^{Sc}, including protease resistance and the ability to sustain conversion of newly synthesized PrP^{C} to a PrP^{Sc} form (18). Finally, artificial expression of PrP in the cytoplasm using a PrP construct lacking the N-terminal signal sequence was found to be toxic to cultured cells, and resulted in a neurodegenerative phenotype in transgenic mice (23). On the basis of these results, the hypothesis has been advanced that mislocalization of PrP in the cytoplasm may be a general mechanism underlying the spontaneous formation of infectious PrP^{Sc}, as well as the pathogenesis of prion diseases (23). In addition, it has been cautioned that the therapeutic use of proteasome inhibitors in clinical settings may increase the risk for development of prion disease (23).

In the present paper, we have undertaken a detailed analysis of the metabolism of wild-type and mutant PrP molecules in cultured cells, and the effect of proteasome inhibitors on the turnover of these proteins. We find that mutant PrP molecules are delayed in their biosynthetic maturation, and exit the ER more slowly than wild-type molecules. In contrast to recent reports, however, we find that neither wild-type nor mutant PrP proteins are major substrates for retrotranslocation and proteasomal degradation. We observe that a small percentage of PrP chains is inefficiently translocated when the protein is expressed at high levels in transfected cells, and these chains are degraded by the proteasome without entering the ER lumen. We also suggest that some of the dramatic effects of proteasome inhibitors observed in previous studies are due to artifactual increases in PrP mRNA levels and protein synthetic rate, rather than to reduction in the catalytic activity of the proteasome. The work presented here clarifies an important current issue in the cell biology of PrP, and suggests reasonable hypotheses for the molecular pathology of prion diseases.

EXPERIMENTAL PROCEDURES

Cells—All expression constructs used in this paper carried a CMV promoter to drive synthesis of PrP in transfected cells. Stably transfected lines of CHO and PC12 cells expressing WT, PG14, or D177N-Met^{128} murine PrP from a pBC12 vector have been described previously (4, 5, 7, 24). The WT and PG14 proteins in these lines carried an epitope tag for the antibody 3F4. Plasmids containing the coding sequences for murine WT, PG14, or D177N-Met^{128} PrP (all 3F4 epitope-tagged) in the vector pcDNA3 (Invitrogen Corp., Carlsbad, CA) were transiently transfected into CHO or BHK cells using LipofectAMINE (Invitrogen) according to the manufacturer's directions. Cells were used 24 h after transient transfection. CHO and BHK cells were maintained in α-minimal essential medium supplemented with 10% fetal calf serum, nonessential amino acids, and penicillin/streptomycin. PC12 cells were grown in Dulbecco's modified Eagle's medium supplemented with 10% horse serum, 5% fetal calf serum, and penicillin/streptomycin.

Cultures of granule cells were prepared from the cerebella of Tg(WT-E1), Tg(PG14-A2), or Tg(PG14-A3) mice (12) at postnatal days 3–6 according to the procedure of Miller and Johnson (25). Briefly, cerebella were dissected, sliced into ~1-mm pieces and incubated at 37 °C for 15 min in Hanks' balanced salt solution containing 0.3 mg/ml trypsin. Trypsin inhibitor was added to a final concentration of 0.5 mg/ml, and the tissue was mechanically dissociated by passing through a flame-polished Pasteur pipette. Cells were plated at 200,000–500,000 cells/cm^2 on plates coated with poly-L-lysine (0.1 mg/ml). Cells were maintained in basal Eagle's medium supplemented with 10% dialyzed fetal bovine serum, penicillin/streptomycin, and KCl (25 mM). Cultures were used 4–7 days after plating. To reduce the number of non-neuronal cells in those cultures maintained for longer than 5 days, aphidicolin (3.3 mg/ml) was added to the medium 36 h after plating. Non-neuronal contamination of the cultures was assessed as described (25), and found to be less than 3%.

Proteasome Inhibitors—PSI 1 was purchased from Calbiochem (La Jolla, CA) and was prepared as a stock solution in ethanol at 10 mM. MG132 was obtained from Sigma, and was prepared as a stock solution in Me_2SO at 10 mM. Control cell cultures were exposed to the vehicle only.

Antibodies—Monoclonal antibodies 3F4 (26) and 8H4 (27), and polyclonal antibody P45-66 (4) against PrP have been described previously. 3F4 was used to recognize transfected murine PrP in all immunoprecipitations and Western blots, except those involving stably transfected CHO cells expressing D177N PrP, in which P45-66 was used because the construct was not epitope-tagged. 8H4 was used for one of the Western blots shown in Fig. 5*A* to recognize both transfected murine PrP and endogenous rat PrP in PC12 cells.

An antibody (anti-SP) that selectively recognizes forms of murine PrP containing an uncleaved signal peptide was generated by immunizing rabbits with a synthetic peptide (TMWTDVGLCKKRPK; amino acids 14–27) that spans the signal peptide cleavage site at residues 22/23. The peptide was conjugated to keyhole limpet hemocyanin. This antibody shows no reactivity toward PrP molecules lacking the signal peptide, and its reactivity is completely blocked by incubation with the peptide immunogen. Detailed characterization of this antibody will be presented elsewhere.[2] For immunofluorescence staining, the antibody was affinity-purified using immobilized peptide immunogen.

A monoclonal antibody to protein-disulfide isomerase (PDI) was obtained from Stressgen Biotechnologies Corp. (Victoria, British Columbia). Alexa 594-conjugated goat anti-mouse and Alexa 488-conjugated goat anti-rabbit IgGs were from Molecular Probes, Inc. (Eugene, OR). Anti-ubiquitin monoclonal antibody MAB1510 was purchased from Chemicon International (Temecula, CA).

Pulse-Chase Labeling and Immunoprecipitation—Cells were incubated for 30 min in methionine- and cysteine-free medium prior to pulse labeling in the same medium containing 250–750 μCi/ml [^{35}S]methionine (Promix; Amersham Biosciences). After washing, cells were chased in regular medium containing unlabeled methionine and cysteine for the indicated times. In some experiments, cycloheximide (100 μg/ml) was included in the chase medium to block completion of polypeptide chains that had been initiated but not completed during the pulse period (28). At the end of the chase period, cells were lysed in 0.5% SDS, 50 mM Tris-HCl (pH 7.5) containing protease inhibitors (pepstatin and leupeptin, 1 μg/ml; phenylmethylsulfonyl fluoride, 0.5 mM; EDTA, 2 mM). The lysates were heated at 95 °C for 5 min and then diluted 5-fold with 0.5% Triton X-100, 50 mM Tris-HCl (pH 7.5) containing protease inhibitors. PrP was then immunoprecipitated using the appropriate anti-PrP antibody and protein A-Sepharose beads, and analyzed by SDS-PAGE and autoradiography. In some cases, immunoprecipitated PrP was eluted from protein A-Sepharose beads at 95 °C using 0.2% SDS, 50 mM Tris-HCl (pH 7.5), and subjected to treatment with

[2] R. S. Stewart and D. A. Harris, manuscript in preparation.

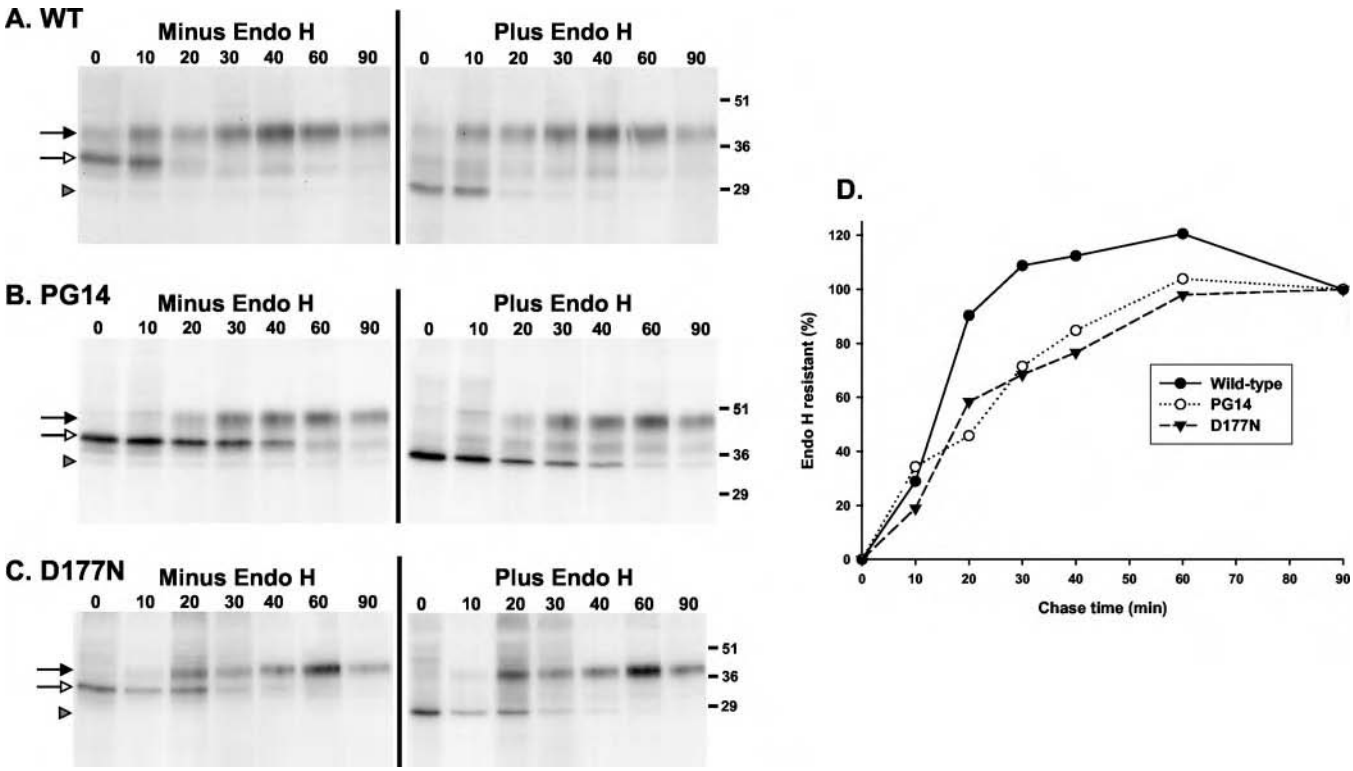

FIG. 1. **Biosynthetic maturation of mutant PrP to an endo H-resistant form in CHO cells is delayed.** Stably transfected CHO cells expressing WT PrP (*A*), PG14 PrP (*B*), or D177N PrP (*C*) were pulse-labeled with [^{35}S]methionine for 20 min, and then chased in medium containing unlabeled methionine for 0, 10, 20, 30, 40, 60, or 90 min. Cells were then lysed, and PrP was isolated by immunoprecipitation. Half of the immunoprecipitated PrP was treated with endo H (*gels* on the *right*) and half was left untreated (*gels* on the *left*) prior to analysis by SDS-PAGE and autoradiography. The *black* and *white arrows* and the *shaded arrowhead* indicate, respectively, the positions of mature (endo H-resistant), immature (endo H-sensitive), and unglycosylated PrP. Molecular mass markers are given in kilodaltons. *D*, the percentage of endo H-resistant PrP at each chase time was calculated from PhosphorImager analysis of the gels shown in *panels A–C*, using the formula $\{1 - [(X\text{-}Y)/T]\} \times 100$, where X = amount of unglycosylated PrP after treatment with endo H; Y = amount of unglycosylated PrP without endo H treatment; T = total PrP. Values were scaled to 0 and 100% endo H-resistance at 0 and 90 min, respectively, to correct for the efficiency of endo H cleavage. The results are representative of five independent experiments.

endoglycosidase H (New England Biolabs, Beverly, MA) for 1 h at 37 °C. The radioactivity in PrP bands on gels was quantitated using a PhosphorImager SI or Storm 860 (Molecular Dynamics, Sunnyvale, CA). Background values measured in a region of the image that did not lie within the protein lanes were subtracted from each determination.

Western Blots, Northern Blots, and Reverse Transcriptase-PCR (RT-PCR)—Western blots were performed as described previously (29). Films exposed using ECL were quantitated with SigmaScan Pro 5.0 (SPSS Science, Chicago, IL).

Total RNA was prepared using the RNAWiz kit (Ambion Inc., Austin, TX). Northern blot analysis was performed using the Gene Images CDP-Star chemiluminescent detection system (Amersham Biosciences). A 485-bp *Kpn*I segment from the 3′ end of the mouse PrP coding region was used as a probe. Under the hybridization conditions used in Fig. 5*C*, this probe cross-reacts with rat PrP mRNA.

RT-PCR was performed using the TITANIUM one-step RT-PCR kit (Clontech, Palo Alto, CA). PrP primers (specific for mouse PrP mRNA) were as follows: sense, 5′-GGACCGCTACTACCGTGAAAAC-3′; antisense, 5′-TGGCCTGTAGTACACTTGGTTAGG-3′. Mouse β-actin primers were supplied by the manufacturer and were included in the same reaction to serve as an internal standard. Control reactions in which the RT was inactivated by heating at 95 °C for 10 min showed no amplified bands. Aliquots were removed from the amplification reaction after 12, 16, and 20 cycles, and were analyzed by electrophoresis on 8% acrylamide/TBE gels followed by staining with SYBR Green I (Molecular Probes). Quantification of band intensities was performed on a Storm 860.

Topology and Detergent Insolubility Assays—For determining the membrane topology of PrP, cells were lysed in 0.25 M sucrose, 10 mM HEPES (pH 7.4) by 10 passages through 27-gauge needles connected to 0.3-mm silastic tubing. After centrifugation at 2,300 × *g* for 2 min, the postnuclear supernatant was aliquoted into three tubes. One sample was left untreated; the second was digested with 250 μg/ml proteinase K for 30 min at 22 °C in 50 mM Tris-HCl (pH 7.5); and the third was digested with proteinase K in the presence of 0.5% Triton X-100 to solubilize membranes. Samples were precipitated with methanol and PrP was analyzed by Western blotting.

To assay detergent insolubility, cells were lysed for 10 min on ice in 0.5% Triton X-100, 0.5% sodium deoxycholate, 50 mM Tris-HCl (pH 7.5). After debris was removed by centrifugation at 16,000 × *g* for 10 min, the supernatant was centrifuged in a TLA 55 rotor at 186,000 × *g* for 40 min. Proteins in the supernatant were precipitated with methanol, and PrP in the supernatant and pellet fractions was analyzed by Western blotting.

Immunofluorescence Staining—CHO cells plated on glass coverslips were fixed for 30 min in PBS containing 4% paraformaldehyde and 5% sucrose, and were then permeabilized for 10 min in PBS containing 0.05% Triton X-100. Cells were subsequently incubated at room temperature as follows: 30 min in PBS containing 2% goat serum (blocking buffer), 60 min with primary antibodies (anti-SP and anti-PDI) in blocking buffer, 15 min in blocking buffer, 60 min with Alexa-conjugated secondary antibodies in blocking buffer. Coverslips were mounted in 50% glycerol/PBS, and cells were visualized by laser-scanning confocal microscopy using a Zeiss LSM-510 microscope.

RESULTS

Maturation of Mutant PrP Molecules Is Delayed—We used pulse-chase labeling to analyze the maturation of newly synthesized PrP molecules in stably transfected CHO cells. We observed that WT PrP migrated as a major 33-kDa species immediately after pulse labeling (Fig. 1*A*, *left panel*). A 38-kDa form, which was barely visible at the end of the pulse period, increased in amount during the first 10 min of chase, and became the predominant species by 20 min. The 38-kDa form subsequently decayed with a half-life of ~3 h (see Fig. 3*A*). The 33-kDa species was shifted to a 25-kDa unglycosylated form after digestion with endoglycosidase H (endo H) (Fig. 1*A*, *right panel*). This shift indicates that the 33-kDa band represents

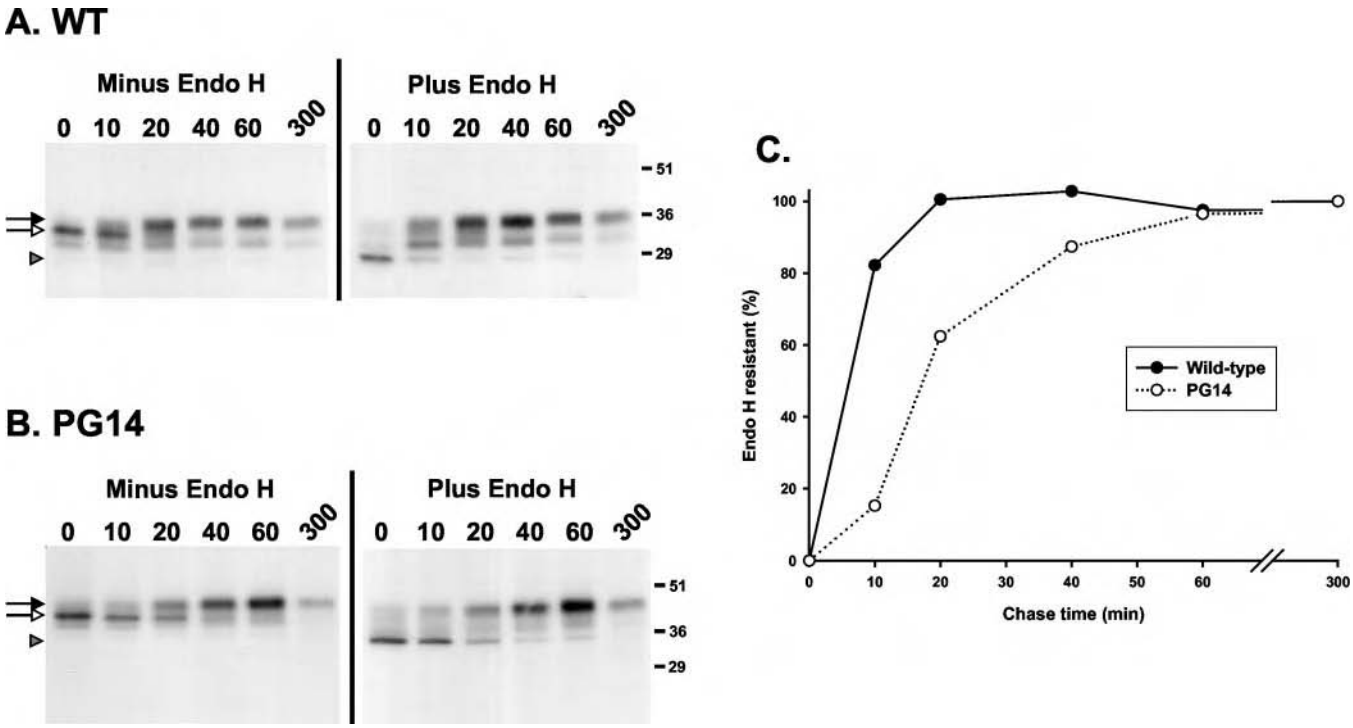

FIG. 2. **Biosynthetic maturation of PG14 PrP to an endo H-resistant form in neurons is delayed.** Cerebellar granule neurons cultured from transgenic mice expressing WT PrP (*A*) or PG14 (*B*) PrP were pulse-labeled with [^{35}S]methionine for 20 min, and then chased in medium containing unlabeled methionine for 0, 10, 20, 40, 60, or 300 min. Cells were then lysed, and PrP was isolated by immunoprecipitation. Half of the immunoprecipitated PrP was treated with endo H (*gels* on the *right*) and half was left untreated (*gels* on the *left*) prior to analysis by SDS-PAGE and autoradiography. The *black* and *white arrows* and the *shaded arrowhead* indicate the positions, respectively, of mature (endo H-resistant), immature (endo H-sensitive), and unglycosylated PrP. *C*, the percentage of endo H-resistant PrP at each chase time was calculated from PhosphorImager analysis of the gels shown in *panels A* and *B*, using the formula given in the legend to Fig. 1*D*. The results are representative of two independent experiments.

immature, core-glycosylated molecules that had not yet transited beyond the mid-Golgi. In contrast, the 38-kDa form was resistant to endo H digestion, and thus represents mature, complex-glycosylated chains that have moved beyond the mid-Golgi to later compartments in the secretory pathway. In addition to the 38-kDa form, which is presumably glycosylated on both asparagine consensus sites, trace amounts of mature, singly glycosylated PrP (~32 kDa) can also be seen throughout the chase period. Quantitation of the bands revealed that a maximum of ~50–60% of radioactivity initially incorporated into the 33-kDa precursor during the pulse was eventually recovered in the mature, 38-kDa form. Thus, maturation of WT PrP molecules in CHO cells is rapid and efficient.

The maturation of PrP molecules carrying either of two pathogenic mutations was noticeably slower. PG14 is our designation for a nine-octapeptide insertion that is associated with a mixed phenotype in human beings having characteristics of both Creutzfeldt-Jakob disease and Gerstmann-Sträussler syndrome (12). PG14 PrP is initially synthesized as a 36-kDa form that matures into a 50-kDa species during the chase period (Fig. 1*B*, *left panel*). The 36-kDa form is shifted by digestion with endo H, confirming that it represents a core-glycosylated precursor, whereas the 50-kDa form is endo H-resistant (Fig. 1*B*, *right panel*). Whereas the endo H-sensitive precursor of WT PrP has largely disappeared by 20 min of chase, the endo H-sensitive precursor of PG14 PrP is still present at 40 min of chase. Delayed maturation was also observed for PrP molecules carrying a second mutation, D177N/Met^{128}, which is linked to fatal familial insomnia (30) (Fig. 1*C*). In this case, the endo H-sensitive precursor (33 kDa) was still present after 20–30 min of chase.

The slower maturation of the two mutant PrPs in comparison with WT PrP is clear from Fig. 1*D*, which plots the percentage of endo H-resistant PrP at different chase times. Of note, there was no appreciable difference between WT and mutant PrPs in the maximum amount of initial label that was chased into the endo H-resistant form (~50–60%), and in the half-life of this form (3–5 h; see Fig. 3, *A–C*). Thus, mutant PrP molecules mature more slowly than WT PrP molecules in CHO cells, but the overall efficiency of maturation and the stability of the final product are similar for both types of PrP. We have seen a similar phenomenon when WT and PG14 PrPs are expressed in transiently transfected BHK cells (not shown).

To confirm that these observations held true for PrP molecules synthesized in neurons, we carried out pulse-chase labeling experiments on cerebellar granule cells cultured from transgenic mice expressing WT and PG14 PrP (12). We observed that WT PrP was fully endo H-resistant by 10–20 min of chase, whereas PG14 PrP required 40 min to become completely endo H-resistant (Fig. 2, *A* and *B*). The delayed maturation of PG14 PrP is apparent when the percentage of endo H-resistant protein is quantitated (Fig. 2*C*). Despite this difference in the kinetics of maturation, there was no significant difference between WT and PG14 PrP in the maximum amount of initial label that was chased into the endo H-resistant form (~60–70%). These results demonstrate that the slower maturation of PG14 PrP compared with WT PrP is seen in neurons as well as in CHO and BHK cells.

Proteasome Inhibitors Do Not Alter the Turnover or Maturation of PrP—The pulse-chase data, combined with our previous morphological results (15), suggested that mutant PrP molecules are delayed in their transit along the early parts of the secretory pathway, probably including the ER. Because proteins retained in the ER are often rapidly degraded by the proteasome after retrotranslocation into the cytoplasm (20, 21), we wondered whether this degradative process might operate

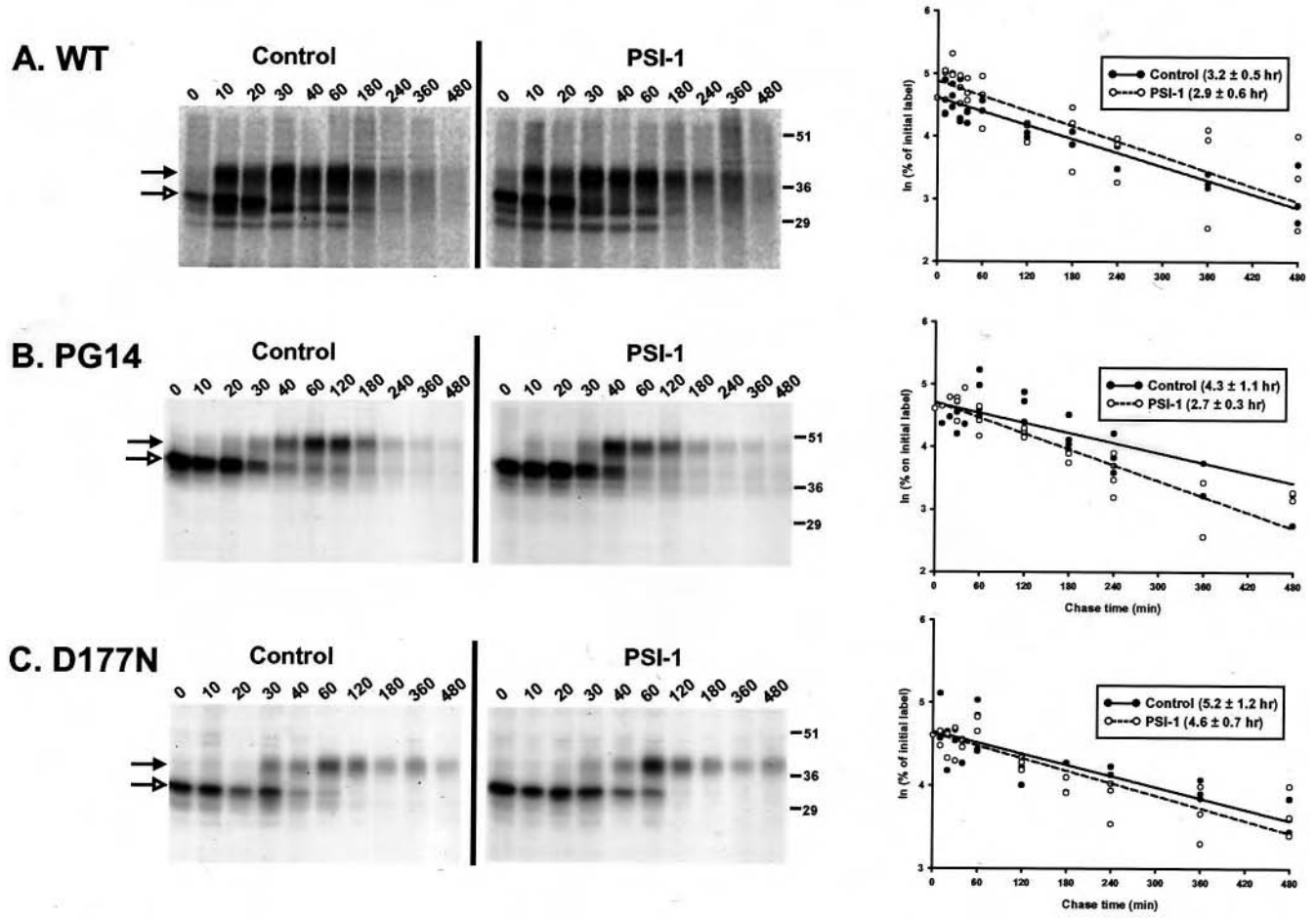

FIG. 3. **Proteasome inhibition does not alter the half-lives of WT or mutant PrPs.** Stably transfected CHO cells expressing WT PrP (*A*), PG14 PrP (*B*), or D177N PrP (*C*) were pulse-labeled with [^{35}S]methionine for 20 min, and then chased in medium containing unlabeled methionine for the indicated times (in min). In one set of cultures (*gels* on the *right*), PSI-1 (20 μM) was present during a 30-min preincubation, as well as during the pulse and chase periods. In the other set of cultures (*gels* on the *left*), an equivalent amount of ethanol vehicle was present. At the end of the chase period, cells were lysed, and PrP was isolated by immunoprecipitation and analyzed by SDS-PAGE and autoradiography. The *black* and *white arrows* indicate the positions, respectively, of mature (endo H-resistant) and immature (endo H-sensitive) PrP. The *graphs* show semi-logarithmic plots of the percentage of initial label present in both PrP bands (mature + immature) at each chase time. Each *circle* represents an independent experiment. The *lines* were fitted by least-squares analysis to obtain the half-life ± S.E.

on mutant PrP molecules during their protracted residence in the ER. We therefore repeated the pulse-chase labeling experiments on CHO cells in the presence and absence of PSI 1 (Z-Ile-Glu(OtBu)-Ala-Leu-al), a peptide aldehyde that reversibly inhibits the chymotryptic activity of the proteasome. We observed that, in the absence of inhibitor, WT, PG14, and D177N PrP molecules had similar half-lives, ranging from 3 to 5 h (Fig. 3, *A–C*). PSI 1 did not significantly prolong these half-lives (Fig. 3, *A–C*). In addition, the inhibitor did not affect the kinetics with which the core-glycosylated precursor of each protein was converted to the mature form, and did not change the maximal percentage of the initial label that was chased into the mature form (~50–60%). We know that PSI 1 was active in these experiments, based on accumulation of high molecular mass ubiquitin-protein conjugates detected on Western blots with an anti-ubiquitin antibody (data not shown). Results similar to those shown in Fig. 3 were obtained using lactacystin, an inhibitor that irreversibly blocks all three catalytic activities of the proteasome (data not shown). We conclude from these data that, although mutant PrP molecules are delayed in their exit from the ER, the majority of them are not substrates for proteasomal degradation following retrotranslocation. Our results do not rule out the possibility that a minority of PrP molecules are degraded by the latter pathway, because in this case a small effect of proteasome inhibitors on PrP half-life might be difficult to detect.

Long Term Treatment of Transfected Cells with Proteasome Inhibitors Artifactually Increases PrP mRNA and Synthetic Rate—Despite the fact that the inhibitor had no effect on PrP metabolism in pulse-chase experiments on CHO cells (Fig. 3), we found that it significantly increased the amount of both WT and mutant PrP observable by Western blotting of these cells (Fig. 4*A*). This effect was observable after 8 h of treatment, and was very dramatic after 18 h. In most cases, PSI 1 increased the amount of both glycosylated and unglycosylated PrP (Fig. 4*A*, *PG14* and *D177N*), although in some cell clones the major species that accumulated was an unglycosylated form (Fig. 4*A*, *WT*). The glycosylated forms that accumulated in response to PSI 1 were resistant to endo H digestion (data not shown). The latter result was particularly surprising, because it seemed to imply that the proteasome was involved in degradation of fully mature PrP molecules that had already left the ER. Similar results were obtained with lactacystin (data not shown).

We suspected that some of these changes were because of secondary effects of PSI 1 that increased the synthetic rate of the protein, rather than to inhibition of the catalytic activity of the proteasome. This suspicion was confirmed by two lines of evidence. First, reverse transcriptase-PCR analysis (Fig. 4*B*) and Northern blot analysis (data not shown) demonstrated that long term exposure of CHO cells to PSI 1 significantly in-

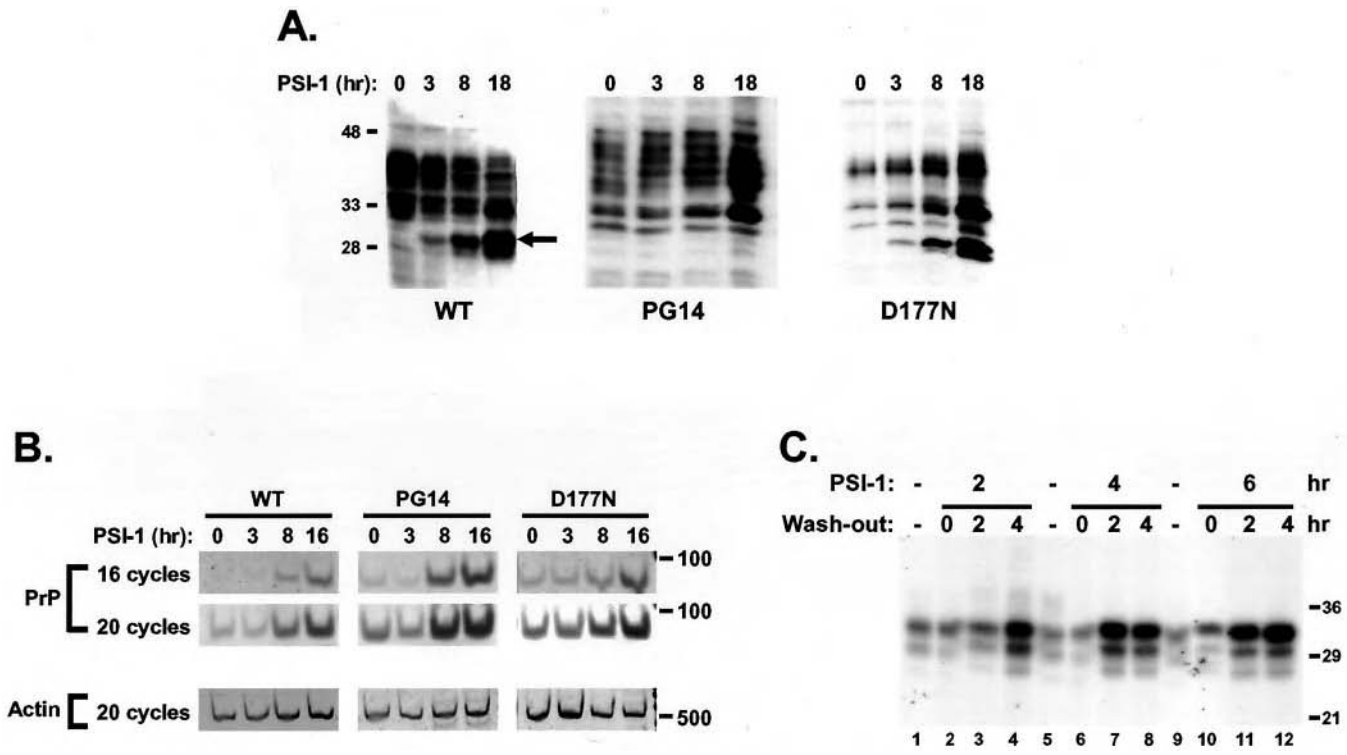

FIG. 4. **Long term treatment of CHO cells with a proteasome inhibitor increases PrP protein, mRNA, and synthetic rate.** *A*, stably transfected CHO cells expressing WT, PG14, and D177N PrPs were treated with PSI 1 (20 μM) for the indicated times. Cells were then lysed, and PrP analyzed by Western blotting. The *arrow* points to an unglycosylated form of WT PrP that is increased by PSI 1 treatment. *B*, the same cell lines used in *A* were treated with PSI 1 for the indicated times, and then PrP and β-actin mRNA were analyzed by RT-PCR. Samples were removed after 16 and 20 cycles of amplification to assess saturation of the signal. Size markers are in nucleotides. *C*, stably transfected CHO cells expressing WT PrP were either treated with ethanol vehicle for 10 h (*lanes 1*, *5*, and *9*), or were incubated with PSI 1 for 2 (*lanes 2–4*), 4 (*lanes 6–8*), or 6 h (*lanes 10–12*). At the end of the PSI 1 incubation, cells were either analyzed immediately (*lanes 2*, *6*, and *10*), or were transferred to inhibitor-free medium for 2 (*lanes 3*, *7*, and *11*) or 4 h (*lanes 4*, *8*, and *12*). At the end of all incubations, cells were pulse-labeled with [^{35}S]methionine for 20 min, after which PrP was immunoprecipitated and analyzed by SDS-PAGE and autoradiography. Autoradiographic analysis of lysates prior to immunoprecipitation revealed equal incorporation of [^{35}S]methionine into total cellular proteins in all samples (not shown).

creased PrP mRNA levels. This effect varied among independent clones of transfected cells, with some clones showing as much as a 10-fold increase in PrP mRNA after overnight treatment with PSI 1. Second, PSI 1 increased the PrP synthetic rate, as measured by the amount of [^{35}S]methionine incorporated in a 20-min pulse (Fig. 4*C*). Remarkably, treatment of cells with PSI 1 for as little as 2 h caused a progressive increase in PrP synthesis 2–4 h after the inhibitor had been removed (Fig. 4*C*, *lanes 4*, *7*, *8*, *11*, and *12*). These effects were not seen in the pulse-chase studies shown in Fig. 3, because in those experiments the cells had been treated with PSI 1 for only 30 min at the time of pulse labeling, a time that would be too short to cause an increase in PrP synthesis.

Proteasome inhibitors also increased PrP protein and mRNA in stably transfected lines of PC12 cells that express WT or PG14 PrP. Fig. 5 shows the effect of the peptide aldehyde inhibitor MG132 (Z-Leu-Leu-Leu-al), and similar results were seen with ALLN (Ac-Leu-Leu-NorLeu-al) and lactacystin (data not shown). An increase in PrP mRNA was first apparent between 2 and 4 h (Fig. 5, *C*, *lanes 6–15*, and *D*), and an increase in PrP protein by 4–8 h (Fig. 5*A*, *top* and *middle panels*, *lanes 6–15,* and *B*). We noted that MG132 did not have any effect on the levels of endogenous rat PrP (detected with 8H4 antibody) or its mRNA, as assayed in control PC12 cells that had been transfected with the empty expression vector lacking the murine PrP insert (Fig. 5, *A* and *C*, *lanes 1–5*, and *B* and *D*). This result suggested that the inhibitor might be selectively altering transcription from expression constructs carrying a heterologous promoter (CMV in this case).

A Small Percentage of PrP Molecules Is Degraded by the Proteasome before Translocation into the ER—To minimize these artifactual effects on PrP mRNA levels and synthetic rate, we restricted treatments with proteasome inhibitors to 8 h or less, and also utilized pools of transiently transfected cells to avoid the clonal variation seen with stably transfected lines. Under these circumstances, the primary effect of PSI 1 was to cause the accumulation of a PrP species that was ~2 kDa larger than the corresponding mature, unglycosylated form (27 kDa for WT and D177N PrP and 33 kDa for PG14 PrP) (Fig. 6, *lanes 2*, *6*, and *10*). The inhibitor-induced bands were not shifted by digestion with either endo H or PNGase F, and were also produced after PSI 1 treatment of cells synthesizing a form of PrP (T182A/T198A) in which both consensus sites for *N*-glycosylation had been mutated (data not shown). These results indicated that the PSI 1-induced species were not alternate glycoforms of PrP. In addition, we found that migration of the 27/33-kDa bands did not shift after treatment with phosphatidylinositol-specific phospholipase C (not shown), indicating that they most likely lacked a C-terminal GPI anchor.

To explain why the 27/33-kDa bands induced by PSI 1 were slightly larger in size than mature, unglycosylated PrP, we hypothesized that they contained an intact signal peptide. To directly test this hypothesis, we reacted Western blots with an antibody (anti-SP) that specifically recognizes the PrP signal peptide. We found that the 27/33-kDa bands were selectively labeled with this antibody (Fig. 6, *lanes 4*, *8*, and *12*). Thus, these bands represent unprocessed forms of PrP that are not glycosylated and from which the signal peptide has not been removed. The fact that these forms accumulate in the presence of PSI 1 indicates that they are normally degraded by the

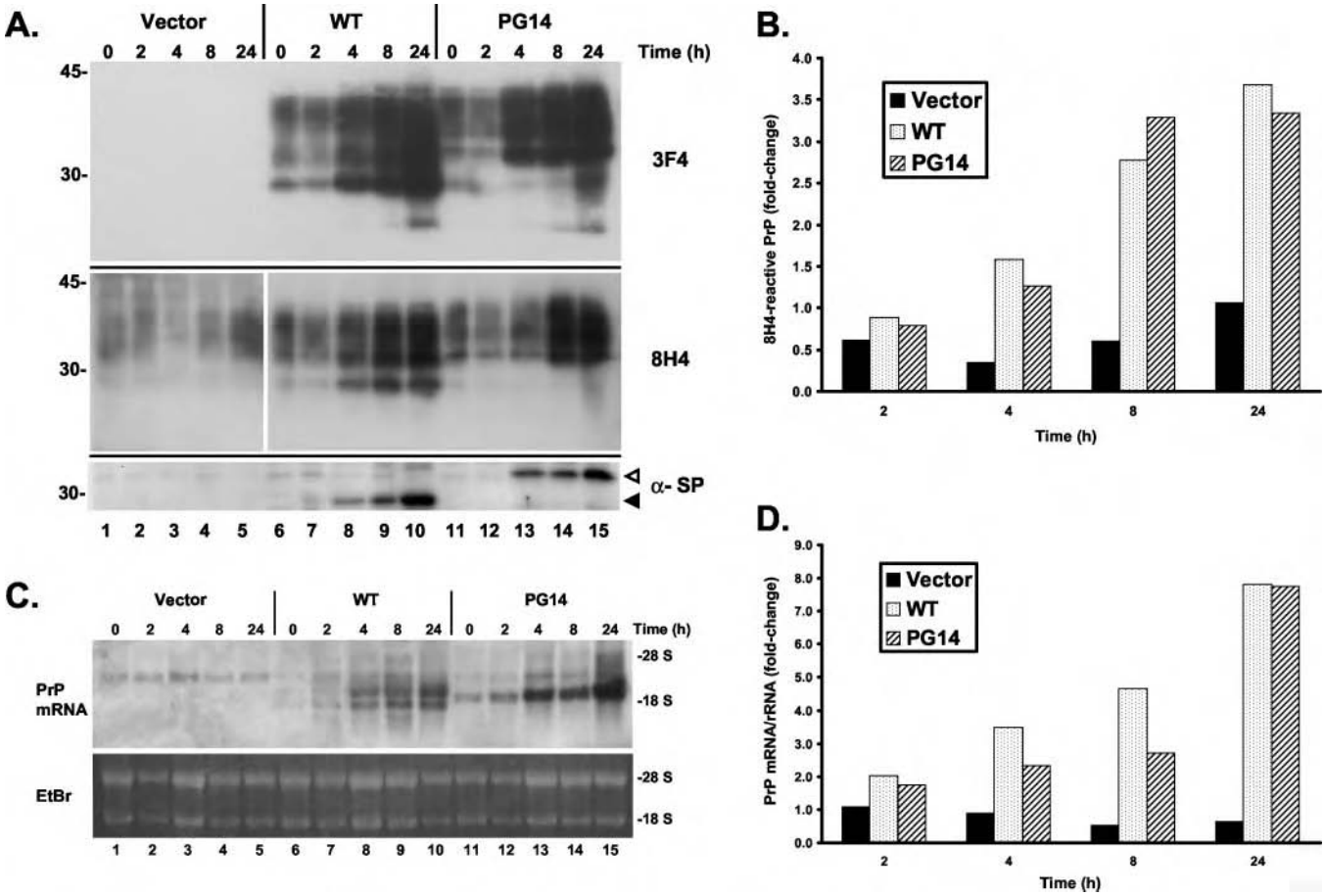

FIG. 5. **Long term treatment of PC12 cells with a proteasome inhibitor increases PrP protein and mRNA.** *A*, PC12 cells stably transfected with the empty expression vector (*lanes 1–5*), or with the vector encoding WT murine PrP (*lanes 6–10*) or PG14 murine PrP (*lanes 11–15*) were exposed to MG132 (10 μM) for the indicated times. Cells were then lysed, and PrP analyzed by Western blotting using either 3F4 antibody (*top panel*) that detects only epitopically tagged murine PrP; 8H4 antibody (*middle panel*) that detects both murine PrP and endogenous rat PrP; or anti-SP antibody (*bottom panel*) that detects signal peptide-bearing forms of murine PrP. For the 8H4 blot, a longer exposure is shown for *lanes 1–5* than for the other lanes. The *black* and *white arrowheads* to the *right* of the *bottom panel* indicate the positions, respectively, of WT and PG14 PrP containing an uncleaved signal peptide. *B*, the PrP signals from the 8H4 blot shown in *A* were quantitated, and expressed relative to the amount of PrP at 0 h of inhibitor treatment. *C*, total RNA was extracted from PC12 cells treated with MG132 as in *A*, and murine and rat PrP mRNA levels were analyzed by Northern blotting (*top panel*). The EtBr-stained gel in the *bottom panel* demonstrates approximately equal loading of all lanes. Size markers are 18 S and 28 S rRNA. *D*, PrP mRNA and EtBr signals from *C* were quantitated, and the ratio of PrP mRNA/rRNA at each time point was expressed relative to the ratio at 0 h of inhibitor treatment.

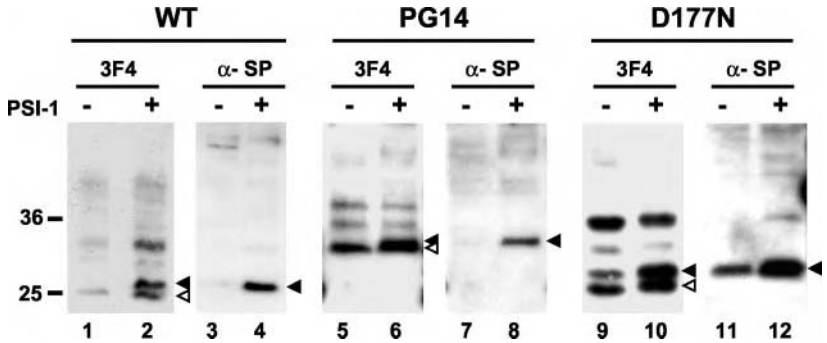

FIG. 6. **An unglycosylated, signal peptide-bearing form of PrP accumulates after treatment of CHO cells with a proteasome inhibitor.** Transiently transfected CHO cells expressing WT, PG14, or D177N PrPs were treated for 8 h with either ethanol vehicle (− *lanes*) or with PSI 1 (20 μM) (+ *lanes*). Cells were then lysed and PrP analyzed by Western blotting using either 3F4 antibody or anti-signal peptide antibody (*α-SP*). The *white* and *black arrowheads* indicate the positions, respectively, of processed (signal peptide-cleaved) and unprocessed (signal peptide-bearing) forms of unglycosylated PrP. These two species are not completely resolved for PG14 PrP, because of the higher M_r of this protein. The slightly faster migration of all bands in *lane 9* compared with those in *lane 10* is an artifact of gel smiling. Transiently transfected cells produce less doubly glycosylated PrP than stably transfected cells, accounting for the difference in the pattern of PrP bands between this figure and Fig. 4*A*.

proteasome. We noted that small amounts of the signal peptide-containing forms were sometimes detectable even in the absence of PSI 1 (Fig. 6, *lanes 9* and *11*). This phenomenon appeared to correlate with the level of PrP expression in a particular transfection experiment, rather than with the PrP sequence being expressed (data not shown). Accumulation of unglycosylated, signal peptide-containing forms of WT and PG14 PrP was also observed after proteasome inhibitor treat-

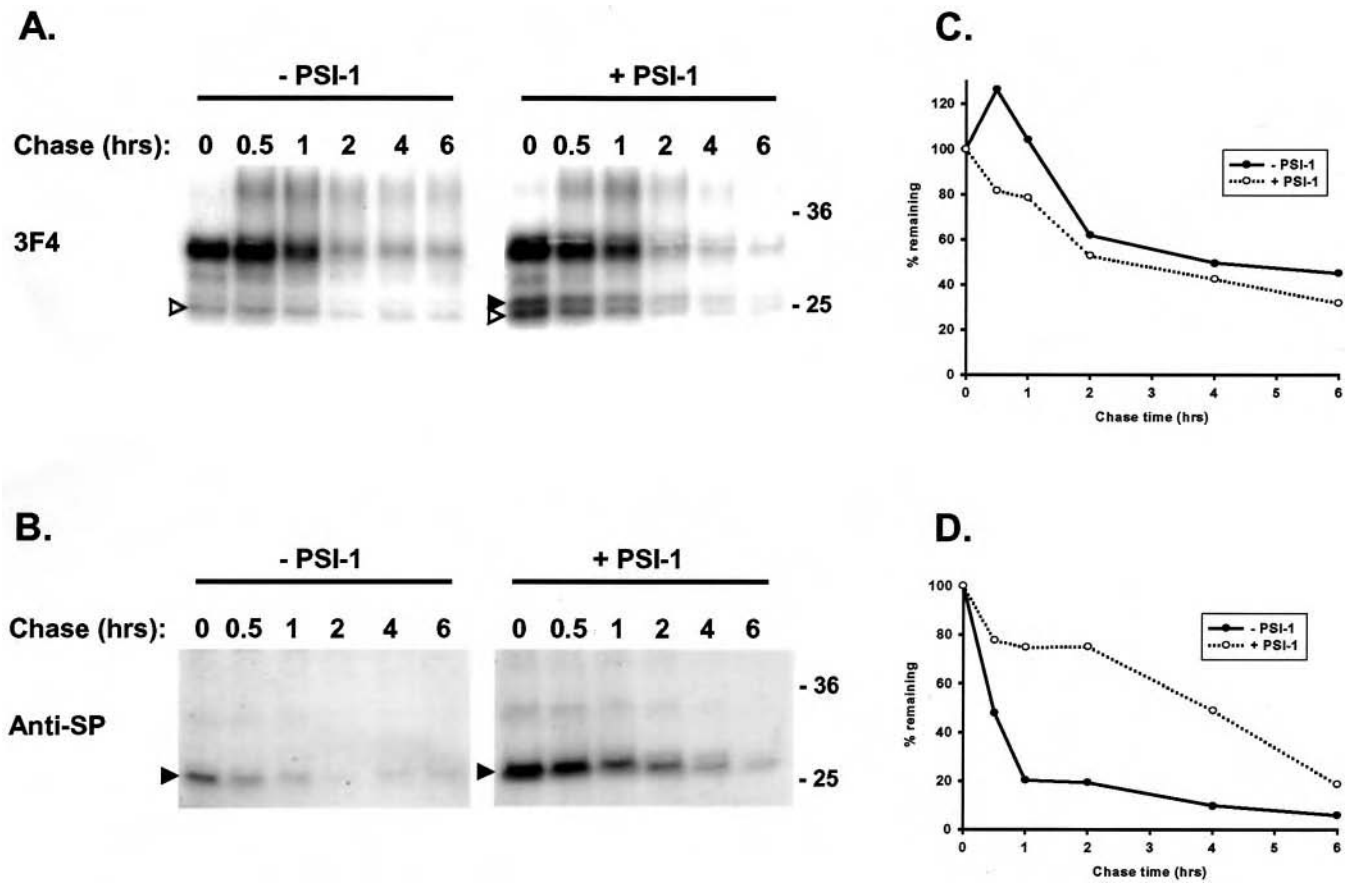

FIG. 7. **The signal peptide-bearing form of PrP has a short metabolic half-life, and is stabilized in the presence of a proteasome inhibitor.** *A* and *B*, transiently transfected CHO cells expressing WT PrP were pulse-labeled with [^{35}S]methionine for 20 min, and then chased in medium containing unlabeled methionine for 0, 0.5, 1, 2, 4, or 6 h. In one set of cultures (*gels* on the *right*), PSI-1 (20 μM) was present during a 30-min preincubation, as well as during the pulse and chase periods. In the other set of cultures (*gels* on the *left*), an equivalent amount of ethanol vehicle was present. At the end of the chase period, cells were lysed, and PrP was immunoprecipitated using either (*A*) 3F4 or (*B*) anti-SP antibodies, and analyzed by SDS-PAGE and autoradiography. The *white* and *black arrowheads* indicate the positions, respectively, of processed (signal peptide-cleaved) and unprocessed (signal peptide-bearing) forms of unglycosylated PrP. *C*, the amount of label in all PrP bands (unglycosylated + glycosylated) was calculated at each chase time as a percentage of the initial label, based on PhosphorImager analysis of the gels shown in *A*. The results are representative of two independent experiments. *D*, the amount of label in the signal peptide-bearing PrP band was calculated at each chase time as a percentage of the initial label, based on PhosphorImager analysis of the gels shown in *B*. The results are representative of two independent experiments.

ment of transfected PC12 cells (Fig. 5*A*, *bottom panel*, *lanes 6–15*).

To further analyze the metabolism of the signal peptide-bearing form, we carried out pulse-chase labeling of transiently transfected CHO cells expressing WT PrP in the presence and absence of proteasome inhibitor, and then subjected cell lysates to immunoprecipitation using either 3F4 or anti-SP antibodies. In untreated cells, the 3F4 antibody recognized glycosylated bands at 32–38 kDa, as well as an unglycosylated band of 25 kDa (Fig. 7*A*, *left panel*). In the presence of PSI 1, a band of 27 kDa appeared (Fig. 7*A*, *right panel*), corresponding to the additional species observed on Western blots of cells treated with inhibitor (Fig. 6, *lane 2*). As expected, only the 27-kDa band was immunoprecipitated by the anti-SP antibody, confirming its identity as an unprocessed, signal peptide-containing form of PrP (Fig. 7*B*, *right panel*). Untreated cells contained lower levels of the 27-kDa form, which could be visualized by immunoprecipitation with anti-SP antibody (Fig. 7*B*, *left panel*). Of note, the half-life of the 27-kDa form was very short ($t_{1/2}$ = 30 min) in untreated cells, and was significantly extended (to ~4 h) by including PSI 1 in the chase medium (Fig. 7*D*), consistent with the conclusion that this form is normally degraded by the proteasome. The fact that PSI 1 increased the amount of the 27-kDa form that was present at the start of the chase period implies that this species undergoes significant proteasomal degradation even within the 20-min period of pulse labeling (compare *0 h lanes* in the *left* and *right panels* of Fig. 7*B*). In contrast, the rest of the PrP species (including both unglycosylated and glycosylated forms lacking a signal peptide) had a half-life of ~3 h, and this value was not affected by PSI 1 (Fig. 7*C*). The latter result is similar to what was observed in experiments on stably transfected cells (Fig. 3).

The presence of the signal peptide on the 27-kDa form of PrP that accumulates in the presence of proteasome inhibitor suggested that this polypeptide had not yet been translocated into the ER lumen where signal peptidase is located. To directly probe the topology of the 27-kDa form, we carried out a protease protection assay on microsomes prepared from control and inhibitor-treated cells synthesizing WT PrP. We found that the 27-kDa band was selectively degraded by protease treatment of intact microsomes, whereas other PrP forms (both glycosylated and unglycosylated), were protected (Fig. 8*A*). This result implies that the 27-kDa polypeptide is present on the cytoplasmic side of the ER membrane. We also observed that, in contrast to the other PrP forms, the untranslocated polypeptide was insoluble in non-ionic detergents (Fig. 8*B*).

To determine the localization of the 27-kDa form in intact cells, we carried out immunofluorescence staining of CHO cells expressing WT PrP using anti-SP antibody and an antibody to PDI as a marker for the ER. We observed very little staining

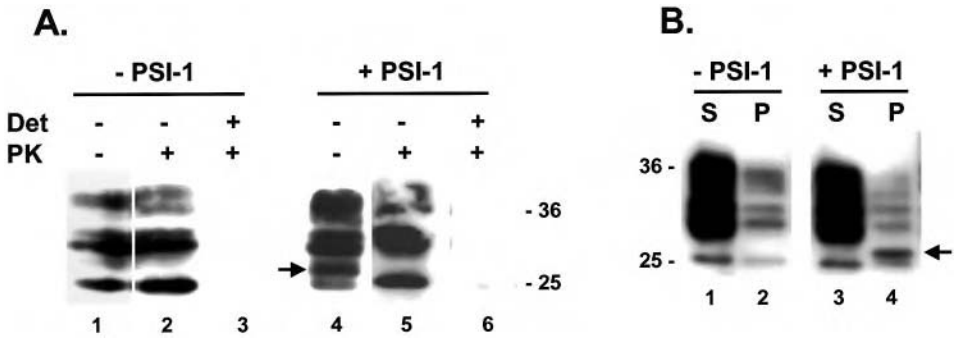

FIG. 8. **The signal peptide-bearing form of PrP that accumulates in the presence of proteasome inhibitor is present on the cytoplasmic side of the ER membrane, and is detergent-insoluble.** *A*, transiently transfected BHK cells expressing WT PrP were treated for 16 h with either ethanol vehicle (*lanes 1–3*) or with PSI 1 (20 μM) (*lanes 4–6*). Postnuclear supernatants were then prepared and were either left untreated (*lanes 1* and *4*), or were incubated with proteinase K in the absence (*lanes 2* and *5*) or presence (*lanes 3* and *6*) of Triton X-100 (*Det*). The *arrow* points to the PSI 1-induced form of PrP (*lane 4*) that is selectively digested with proteinase K in the absence of detergent (*lane 5*). *B*, transiently transfected CHO cells expressing WT PrP were treated for 16 h with either ethanol vehicle (*lanes 1* and *2*) or with PSI 1 (20 μM) (*lanes 3* and *4*). Cell lysates were first pre-cleared by centrifugation at 16,000 $\times$ *g*, and were subjected to centrifugation at 186,000 $\times$ *g* for 40 min. PrP in equivalent amounts of supernatants (*lanes 1* and *3*) and pellets (*lanes 2* and *4*) was then visualized by Western blotting. The *arrow* indicates the position of the PSI 1-induced form of PrP, which is detergent-insoluble (*lane 4*).

with anti-SP antibody in untreated cells (Fig. 9*A*). Treatment with PSI 1 caused marked accumulation of anti-SP-reactive PrP in an intracellular distribution that colocalized with PDI (Fig. 9, *D–F*). In conjunction with the results of the topology assay, the immunofluorescence data imply that the signal peptide-bearing form of PrP that accumulates in the presence of proteasome inhibitors is closely associated with the cytoplasmic surface of the ER membrane.

Taken together, our data indicate that a fraction of newly synthesized PrP molecules are never translocated or processed. These chains are normally degraded by the proteasome, probably in close apposition to the cytoplasmic surface of the ER membrane.

Proteasome Inhibitors Do Not Cause Accumulation of PrP in Cerebellar Granule Neurons—We found that treatment of neurons expressing either WT or PG14 PrP with MG132 for up to 8 h had no effect on any of the PrP bands seen by Western blotting using 3F4 antibody, including both glycosylated and unglycosylated species (Fig. 10, *A* and *B*, *upper panels*). Blots of the same cell lysates developed with an anti-ubiquitin antibody revealed accumulation of high molecular mass, ubiquitinated proteins, demonstrating the efficacy of the inhibitor treatment (Fig. 10, *A* and *B*, *lower panels*). PrP levels decreased after 24 h of exposure, but this is likely because of the death of a significant proportion of the neurons that had occurred by this time (data not shown). Prolonged treatment of cerebellar granule neurons with proteasome inhibitors is known to induce apoptosis (31). Results similar to those shown in Fig. 10, *A* and *B*, were obtained with other inhibitors, including ALLN (50–200 μM), lactacystin (0.1–10 μM), and lactacystin β-lactone (10 μM), and with neurons from non-transgenic C57BL/6J mice (data not shown).

Blotting of the same samples from MG132-treated neurons with anti-SP antibody failed to reveal the presence of signal peptide-bearing forms of either WT or PG14 PrP (Fig. 10*C*, *lanes 1–12*). Lysates from transfected PC12 cells treated with MG132 for 24 h were used to provide markers for the sizes of the signal peptide-containing forms (27 for WT and 33 kDa for PG14) (Fig. 10*C*, *lane 13*). The faint bands seen at 27 kDa after inhibitor treatment of neurons expressing WT PrP (Fig. 10*C*, *upper panel*, *lanes 11* and *12*) are likely to be nonspecific, because they were not apparent in the blot developed with 3F4 antibody (Fig. 10*A*, *upper panel*, *lanes 11* and *12*), and because we did not observe them in every experiment. We also failed to see PrP forms reactive with anti-SP antibody after metabolic labeling of cerebellar granule neurons (data not shown).

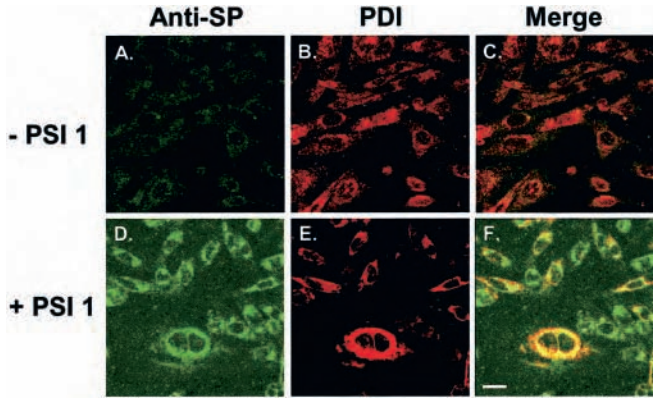

FIG. 9. **The signal peptide-bearing form of PrP that accumulates in the presence of proteasome inhibitor co-localizes with an ER marker.** Stably transfected CHO cells expressing WT PrP were left untreated (*A–C*), or were treated for 15 h with 20 μM PSI (*D–F*). Cells were then fixed and permeabilized, and stained with anti-SP and anti-PDI primary antibodies, followed by Alexa 488- and Alexa 594-conjugated secondary antibodies. Cells were viewed with *green* excitation/emission settings to detect signal peptide-bearing PrP (*A* and *D*), and with *red* excitation/emission settings to detect PDI (*B* and *E*). *Merged red* and *green* images are shown in *C* and *F*. All cells in *F* show colocalization of PrP and PDI, although several cells do not appear yellow because they contain lower levels of PDI, so the *red* and *green* signals are not matched in intensity. The *scale bar* in *F* is 50 μM (applicable to all panels).

We conclude that PrP is not subject to proteasomal degradation in these neurons, either before translocation or after retrotranslocation.

DISCUSSION

The present work addresses a question that has become a recent focus of interest in the prion field: how is PrP synthesized and metabolized by the cell, and how might pathogenic mutations alter these processes? We demonstrate here that PrP molecules carrying disease-associated mutations are significantly delayed in their transit along the early part of the secretory pathway. This phenomenon appears to be a general feature of the biosynthesis of at least a subset of mutant PrPs, because it is observed with two different mutations, and is apparent in transfected CHO and BHK cells, as well as in cultured neurons from transgenic mice. We find that, in contrast to some other secretory proteins that misfold during their biosynthesis, mutant PrPs are not subject to ER-associated degradation, involving retrotranslocation into the cytoplasm

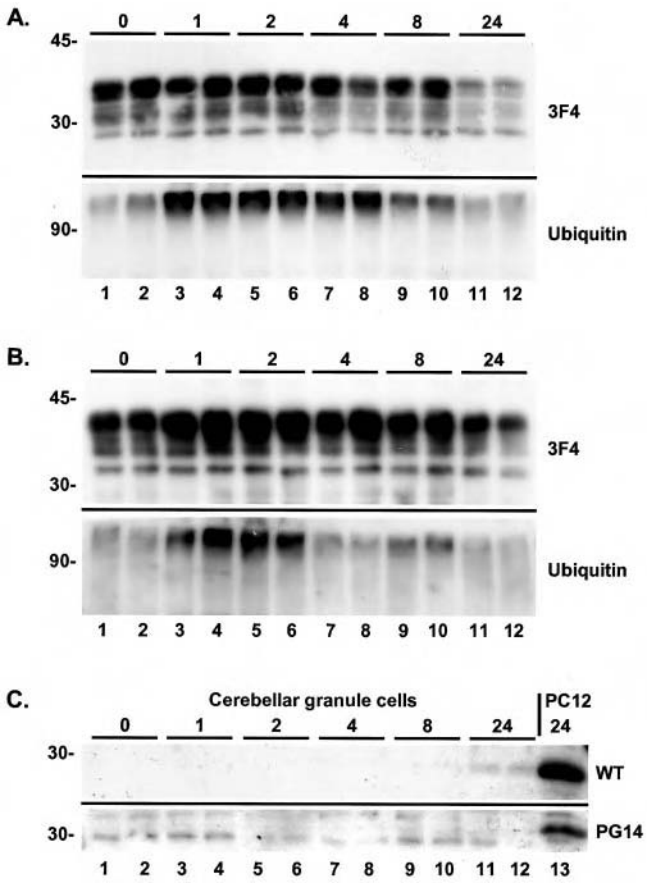

FIG. 10. **Proteasome inhibitors do not cause accumulation of PrP in cerebellar granule neurons.** Cerebellar granule neurons from transgenic mice expressing either WT PrP (*A*) or PG14 PrP (*B*) were treated with MG132 (5 μM) for 0, 1, 2, 4, 8, or 24 h. Cells were then lysed and analyzed by Western blotting using either 3F4 antibody (*upper panel*) or anti-ubiquitin antibody (*lower panel*). Each pair of lanes represents duplicate cultures. *C*, the same lysates used in *panels A* and *B* were Western blotted using anti-SP antibody (*lanes 1–12*). Lysates of transfected PC12 cells expressing WT or PG14 PrP that had been treated for 24 h with MG132 (10 μM) were run in *lane 13* to serve as size markers for the respective signal peptide-containing forms.

and then degradation by the proteasome. A small number of PrP molecules, both mutant and WT, are degraded by the proteasome, but these represent aberrant chains that have been translated in the cytoplasm, but have not been translocated into the ER lumen. Our results strongly contrast with those of two other groups that have recently claimed a role for the proteasome in the degradation of retrotranslocated PrP.

Mutant PrP Is Delayed in Its Exit from the ER—*N*-Linked oligosaccharide chains become resistant to cleavage by endo H in the mid-Golgi, as a result of the action of Golgi mannosidase II. The slower maturation of mutant PrPs from an endo H-sensitive to an endo H-resistant form therefore suggests that these proteins transit the early part of the secretory pathway more slowly than WT PrP. This observation is consistent with a previous study in which we localized mutant PrP molecules in transfected cells using immunofluorescence and immunoelectron microscopy, and by fluorescence microscopy of PrP-EGFP fusion proteins (15). We found that several different mutant PrPs, including PG14 and D177N, were present on the cell surface at reduced levels compared with WT PrP. In addition, many cells showed accumulation of mutant PrP in the ER. Similar observations regarding the cellular distribution of mutant PrPs have been made by several other laboratories (9, 32–35). The combined results of localization and biosynthetic studies therefore suggest that mutant PrP molecules are delayed in their export from the ER. This delay results in a steady-state distribution in which the proteins are concentrated in the ER, and are expressed at lower levels on the cell surface. Although it was originally thought that exit of newly synthesized proteins from the ER was a default process, it is now clear that a number of factors may influence the anterograde transport rate (36–38). These include the kinetics of polypeptide chain folding, association with ER chaperones, interaction with cargo receptors and coat proteins in ER transport vesicles, binding to specific ligands, and self-aggregation. One or more of these factors may play a role in retarding transit of mutant PrPs out of the ER.

The Role of the Proteasome in PrP Degradation—Secretory or membrane proteins that are retained in the ER are sometimes subject to a quality control process in which they are retrotranslocated into the cytoplasm and degraded by the proteasome (20, 21). This mechanism is meant to ensure that abnormally folded proteins, or those that are not properly modified or assembled into multisubunit complexes, do not reach the plasma membrane where they might cause cellular damage. Several pieces of evidence presented here argue strongly that the majority of PrP molecules, both mutant and WT, are not subject to ER-associated degradation involving the proteasome. First, proteasome inhibitors do not affect the half-life of WT or mutant PrPs in pulse-chase experiments. Second, the inhibitors do not alter the kinetics with which core-glycosylated precursors of PrP are converted to mature, endo H-resistant forms. Third, the percentage of the initial radioactive label that is chased into mature forms is high (50–70%), and is not influenced by the presence of proteasome inhibitors. If significant numbers of PrP molecules were being degraded by the proteasome after retrotranslocation from the ER, then proteasome inhibitors would be expected to rescue disappearance of immature forms early in the chase period, resulting in an increase in the half-life and in the steady-state levels of the protein. These effects have been observed for other proteins, such as T-cell receptor α-chain (39), major histocompatibility complex class I heavy chain (40), Ig light chain (41), and α_1-antitrypsin Z (42) that are known to be substrates for retrotranslocation and proteasomal degradation. Cystic fibrosis transmembrane regulator, the classic example of a protein subject to ER-associated degradation, is also stabilized by proteasome inhibitors in pulse-chase experiments, although in this case it is high molecular weight, ubiquitinated intermediates that accumulate (43). For some substrates, proteasome inhibitors cause accumulation of retrotranslocated forms that have been stripped of their oligosaccharide chains by cytoplasmic glycosidases (39, 40). In contrast, the primary form of PrP that we observe after short term treatment of cells with inhibitors is a signal peptide-bearing species that has most likely never been translocated or glycosylated (see below).

In contrast to the two PrP mutants we have analyzed here (one insertional and one missense), two stop codon mutants (Y145stop, Q160stop) do appear to be degraded primarily by the retrotranslocation/proteasome pathway. These molecules are turned over rapidly, are stabilized by proteasome inhibitors, and are found to accumulate intracellularly in the cytoplasm and nucleus under some circumstances (10, 44). Presumably, the absence of the C-terminal part of the polypeptide chain and the GPI anchor causes these mutants to interact with the ER quality control machinery in a way that full-length molecules do not.

Our results demonstrate that a small fraction of PrP molecules, both wild-type and mutant, is subject to proteasomal degradation in transfected cells by a pathway that does not involve retrotranslocation from the ER lumen. Proteasome in-

hibitors cause the selective accumulation of a form of PrP (27 kDa for WT and D177N, and 33 kDa for PG14) that is ~2-kDa larger than the mature, unglycosylated species. This form, which is the major one that accumulates on Western blots after short term treatment of cells with proteasome inhibitors (≤8 h), is turned over rapidly ($t_{½}$ = 30 min), and its half-life is significantly prolonged by the inhibitors. Our data strongly suggest that the 27/33-kDa forms represent PrP molecules that reside on the cytoplasmic face of the ER membrane, and that have never been translocated into the lumen for further processing. The most decisive observation is that these species react with an antibody that is specific for PrP molecules bearing an intact signal peptide. This feature indicates that the proteins have not been exposed to signal peptidase, which resides in the lumen of the ER. The presence of the signal peptide argues persuasively against the possibility that the 27/33-kDa forms are delivered to the cytoplasm by a process of retrotranslocation, because in that case the signal peptide would have been removed during cotranslational insertion into the ER lumen. In addition, the 27/33-kDa forms lack *N*-linked glycans and a GPI anchor, based on the fact that their migration is not shifted by treatment with glycosidases or phosphatidylinositol-specific phospholipase C. These features are consistent with the lack of processing by oligosaccharyl transferase and GPI transamidase, both of which reside in the ER lumen. Topology analysis using a protease protection assay demonstrates directly that the 27-kDa protein is located entirely on the cytoplasmic side of the ER membrane. Finally, immunolocalization studies indicate that the 27-kDa form accumulates in an ER pattern after proteasome inhibitor treatment. Taken together, our results indicate that a small fraction of PrP chains fail to be translocated into the ER lumen during their synthesis, and these remain closely associated with the cytoplasmic face of the ER membrane where they are rapidly degraded by the proteasome. We suspect that these chains are ubiquitinated prior to proteasomal attack, because we have sometimes observed a ladder of higher molecular mass PrP species above the 27/33-kDa band, with steps separated by ~8 kDa, after treatment of cells with proteasome inhibitors (data not shown). The phenomenon of abortive translocation we have observed here is not unique to PrP, and we think it is likely to reflect saturation of one or more components of the translocation machinery at the elevated expression levels typical of transfected cells. Untranslocated PrP does not accumulate in cultured cerebellar granule cells treated with proteasome inhibitors, implying that this species is unlikely to be an obligate by-product of PrP biosynthesis in neurons. Untranslocated, signal peptide-bearing forms of other proteins have been found to accumulate in transfected cells treated with proteasome inhibitors (39).

Artifactual Effects of Proteasome Inhibitors—We have uncovered a previously unappreciated side effect of proteasome inhibitors. Although the toxic and stress-inducing effects of these drugs are well known, we have found that proteasome inhibitors are also capable of increasing the synthesis of a specific protein, PrP, and its mRNA in transfected cells. Preliminary experiments indicate that the inhibitors may have a similar effect on other heterologously expressed proteins.[3] The effect of proteasome inhibitors on PrP mRNA and synthetic rate first became apparent after 2–4 h of treatment, and was very marked after 18–24 h. Our evidence suggests that the effect is related to the CMV promoter driving expression of PrP, because proteasome inhibitors did not alter levels of PrP protein or mRNA derived from the endogenous rat gene in PC12 cells, or from the mouse PrP gene (either endogenous or carried on a transgene) in cultured neurons. The mechanism underlying this unexpected effect of proteasome inhibitors could be related to stabilization of the turnover of transcription or translation factors, or to activation of signaling pathways that impinge on transcription from the CMV promoter (45–48). Because the effect varied between different clones of stably transfected cells, it seems likely that the insertion site in the chromatin could also play a role. Whatever its cause, this potential artifact is important to bear in mind when interpreting experiments using proteasome inhibitors, particularly those involving expression of proteins from heterologous promoters, and those in which the drugs are applied for extended periods of time.

The Role of ER Accumulation in Disease Pathogenesis—A number of inherited human diseases are attributable to defects in export of a mutant protein from the ER (22, 36, 49, 50). In some cases, such as cystic fibrosis and hereditary hemochromatosis, the mutant protein is retrotranslocated from the ER and degraded by the proteasome, resulting in failure of the protein to reach its normal cellular destination. In other disorders, such as hereditary emphysema (PiZ variant) and congenital hypothyroidism, the retained protein accumulates in the ER without being degraded. In these cases, the disease phenotype is due to a toxic effect of the accumulated protein, which stimulates one or more ER stress response pathways. Based on the data presented here, we hypothesize that some inherited prion disorders, such as those associated with PG14 and D177N, are members of this second category of ER retention diseases. Although transit of these mutant PrP molecules out of the ER is not completely blocked, their export rate is reduced sufficiently to cause an accumulation of the protein in the ER at steady state. We are currently investigating whether build-up of mutant PrP in the ER activates pro-apoptotic stress pathways. Regardless of the pathway involved, it is clear that PG14 PrP is a potent trigger of neuronal death, because transgenic mice expressing this protein develop a fatal neurodegenerative illness characterized by massive apoptosis of cerebellar granule cells (11, 12).

Comparison with Other Studies—Our results require a major shift in the interpretation of several previously published studies on the role of the proteasome in the metabolism of PrP. Two other laboratories have reported that proteasome inhibitors cause the accumulation of a 26–27-kDa, unglycosylated form of wild-type PrP in several different cultured cell types (17, 19). The accumulated PrP was present in the cytoplasm by immunofluorescence staining, partially colocalizing with the cytoplasmic heat shock protein Hsc70 (17). Based on the fact that the 26-kDa species migrated on SDS-PAGE at the position of recombinant PrP 23–230, it was suggested that this form was processed at both the N and C termini (*i.e.* the signal peptide and GPI addition sequence had been removed in the ER) (17). These authors therefore concluded that a population of PrP molecules was normally subject to retrotranslocation into the cytoplasm after insertion into the ER lumen, followed by rapid proteasomal degradation. The absence of oligosaccharide chains on the retrotranslocated molecules was suggested to be due to the action of cytoplasmic glycosidases.

In contrast, our results make it clear that the unglycosylated PrP molecules that accumulate after proteasome treatment are not fully processed polypeptide chains derived by retrotranslocation. Rather, they are abortive translocation products that have never left the cytoplasm, and that therefore have intact signal peptides and GPI addition sequences. These molecules represent a relatively small fraction of the total PrP chains synthesized, and their production is associated with high expression levels in transfected cells. The fact that, in our hands,

[3] R. Chiesa and E. Biasini, unpublished data.

short term treatment of cells with proteasome inhibitors has no consistent effect other than stabilization of this untranslocated species indicates that neither wild-type or mutant PrP molecules are major substrates for degradation by ER quality control mechanisms. Similar to Yedidia *et al.* (19), we find that long term inhibitor treatment causes accumulation of mature, glycosylated PrP forms, but this effect is very likely attributable to the artifactual increase in PrP mRNA and synthetic rate that we have shown occurs under these conditions.

It has been suggested that some of the cytoplasmic PrP that accumulates in the presence of proteasome inhibitors has been converted to a PrP^{Sc}-like conformation, based on its detergent insolubility and protease resistance (18, 51). In support of the claim that this conformation is self-perpetuating (infectious), it was reported that aggregated and protease-resistant PrP continued to accumulate in transfected cells for a number of hours after removal of proteasome inhibitors (18). In light of the results reported here, however, we would offer an alternative explanation for this result. We suggest that the initial inhibitor treatment caused a sustained increase in the synthesis of PrP that continued even after the inhibitor was removed. This is the same phenomenon that we have illustrated in Fig. 4*C*, and is likely to result in the accumulation of multiple forms of PrP, including glycosylated, unglycosylated, and untranslocated species. Thus, increased PrP synthesis, rather than a self-propagating conformational change, probably accounts for the continued accumulation of PrP after transient treatment with proteasome inhibitors.

On the basis of several kinds of observations in both cultured cells and transgenic mice, it has been proposed that cytosolic PrP is highly cytotoxic, and that accumulation of this form may represent the first step in a pathogenic cascade operative in both inherited and infectiously acquired prion diseases (23). While the results reported here argue strongly against retrotranslocation as a mechanism for generation of cytosolic PrP, they do not address the potential toxicity of PrP that might accumulate in the cytoplasm as a result of other processes, for example, abortive translocation. It has been reported that artificial targeting of PrP to the cytoplasm by deletion of the N-terminal signal sequence is toxic to transfected cells and transgenic mice (23). However, in the absence of evidence that cytosolic PrP increases during the course of a natural prion disease, it is difficult to be certain of the pathogenic role of this form. Our data argue that accumulation of misfolded forms of mutant PrP in the lumen of the ER, rather than in the cytoplasm, represents a more likely instigating event in at least a subset of inherited prion disorders.

Acknowledgments—We thank Gianluigi Zanusso and Man-Sun Sy for 8H4 antibody, as well as Richard Kascsak for 3F4 antibody. We also acknowledge Michael Green for critical reading of the manuscript.

REFERENCES

1. Prusiner, S. B. (1998) *Proc. Natl. Acad. Sci. U. S. A.* **95,** 13363–13383
2. Collinge, J. (2001) *Annu. Rev. Neurosci.* **24,** 519–550
3. Young, K., Piccardo, P., Dlouhy, S., Bugiani, O., Tagliavini, F., and Ghetti, B. (1999) in *Prions: Molecular and Cellular Biology* (Harris, D. A., ed) pp. 139–175, Horizon Scientific Press, Wymondham, UK
4. Lehmann, S., and Harris, D. A. (1995) *J. Biol. Chem.* **270,** 24589–24597
5. Lehmann, S., and Harris, D. A. (1996) *J. Biol. Chem.* **271,** 1633–1637
6. Lehmann, S., and Harris, D. A. (1996) *Proc. Natl. Acad. Sci. U. S. A.* **93,** 5610–5614
7. Chiesa, R., and Harris, D. A. (2000) *J. Neurochem.* **75,** 72–80
8. Priola, S. A., and Chesebro, B. (1998) *J. Biol. Chem.* **273,** 11980–11985
9. Singh, N., Zanusso, G., Chen, S. G., Fujioka, H., Richardson, S., Gambetti, P., and Petersen, R. B. (1997) *J. Biol. Chem.* **272,** 28461–28470
10. Lorenz, H., Windl, O., and Kretzschmar, H. A. (2002) *J. Biol. Chem.* **277,** 8508–8516
11. Chiesa, R., Drisaldi, B., Quaglio, E., Migheli, A., Piccardo, P., Ghetti, B., and Harris, D. A. (2000) *Proc. Natl. Acad. Sci. U. S. A.* **97,** 5574–5579
12. Chiesa, R., Piccardo, P., Ghetti, B., and Harris, D. A. (1998) *Neuron* **21,** 1339–1351
13. Daude, N., Lehmann, S., and Harris, D. A. (1997) *J. Biol. Chem.* **272,** 11604–11612
14. Narwa, R., and Harris, D. A. (1999) *Biochemistry* **38,** 8770–8777
15. Ivanova, L., Barmada, S., Kummer, T., and Harris, D. A. (2001) *J. Biol. Chem.* **276,** 42409–42421
16. Stewart, R. S., Drisaldi, B., and Harris, D. A. (2001) *Mol. Biol. Cell* **12,** 881–889
17. Ma, J., and Lindquist, S. (2001) *Proc. Natl. Acad. Sci. U. S. A.* **98,** 14955–14960
18. Ma, J., and Lindquist, S. (2002) *Science* **298,** 1785–1788
19. Yedidia, Y., Horonchik, L., Tzaban, S., Yanai, A., and Taraboulos, A. (2001) *EMBO J.* **20,** 5383–5391
20. Bonifacino, J. S., and Weissman, A. M. (1998) *Annu. Rev. Cell Dev. Biol.* **14,** 19–57
21. Tsai, B., Ye, Y., and Rapoport, T. A. (2002) *Nat. Rev. Mol. Cell. Biol.* **3,** 246–255
22. Aridor, M., and Hannan, L. A. (2000) *Traffic* **1,** 836–851
23. Ma, J., Wollmann, R., and Lindquist, S. (2002) *Science* **298,** 1781–1785
24. Lehmann, S., and Harris, D. A. (2000) *J. Biol. Chem.* **275,** 1520
25. Miller, T. M., and Johnson, E. M., Jr. (1996) *J. Neurosci.* **16,** 7487–7495
26. Kascsak, R. J., Rubinstein, R., Merz, P. A., Tonna-DeMasi, M., Fersko, R., Carp, R. I., Wisniewski, H. M., and Diringer, H. (1987) *J. Virol.* **61,** 3688–3693
27. Zanusso, G., Liu, D., Ferrari, S., Hegyi, I., Yin, X., Aguzzi, A., Hornemann, S., Liemann, S., Glockshuber, R., Manson, J. C., Brown, P., Petersen, R. B., Gambetti, P., and Sy, M. S. (1998) *Proc. Natl. Acad. Sci. U. S. A.* **95,** 8812–8816
28. Braakman, I., Hoover-Litty, H., Wagner, K. R., and Helenius, A. (1991) *J. Cell Biol.* **114,** 401–411
29. Harris, D. A., Huber, M. T., van Dijken, P., Shyng, S.-L., Chait, B. T., and Wang, R. (1993) *Biochemistry* **32,** 1009–1016
30. Goldfarb, L. G., Petersen, R. B., Tabaton, M., Brown, P., LeBlanc, A. C., Montagna, P., Cortelli, P., Julien, J., Vital, C., Pendelbury, W. W., Haltia, M., Wills, P. R., Hauw, J. J., McKeever, P. E., Monari, L., Schrank, B., Swergold, G. D., Autilio-Gambetti, L., Gajdusek, D. C., Lugaresi, E., and Gambetti, P. (1992) *Science* **258,** 806–808
31. Porcile, C., Piccioli, P., Stanzione, S., Bajetto, A., Bonavia, R., Barbero, S., Florio, T., and Schettini, G. (2002) *Ann. N. Y. Acad. Sci.* **973,** 402–413
32. Jin, T., Gu, Y., Zanusso, G., Sy, M., Kumar, A., Cohen, M., Gambetti, P., and Singh, N. (2000) *J. Biol. Chem.* **275,** 38699–38704
33. Capellari, S., Parchi, P., Russo, C. M., Sanford, J., Sy, M.-S., Gambetti, P., and Petersen, R. B. (2000) *Am. J. Pathol.* **157,** 613–622
34. Petersen, R. B., Parchi, P., Richardson, S. L., Urig, C. B., and Gambetti, P. (1996) *J. Biol. Chem.* **271,** 12661–12668
35. Negro, A., Ballarin, C., Bertoli, A., Massimino, M. L., and Sorgato, M. C. (2001) *Mol. Cell. Neurosci.* **17,** 521–538
36. Aridor, M., and Balch, W. E. (1999) *Nat. Med.* **5,** 745–751
37. Aridor, M., and Balch, W. E. (2000) *Science* **287,** 816–817
38. Aridor, M., and Balch, W. E. (1996) *Trends Cell Biol.* **6,** 315–320
39. Yu, H., Kaung, G., Kobayashi, S., and Kopito, R. R. (1997) *J. Biol. Chem.* **272,** 20800–20804
40. Wiertz, E. J., Jones, T. R., Sun, L., Bogyo, M., Geuze, H. J., and Ploegh, H. L. (1996) *Cell* **84,** 769–779
41. O'Hare, T., Wiens, G. D., Whitcomb, E. A., Enns, C. A., and Rittenberg, M. B. (1999) *J. Immunol.* **163,** 11–14
42. Qu, D., Teckman, J. H., Omura, S., and Perlmutter, D. H. (1996) *J. Biol. Chem.* **271,** 22791–22795
43. Gelman, M. S., Kannegaard, E. S., and Kopito, R. R. (2002) *J. Biol. Chem.* **277,** 11709–11714
44. Zanusso, G., Petersen, R. B., Jin, T., Jing, Y., Kanoush, R., Ferrari, S., Gambetti, P., and Singh, N. (1999) *J. Biol. Chem.* **274,** 23396–23404
45. Nakayama, K., Furusu, A., Xu, Q., Konta, T., and Kitamura, M. (2001) *J. Immunol.* **167,** 1145–1150
46. Kawazoe, Y., Nakai, A., Tanabe, M., and Nagata, K. (1998) *Eur. J. Biochem.* **255,** 356–362
47. Zimmermann, J., Erdmann, D., Lalande, I., Grossenbacher, R., Noorani, M., and Furst, P. (2000) *Oncogene* **19,** 2913–2920
48. Wu, H. M., Wen, H. C., and Lin, W. W. (2002) *Am. J. Respir. Cell Mol. Biol.* **27,** 234–243
49. Kim, P. S., and Arvan, P. (1998) *Endocr. Rev.* **19,** 173–202
50. Aridor, M., and Hannan, L. A. (2002) *Traffic* **3,** 781–790
51. Ma, J., and Lindquist, S. (1999) *Nat. Cell Biol.* **1,** 358–361

Neurobiology of Disease

Neurodegenerative Illness in Transgenic Mice Expressing a Transmembrane Form of the Prion Protein

Richard S. Stewart,[1] Pedro Piccardo,[2,3] Bernardino Ghetti,[2] and David A. Harris[1]

[1]Department of Cell Biology and Physiology, Washington University School of Medicine, St. Louis, Missouri 63110, [2]Division of Neuropathology, Indiana University School of Medicine, Indianapolis, Indiana 46202, and [3]Center for Biologics Evaluation and Research, Food and Drug Administration, Rockville, Maryland 20852

Although PrP^{Sc} is thought to be the infectious form of the prion protein, it may not be the form that is responsible for neuronal cell death in prion diseases. ^{Ctm}PrP is a transmembrane version of the prion protein that has been proposed to be a neurotoxic intermediate underlying prion-induced pathogenesis. To investigate this hypothesis, we have constructed transgenic mice that express L9R-3AV PrP, a mutant prion protein that is synthesized exclusively in the ^{Ctm}PrP form in transfected cells. These mice develop a fatal neurological illness characterized by ataxia and marked neuronal loss in the cerebellum and hippocampus. ^{Ctm}PrP in neurons cultured from transgenic mice is localized to the Golgi apparatus, rather than to the endoplasmic reticulum as in transfected cell lines. Surprisingly, development of the neurodegenerative phenotype is strongly dependent on coexpression of endogenous, wild-type PrP. Our results provide new insights into the cell biology of ^{Ctm}PrP, the mechanism by which it induces neurodegeneration, and possible cellular activities of PrP^{C}.

Key words: **prion; transgenic; neurodegeneration; Golgi; transmembrane; mutation**

Introduction

Prion diseases are associated with conformational conversion of an endogenous, neuronal glycoprotein (PrP^{C}) into an aggregated, β-sheet-rich isoform (PrP^{Sc}) that is infectious in the absence of nucleic acid (Prusiner, 1998; Weissmann, 2004). Because PrP^{Sc} accumulates in the brains of infected animals and humans, it has usually been assumed that this isoform is the cause of prion-induced neurodegeneration. However, several lines of evidence now suggest that, although PrP^{Sc} is the infectious form of PrP, it may not be the form directly responsible for neuronal death in prion diseases (for review, see Chiesa and Harris, 2001). Thus, there has been an attempt to identify the PrP species that initiate the neurodegenerative process. The present work focuses on one candidate for such a neurotoxic form of PrP, designated ^{Ctm}PrP.

PrP can be synthesized in the endoplasmic reticulum (ER) in three topological forms, designated ^{Sec}PrP, ^{Ntm}PrP, and ^{Ctm}PrP. ^{Sec}PrP molecules are attached to the outer leaflet of the lipid bilayer exclusively by a C-terminal glycosyl-phosphatidylinositol (GPI) anchor. ^{Ntm}PrP and ^{Ctm}PrP molecules span the lipid bilayer via a central hydrophobic region (amino acids 111–134), with either the N terminus or C terminus, respectively, on the extracytoplasmic side of the membrane (Hegde et al., 1998b; Hölscher et al., 2001; Kim et al., 2001; Stewart et al., 2001). ^{Ctm}PrP has been hypothesized to be a key pathogenic intermediate in both familial and infectiously acquired prion diseases (Hegde et al., 1999). In support of this proposition, transgenic mice expressing PrP with ^{Ctm}PrP-favoring mutations develop a scrapie-like neurological illness, but without PrP^{Sc} (Hegde et al., 1998b, 1999). However, a general role for ^{Ctm}PrP in prion diseases has been called into question by recent observations (Stewart and Harris, 2001, 2003), leaving the biological significance of this form unresolved.

A major difficulty in studying ^{Ctm}PrP is that it has not been possible to synthesize this form in either cultured cells or brain in the absence of the other two topological variants (^{Ntm}PrP and ^{Sec}PrP). To overcome this limitation, we identified nonconservative mutations in the hydrophobic core of the PrP signal peptide that markedly increased the proportion of ^{Ctm}PrP (Stewart et al., 2001; Stewart and Harris, 2003). Combining one of these mutations (L9R) with 3AV, a mutation within the transmembrane domain, to create L9R-3AV resulted in a protein that was synthesized exclusively as ^{Ctm}PrP, in both *in vitro* translation reactions and transfected cells (Stewart et al., 2001). The availability of L9R-3AV PrP provided us with the ability to analyze the properties of ^{Ctm}PrP in a cellular context in the absence of the other two topological variants (Stewart et al., 2001).

In the present study, we report on transgenic mice that express PrP carrying the L9R-3AV mutation. These Tg(L9R-3AV) mice develop a severe neurological illness accompanied by marked neuronal degeneration in several brain areas. Unexpectedly, we find that this phenotype is strongly dependent on coexpression of

Received Oct. 29, 2004; revised Feb. 15, 2005; accepted Feb. 16, 2005.

This work was supported by Department of Defense Grant DAMD-03-0531 (R.S.S.) and National Institutes of Health Grants NS40975 (D.A.H.) and P30 AG10133 (B.G.). No official endorsement of this article by the Food and Drug Administration is intended or should be inferred. We thank Charles Weissmann for *Prn-p*$^{0/0}$ mice, Richard Kascsak for 3F4 antibody, and Man-Sun Sy for 8H4 and 8B4 antibodies. We are grateful to Cheryl Adles and Michelle Kim for mouse colony maintenance and genotyping and to Rose Richardson and Constance Alyea for preparing histological specimens. We thank Mike Green for critically reading this manuscript.

Correspondence should be addressed to Dr. David A. Harris, Department of Cell Biology and Physiology, Washington University School of Medicine, 660 South Euclid Avenue, St. Louis, MO 63110. E-mail: dharris@cellbiology.wustl.edu.

DOI:10.1523/JNEUROSCI.0105-05.2005

 0270-6474/05/253469-09$15.00/0

endogenous, wild-type PrP. Our results have important implications for the cell biology of ^{Ctm}PrP, the mechanism by which it induces neurodegeneration, and possible physiological functions of PrP^{C}.

Materials and Methods

Transgenic mice. Construction of a plasmid that encodes mouse PrP containing the L9R-3AV mutation and the 3F4 antibody epitope (see Fig. 1) has been described previously (Stewart et al., 2001). The coding region of this plasmid was amplified by PCR using the following primers: GACCAGCTCGAGATGGCGAACCTTGGCTACTGG (sense); GACCAGCTCGAGTCATCCCACGATCAGGAAGAT (antisense). The amplified PCR product was digested with *Xho*I and inserted into the MoPrP.Xho vector (Borchelt et al., 1996). Purified DNA was injected into pronuclei of fertilized eggs from an F_2 cross of C57BL/6J × CBA/J F_1 parental mice. Founder animals were identified by PCR amplification of tail DNA using the following primers: AACCGAGCTGAAGCATTCTGCC (sense); CACGAGAAATGCGAAGGAACAAGC (antisense). Founders were bred to C57BL/6J × CBA/J (*Prn-p*$^{+/+}$) mice or to *Prn-p*$^{0/0}$ mice obtained from Charles Weissmann (Scripps Research Institute, West Palm Beach, FL). The latter mice, which were created on a C57BL/6J/129 background (Büeler et al., 1992), have been maintained in our laboratory by crossing onto the C57BL/6J × CBA/J background. For one line (B), transgenic animals were intercrossed to obtain progeny that were homozygous for the transgene array. The latter animals were identified by quantitative PCR. Tg(WT-E1)/*Prn-p*$^{0/0}$ and Tg(PG14-A2)/*Prn-p*$^{0/0}$ mice have been described previously (Chiesa et al., 1998). The transgenically encoded PrP in both of these lines carries the 3F4 epitope.

Animals were scored as ill if they displayed ataxia on a horizontal grid test (Chiesa et al., 1998), and they were considered to be terminal and were killed when they could no longer walk or feed themselves.

Histological analysis. Brain tissue was fixed, processed, and sectioned sagittally as described previously (Chiesa et al., 1998). Tissue sections were stained with hematoxylin and eosin. For detection of GFAP, sections were stained with an antibody from Biogenex (San Ramon, CA) at a 1:50 dilution, followed by visualization using the peroxidase–antiperoxidase (PAP) method with goat anti-rabbit IgG and rabbit PAP (Sternberger Monoclonals, Baltimore, MD). 3,3′-Diaminobenzidine was used as a chromogen. Sections were counterstained lightly with hematoxylin to reveal the localization of the cells.

Western blotting. Brain tissue was homogenized using a Teflon pestle in 10 vol of PBS containing protease inhibitors (in μg/ml: 20 PMSF, 10 leupeptin, and 10 pepstatin). Homogenates were clarified by centrifugation at 2000 × *g* for 5 min. Cultured neurons were lysed in 0.5% SDS and 50 mM Tris-HCl, pH 7.5, and the lysates were heated at 95°C for 10 min. Protein was quantified using a BCA assay (Pierce, Rockford, IL). Samples were analyzed by SDS-PAGE followed by immunoblotting with 3F4 antibody (Bolton et al., 1991) or 8H4 antibody (Zanusso et al., 1998).

Reverse transcriptase-PCR. RNA was extracted from freshly dissected forebrain or cerebellum using RNAWiz (Ambion, Austin, TX) according to the manufacturer's instructions. RNA was reverse transcribed and amplified in a one-step reaction using the Titanium kit (Clontech, Palo Alto, CA). The primers used to detect mRNA encoding transgene-derived PrP were CGCTGCGTCGCATCGGTGG (sense) and GCCATCTCGAGGTACCAC (antisense). The primers used to detect mRNA encoding endogenous PrP were GCCAAGCAGACTATCAG (sense) and CGGCTGTAGTCAGGTGTATCA (antisense). Mouse β-actin primers supplied by the manufacturer were included as an internal standard to correct for RNA input. Samples were removed every four cycles and analyzed on 8% polyacrylamide/Tris-borate EDTA gels. DNA band intensities were quantified by staining gels with SYBRGreen (Molecular Probes, Eugene, OR) and imaging with a Storm 860 phosphorimager (Amersham Biosciences, Arlington Heights, IL). The data shown were from those samples in which band intensities for both PrP and actin were within the linear range of amplification (generally 18 cycles).

Culturing and metabolic labeling of cerebellar granule cells. Primary cultures from 5-d-old pups were prepared as described previously (Miller and Johnson, 1996). Dissociated cells were resuspended in cerebellar granule neuron (CGN) medium (basal medium Eagle's, 10% dialyzed fetal bovine serum, 25 mM KCl, 2 mM glutamine, and 50 μg/ml gentamycin) and plated at a density of 500,000 cells/cm^2 in polylysine-coated plastic plates or 8-well glass chamber slides. Cells were used after 4–5 d in culture. These cultures contained >95% neurons, as assessed by staining with antibody to GFAP.

Cerebellar granule cells were labeled with 200 μCi/ml ^{35}S-Promix (Amersham Biosciences) in CGN medium lacking methionine, cysteine, and bovine serum and containing vitamin B27 supplement (Invitrogen, Carlsbad, CA). Cells were lysed in 0.5% SDS and 50 mM Tris-HCl, pH 7.5, and immunoprecipitation of PrP was performed as described previously (Drisaldi et al., 2003) using 3F4 or 8H4 antibody.

PrP membrane topology assay. Metabolically labeled cells were scraped with a pipette tip into PBS, spun at 2000 × *g* for 5 min, and resuspended in ice-cold homogenization buffer (in mM: 250 sucrose, 5 KCl, 5 $MgCl_2$, and 50 Tris-HCl, pH 7.5). Cells were lysed by 12 passages through SILASTIC tubing (inner diameter, 0.3 mm) connecting two syringes with 27 gauge needles, and nuclei were removed by centrifugation at 5000 × *g* for 10 min. Aliquots of the postnuclear supernatant were diluted into 50 mM Tris-HCl, pH 7.5, and incubated for 60 min at 4°C with 250 μg/ml proteinase K (PK) in the presence or absence of 0.5% Triton X-100. Digestion was terminated by the addition of PMSF (5 mM final concentration), and PrP was immunoprecipitated with 3F4 antibody and deglycosylated by treatment with peptide-*N*-(acetyl-β-glucosaminyl)-asparagine amidase (New England Biolabs, Beverly, MA).

Immunofluorescent labeling of brain sections and cultured neurons. Mice were perfused transcardially with 4% paraformaldehyde, after which the brains were postfixed for 3 h in the same solution and transferred to 0.1 M sodium phosphate, pH 7.2. Vibratome sections (50 μm) were incubated in blocking solution (PBS plus 2% goat serum and 0.2% Triton X-100) and stained with anti-PrP antibody 8B4 (Zanusso et al., 1998) and anti-giantin antibody (Covance, Berkeley, CA). Primary antibodies were visualized with a mixture of Alexa 488-coupled goat anti-mouse IgG and Alexa 594-coupled goat anti-rabbit IgG (Molecular Probes).

For surface labeling of cultured CGNs, cells were transferred to CGN medium containing vitamin B27 supplement instead of calf serum and stained in the living state for 10 min at 37°C with anti-PrP antibody 8H4. After rinsing with PBS, cells were fixed in 4% paraformaldehyde, 5% sucrose, and PBS for 10 min at room temperature and incubated in blocking solution (2% goat serum and PBS) for 10 min at room temperature. Cells were then stained with Alexa 488-coupled goat anti-mouse IgG, rinsed with PBS, and mounted in 50% glycerol and PBS. In some cases, cultures were incubated with phosphatidylinositol-specific phospholipase C (PIPLC) [final concentration, 1 U/ml; purified from *Bacillus thuringiensis* as described by Shyng et al. (1995)] before surface staining.

For internal labeling of cultured granule neurons, cells were fixed as above and permeabilized for 10 min at room temperature with 0.05% Triton X-100 in PBS. Cells were then incubated in blocking solution and stained with anti-PrP antibody 8B4 and anti-giantin antibody. Primary antibodies were visualized with a mixture of Alexa 488-coupled goat anti-mouse IgG and Alexa 594-coupled goat anti-rabbit IgG.

Cultured neurons and brain sections were viewed with a Zeiss (Oberkochen, Germany) LSM 510 confocal microscope equipped with an Axiovert 200 laser scanning system.

Assay of PrP^{Sc} properties. Cultures of cerebellar granule cells were labeled with ^{35}S-Promix as above. To assay detergent solubility, cells were lysed in buffer A (50 mM NaCl, 0.5% Triton X-100, 0.5% sodium deoxycholate, and 50 mM Tris-HCl, pH 7.5) at 4°C for 10 min. Lysates were first centrifuged at 14,000 × *g* for 10 min, and then the supernatant was centrifuged again at 180,000 × *g* for 40 min. PrP in supernatant and pellet fractions from the second centrifugation was immunoprecipitated and analyzed by SDS-PAGE.

To assay PK resistance, labeled cells were lysed in PK buffer (PBS plus 0.5% Triton X-100, 0.5% NP-40, 0.5% sodium deoxycholate, and 0.2% Sarkosyl), and the lysates were centrifuged at 10,000 × *g* for 10 min. Aliquots of the supernatant were treated with varying amounts of PK at 37°C for 20 min, and digestion was terminated by the addition of PMSF to a final concentration of 5 mM. PrP was then recovered by immunoprecipitation and analyzed by SDS-PAGE.

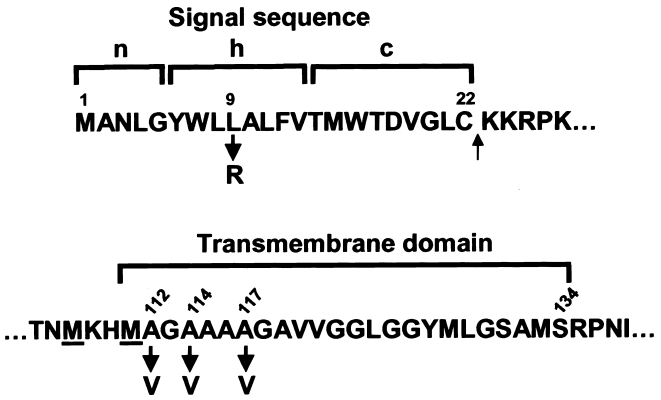

Figure 1. The amino acid sequence of murine PrP, with the L9R and 3AV mutations in the signal sequence and transmembrane domains, respectively, is shown. n, h, and c indicate, respectively, the N-terminal, hydrophobic, and C-terminal regions of the signal sequence. 3AV is the designation for the triple mutation A112V/A114V/A117V. The two underlined methionine residues at positions 108 and 111 were introduced to create an epitope for the 3F4 antibody, which allows discrimination of transgenically encoded and endogenous PrP. The upward arrow following residue 22 indicates the signal peptide cleavage site.

Table 1. Time course of neurological illness in Tg(L9R-3AV) mice

Line	Endogenous PrP (*Prn-p*)	Age at initial symptoms[a]	Age at death[a]	Number of animals
A/−	+/+	17 ± 2	21 ± 1	4[b]
B/−	+/+	172 ± 7	389 ± 12	26
B/−	0/0	>650	>650	20
B/B	+/+	38 ± 2	79 ± 3	10
B/B	0/0	72 ± 6	138 ± 10	6
C/−	+/+	85 ± 3	159 ± 5	46
C/−	+/0	104 ± 2	>300	18
C/−	0/0	144 ± 4	>300	18
D/−[c]	+/+	67	79	1

Founder mice were designated A, B, C, and D. A/−, B/−, C/−, and D/− indicate mice that are hemizygous for the transgene array. B/B indicates mice that are homozygous for the transgene array.

[a]Mean number of days ± SEM.

[b]Four of 70 offspring were transgene positive.

[c]Founder did not breed.

The conformation-dependent immunoassay was performed as described by Chiesa et al. (2003). Lysates of labeled cells prepared in buffer A were subjected to immunoprecipitation using 3F4 antibody, either with or without previous denaturation in 0.5% SDS at 95°C. The immunoprecipitated PrP was then resolved by SDS-PAGE.

Results

Spontaneous neurological illness in Tg(L9R-3AV)/*Prn-p*$^{+/+}$ mice

We introduced a murine PrP cDNA carrying the L9R-3AV mutation (Fig. 1) into the moPrP.Xho vector (Borchelt et al., 1996). This vector directs transgene expression in a pattern similar to that of endogenous PrP, with the exception that there is no expression in cerebellar Purkinje cells (Fischer et al., 1996). The mutant PrP carried an epitope for monoclonal antibody 3F4 (Bolton et al., 1991), which allowed transgenically encoded PrP to be distinguished from endogenous, murine PrP. Four founder mice (designated A–D) were obtained by pronuclear injection of fertilized oocytes from C57BL/6J × CBA/J parents (Table 1). Lines that were hemizygous for the transgene array were established from two of the founders (B and C) by breeding with nontransgenic (C57BL/6J × CBA/J) mates carrying the endogenous *Prn-p* gene.

All Tg(L9R-3AV)/*Prn-p*$^{+/+}$ mice spontaneously developed a progressive neurological illness characterized by ataxia, hindlimb paresis, and wasting (Table 1). Animals from the C line displayed an earlier onset of symptoms and shorter clinical phase before being killed than those from the B line. We intercrossed mice from the B line to produce animals homozygous for the transgene array. These animals developed symptoms shortly after weaning (38 ± 2 d), much earlier than the hemizygous B mice (172 ± 7 d), suggesting that disease onset is proportional to the expression level of mutant PrP (see below). The D founder mouse became ill at 67 d and was killed at 79 d before it could produce offspring. The A founder displayed an unusual breeding pattern. Only a small proportion (4 of 70) of transgene-positive progeny were obtained, and these were all severely runted and killed at weaning. Although this phenomenon was not investigated further, it could be attributable either to embryonic lethality of the transgene or to the presence of the transgene in only a fraction of the germ cells. In a previous study, we found that Tg(WT-E1) mice, which express wild-type PrP from the moPrP.Xho vector at levels approximately four times the endogenous PrP level, never develop clinical symptoms (Chiesa et al., 1998). Thus, the neurological illness seen in Tg(L9R-3AV) mice is related to the presence of the L9R-3AV mutation.

Neuropathology in Tg(L9R-3AV)/*Prn-p*$^{+/+}$ mice

Pathological changes were observed in the cerebellum and hippocampus of Tg(L9R-3AV)/*Prn-p*$^{+/+}$ mice from both the B and C lines. The most obvious abnormality was a marked reduction in the number of granule cells in the cerebellar cortex and a decrease in the thickness of the molecular layer (Fig. 2*A*). Loss of granule cells was most severe in the lobulus centralis, culmen, declive, uvula, and nodulus, whereas the crus II, lobulus paramedianus, and pyramis were less severely involved. Granule cells were not only fewer in number, they were also not as densely packed as normal. The molecular layer was hypercellular, and the dendrites of the Purkinje cells appeared reduced in number, although the total number of Purkinje cells appeared unchanged based on calbindin staining (data not shown). Immunohistochemical staining using anti-GFAP antibody demonstrated gliosis and astrocytic hypertrophy (Fig. 2*D*). The molecular layer displayed markedly hypertrophic Bergmann glial fibers. No spongiform changes were seen.

The hippocampus of Tg(L9R-3AV)/*Prn-p*$^{+/+}$ mice was atrophic, with reduced thickness of the pyramidal cell layer and the stratum oriens (Fig. 3*A*). The CA1 sector of the pyramidal cell layer was particularly affected. Immunohistochemical staining using anti-GFAP antibody demonstrated gliosis and astrocytic hypertrophy in the hippocampus (Fig. 3*D*).

The neurodegeneration observed in Tg(L9R-3AV)/*Prn-p*$^{+/+}$ mice was progressive, as illustrated by analysis of the cerebella of C line mice at different ages (Fig. 4). At 60 d of age, before development of symptoms, the cerebellum appeared relatively normal (Fig. 4*A*). At 85 and 99 d, after the onset of clinical symptoms, there was thinning of the granule cell and molecular layers (Fig. 4*B*,*C*). By 161 d, when animals were terminally ill, very few granule cells remained, and the cerebellum was severely atrophic (Fig. 4*D*). Our observations indicate that there is a progressive degeneration of neurons in several brain regions of Tg(L9R-3AV)/*Prn-p*$^{+/+}$ mice, although we do not rule out the possibility that there could also be effects on neuronal development and migration.

No pathological abnormalities were observed in age-matched, nontransgenic littermate mice (Figs. 2*C*,*F*, 3*C*,*F*) or in Tg(WT-E1) mice (Chiesa et al., 1998).

Neurological illness in Tg(L9R-3AV) mice is strongly dependent on coexpression of wild-type PrP

To test the effect of endogenous, wild-type PrP on the phenotype of Tg(L9R-3AV) mice, we crossed transgenic mice of the B and C lines with *Prn-p*$^{0/0}$ mice (Büeler et al., 1992) to eliminate the *Prn-p* allele. None of 20 Tg(L9R-3AV-B$^{+/-}$)/*Prn-p*$^{0/0}$ mice have shown symptoms of neurological illness, with the oldest of these living >650 d before dying of non-neurological causes (Table 1). In comparison, Tg(L9R-3AV-B$^{+/-}$)/*Prn-p*$^{+/+}$ mice first displayed symptoms at 172 d and were terminally ill by 389 d. A strong mitigating effect of eliminating the *Prn-p* allele was also evident in B line mice that were homozygous for the transgene array. Tg(L9R-3AV-B$^{+/+}$)/*Prn-p*$^{0/0}$ animals first showed symptoms at 72 d of age and became terminally ill at 138 d (Table 1). In contrast, mice homozygous for the B transgene array on the *Prn-p*$^{+/+}$ background became ill at 38 d and were terminal by 79 d. Finally, we also generated littermate Tg(L9R-3AV-C$^{+/-}$) mice on the *Prn-p*$^{+/0}$ and *Prn-p*$^{0/0}$ backgrounds. We observed that elimination of one *Prn-p* allele prolonged the onset of illness from 85 to 104 d, and elimination of both alleles delayed the onset further to 144 d. Tg(L9R-3AV-C$^{+/-}$) mice on both the *Prn-p*$^{+/0}$ and *Prn-p*$^{0/0}$ backgrounds were still alive at 300 d compared with mice on the *Prn-p*$^{+/+}$ background that were terminal by 159 d, on average. These data indicate a dose-dependent effect of endogenous PrP on the phenotype of Tg(L9R-3AV) mice.

Histological analysis confirmed the clinical results. Tg(L9R-3AV-B$^{+/-}$)/*Prn-p*$^{0/0}$ mice showed markedly improved survival of cerebellar granule cells and hippocampal pyramidal cells, as well as minimal astrogliosis, compared with age-matched Tg(L9R-3AV-B$^{+/-}$)/*Prn-p*$^{+/+}$ mice (Figs. 2*A*,*B*,*D*,*E*, 3*A*,*B*,*D*,*E*).

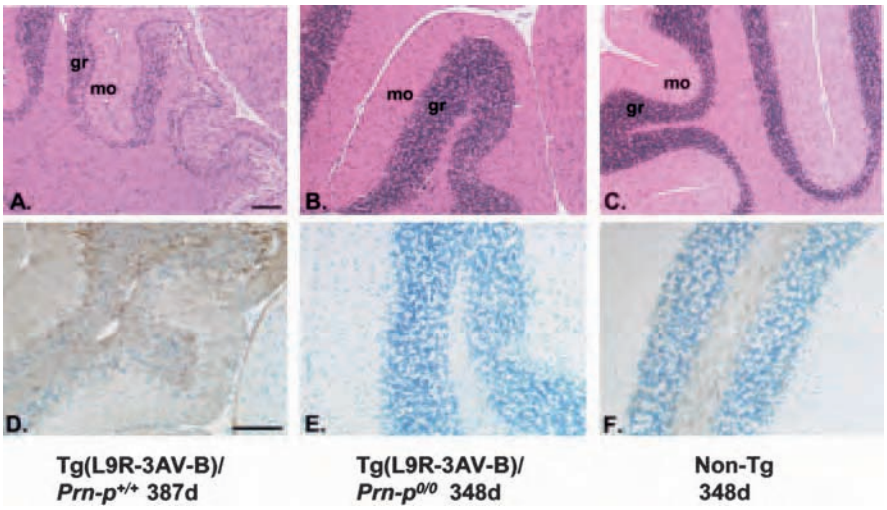

Figure 2. The histology of the cerebellum in Tg(L9R-3AV) and control mice is shown. Sections were from a Tg(L9R-3AV-B$^{+/-}$)/*Prn-p*$^{+/+}$ mouse (387 d old, symptomatic) (***A***, ***D***), a Tg(L9R-3AV-B$^{+/-}$)/*Prn-p*$^{0/0}$ mouse (348 d old, healthy) (***B***, ***E***), and a nontransgenic *Prn-p*$^{0/0}$ mouse (348 d old, healthy) (***C***, ***F***). Sections were stained with hematoxylin/eosin (***A–C***) or anti-GFAP antibody (***D–F***). gr, Granule cell layer; mo, molecular layer. Scale bars: ***A*** (for ***A–C***), ***D*** (for ***D–F***), 100 μm.

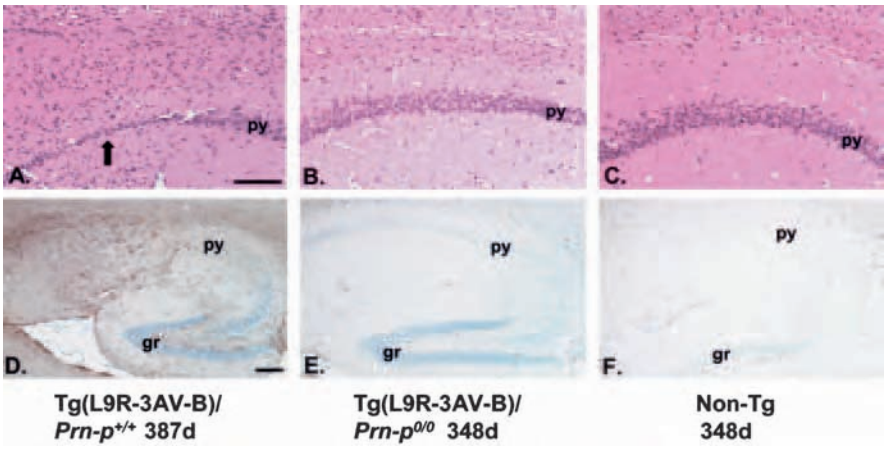

Figure 3. The histology of the hippocampus in Tg(L9R-3AV) and control mice is shown. Sections were from a Tg(L9R-3AV-B$^{+/-}$)/*Prn-p*$^{+/+}$ mouse (387 d old, symptomatic) (***A***, ***D***), a Tg(L9R-3AV-B$^{+/-}$)/*Prn-p*$^{0/0}$ mouse (348 d old, healthy) (***B***, ***E***), and a nontransgenic *Prn-p*$^{0/0}$ mouse (348 d old, healthy) (***C***, ***F***). Sections were stained with hematoxylin/eosin (***A–C***) or with anti-GFAP antibody (***D–F***). py, Pyramidal cell layer; gr, granule cell layer of the dentate gyrus. The arrow in ***A*** indicates severe loss of neurons in the pyramidal cell layer. The section shown in ***F*** was cut in a slightly different sagittal plane than those shown in ***D*** and ***E***, so the hippocampus appears larger. Scale bars: ***A*** (for ***A–C***), ***D*** (for ***D–F***), 100 μm.

Together, these results demonstrate that the neurotoxicity caused by expression of L9R-3AV PrP is dramatically accentuated by the presence of endogenous, wild-type PrP.

Transgene expression levels

Western blotting of brain homogenates from Tg(L9R-3AV) mice with 3F4 antibody revealed the presence of faint, transgene-specific PrP bands that migrated at 32–35 kDa (Fig. 5*A*, lanes 2–6). The specificity of these bands was confirmed by their absence in brain homogenates from *Prn-p*$^{0/0}$ mice (Fig. 5*A*, lane 7). The amount of L9R-3AV PrP in the runted offspring of the A founder (Fig. 5*A*, lane 2) was consistently approximately threefold higher than in mice from the B, C, or D line (Fig. 5*A*, lanes 3–5), confirming that the onset of the neurological illness in Tg(L9R-3AV) mice is correlated with the expression level of mutant PrP. However, the levels of L9R-3AV PrP observed by Western blotting in all transgenic lines were extremely low, ~1–5% of the level of endogenous PrP (data not shown) or of transgenically encoded PrP in Tg(WT-E1) mice (Fig. 5*A*, lane 1). This fact made it difficult to reliably compare the relative expression levels of the B, C, and D lines. However, our impression is that the C line expresses slightly more PrP than the B line, thus accounting for the earlier disease onset seen in the former line (Table 1).

Two kinds of experiments indicated that Western blotting significantly underestimated the amount of L9R-3AV PrP. First, reverse transcriptase (RT)-PCR was performed to estimate the levels of both transgene-derived and endogenous PrP mRNA in the brain using primer pairs specific to each species (Fig. 5*B*). Because the two PrP mRNAs were amplified in separate reactions, β-actin mRNA was used as an internal standard for RNA input to allow comparison of the PrP mRNA signals from the two reactions. The ratios of transgenic:endogenous PrP mRNA were 2.9, 1.3, and 1.4 for mice from the A, B, and C lines, respectively

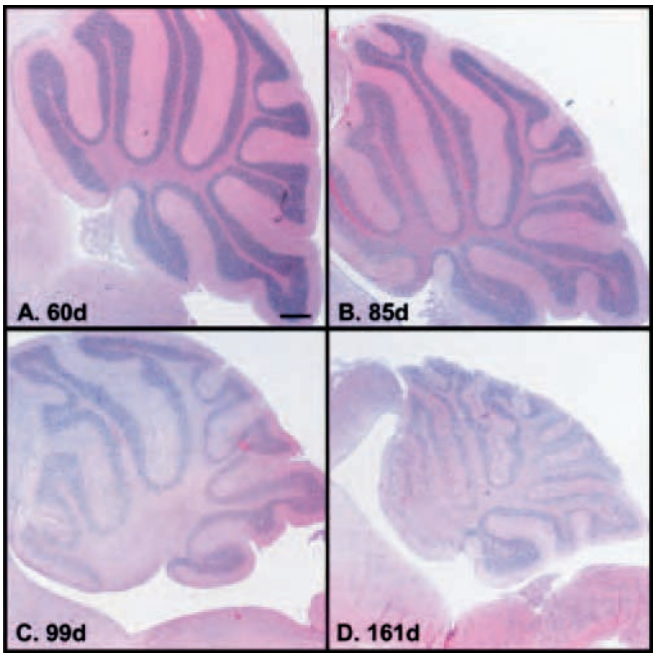

Figure 4. Neurodegeneration in the cerebellum of Tg(L9R-3AV) is progressive. Sections from Tg(L9R-3AV-C $^{+/-}$)/*Prn-p* $^{+/+}$ mice of the indicated ages were stained with hematoxylin/eosin. The 60-d-old mouse (***A***) was healthy, the 85- and 99-d-old mice (***B*** and ***C***, respectively) were symptomatic, and the 161-d-old mouse (***D***) was terminal. Scale bar: (in ***A***) ***A–D***, 100 μm.

(Fig. 5*B*, lanes 2–4). In comparison, Tg(PG14) and Tg(WT) mice (Chiesa et al., 1998) showed ratios of 1.0 and 3.6, respectively, consistent with their previously determined PrP protein expression levels of 1× and 3.6× endogenous (Fig. 5*B*, lanes 7, 8). As expected, nontransgenic *Prn-p* $^{+/+}$ mice showed only a band corresponding to endogenous PrP mRNA (Fig. 5*B*, lane 1), and nontransgenic *Prn-p* $^{0/0}$ mice showed no PrP mRNA bands (Fig. 5*B*, lane 5). Thus, we estimate that transgene mRNA is expressed in the brain at levels well above those that would be predicted based on Western blotting for PrP protein.

In a second experiment, we compared PrP protein levels in CGNs cultured from Tg(L9R-3AV-B $^{+/-}$)/*Prn-p* $^{0/0}$ and Tg(WT) mice using either immunoprecipitation or Western blotting. Immunoprecipitation of PrP from [^{35}S]methionine-labeled cells using either the 8H4 or 3F4 antibody revealed that the amount of PrP in Tg(L9R-3AV) neurons was 30% of the amount in Tg(WT) neurons (Fig. 5*C*, IP). Because the endogenous PrP level in nontransgenic mice is ~30% of the level of transgenic PrP in Tg(WT) mice (Chiesa et al., 1998), the immunoprecipitation results imply that Tg(L9R-3AV-B $^{+/-}$) mice express mutant PrP at approximately endogenous levels. In contrast, when samples from parallel cultures were subjected to Western blotting using the 8H4 or 3F4 antibody (Fig. 5*C*, WB), the amount of L9R-3AV PrP detected was only 1–5% of the amount of wild-type PrP. This discrepancy between the immunoprecipitation and Western blot results does not result from rapid metabolic turnover of L9R-3AV PrP, which has a half-life in neurons similar to that of the wild-type protein (Stewart and Harris, 2005). Rather, our results indicate that L9R-3AV PrP reacts poorly on Western blots, although it is detected efficiently by immunoprecipitation after SDS denaturation. The explanation for the poor reactivity of the mutant PrP on Western blots is unknown but may be related to masking of antibody epitopes in the protein when it is bound to the Nylon membrane either as a result of the mutations or the presence of the hydrophobic signal peptide (Stewart and Harris, 2005).

Using both Western blotting (Fig. 5*A*, lanes 3, 6) and RT-PCR (Fig. 5*B*, lanes 3, 6), we have confirmed that transgene expression levels are similar in Tg(L9R-3AV) mice on the *Prn-p* $^{0/0}$ and *Prn-p* $^{+/+}$ backgrounds. Thus, a reduction in expression of mutant PrP cannot account for the ameliorated phenotype of Tg(L9R-3AV)/*Prn-p* $^{0/0}$ mice.

Tg(L9R-3AV) neurons produce both ^{Ctm}PrP and ^{Sec}PrP

To assay the membrane topology of PrP in neurons from Tg(L9R-3AV) mice, we used primary cultures of cerebellar granule cells, which comprise one of the neuronal populations that degenerate *in vivo* in these animals. Dissociated neurons were labeled with [^{35}S]methionine, and then microsomes present in a postnuclear supernatant were subjected to protease digestion, followed by immunoprecipitation of PrP using 3F4 antibody. In this assay, fully translocated PrP (^{Sec}PrP) is completely protected from digestion, yielding a 25–27 kDa band after enzymatic deglycosylation. ^{Ctm}PrP produces a 19 kDa protected fragment, representing the lumenal and transmembrane domains of the protein. We found that microsomes from Tg(L9R-3AV-B $^{+/-}$)/*Prn-p* $^{+/+}$ neurons yielded approximately equal amounts of the 27 and 19 kDa bands, implying that these cells contained equal proportions of ^{Sec}PrP and ^{Ctm}PrP (Fig. 6, lane 5). We did not detect a 15 kDa fragment indicative of ^{Ntm}PrP. Protease treatment of microsomes in the presence of detergent eliminated both the 19 and 27 kDa bands (Fig. 6, lane 6), confirming that these species arose from protection by the microsomal membrane, rather than from intrinsic protease resistance of PrP. Identical results were obtained with neurons cultured from Tg(L9R-3AV-B $^{+/-}$)/*Prn-p* $^{0/0}$ and Tg(L9R-3AV-C $^{+/-}$)/*Prn-p* $^{+/+}$ mice (data not shown). As expected, microsomes from Tg(WT) neurons showed only a fully protected band of 25 kDa corresponding to ^{Sec}PrP (Fig. 6, lane 2). We confirmed, as reported previously (Stewart et al., 2001), that L9R-3AV PrP expressed in transfected Chinese hamster ovary (CHO) cells produces only a single, protease-protected band of 19 kDa (Fig. 6, lane 8). Thus, CHO cells synthesize the mutant protein exclusively with the ^{Ctm}PrP topology, without detectable ^{Sec}PrP. These results indicate that the L9R-3AV mutation significantly increases the ratio of ^{Ctm}PrP to ^{Sec}PrP in CGNs as well as in CHO cells, but the effect is less pronounced in the neurons.

^{Sec}PrP is localized to the cell surface, and ^{Ctm}PrP is localized to the Golgi apparatus

We used immunofluorescence staining in conjunction with phospholipase treatment to determine the subcellular distribution of ^{Ctm}PrP and ^{Sec}PrP in neurons from Tg(L9R-3AV) mice. PIPLC is a bacterial enzyme that cleaves the GPI anchor at the C terminus of PrP. PIPLC treatment is predicted to release ^{Sec}PrP but not ^{Ctm}PrP from cell membranes, because the latter form has a transmembrane anchor in addition to a GPI anchor. When we stained living (nonpermeabilized) neurons from Tg(L9R-3AV-B $^{+/-}$)/*Prn-p* $^{0/0}$ mice with any of several anti-PrP antibodies, we found that the mutant protein was distributed along the surface of neuronal processes that formed a dense meshwork in the culture (Fig. 7*A*). When cultures were treated with PIPLC, virtually all of the PrP was released from the neuronal surface (Fig. 7*B*). This result implies that most of the surface PrP has the ^{Sec}PrP topology. Identical results were obtained with neurons from Tg(L9R-3AV-B $^{+/-}$)/*Prn-p* $^{+/+}$ mice (data not shown).

Because little ^{Ctm}PrP was present on the surface, most of this form must be localized to intracellular compartments. We

stained Triton X-100-permeabilized neurons to visualize intracellular PrP. We observed that the mutant protein was present in discrete, perinuclear structures in the soma that colocalized with the Golgi marker protein giantin (Fig. 7*C–E*). Surface staining was less prominent in these permeabilized neurons, because Triton X-100 partially extracts PrP from the plasma membrane and also enhances the reactivity of cytoplasmic epitopes of Golgi-resident PrP (our unpublished observations). The distribution of PrP was identical in neurons from Tg(L9R-3AV)/*Prn-p*$^{+/+}$ and Tg(L9R-3AV)/*Prn-p*$^{0/0}$ mice from both the B and C lines (data not shown). Using immunofluorescence staining in conjunction with methods for differential permeabilization of the plasma membrane and intracellular membranes, we have demonstrated directly that PrP in the Golgi of Tg(L9R-3AV) neurons has the ^{Ctm}PrP topology (Stewart and Harris, 2005). In control experiments (data not shown), we found that wild-type PrP in neurons from nontransgenic mice was distributed primarily along the surface of neuronal processes, with little detectable intracellular staining. Thus, the ^{Ctm}PrP form of L9R-3AV PrP is concentrated in the Golgi apparatus of neurons, whereas the ^{Sec}PrP form is present on the surface of neuronal processes.

To confirm that the results obtained in cultured neurons were also applicable to brain tissue, we performed immunohistochemical staining of PrP in Triton X-100-permeabilized brain sections from Tg(L9R-3AV) mice. In the granule cell layer of the cerebellum, we found that L9R-3AV PrP was concentrated in small foci within granule cell bodies that colocalized with giantin (Fig. 7*F–H*), similar to the distribution of the protein in cultured neurons. In contrast, sections from nontransgenic control mice showed strong staining for wild-type PrP in the glomeruli surrounding granule neurons but little staining within the granule cell bodies themselves (Fig. 7*I–K*). Staining of Triton X-100-treated sections from the cerebral cortex and hippocampus of Tg(L9R-3AV) mice also revealed Golgi-localized PrP in the cell bodies of many neurons (data not shown).

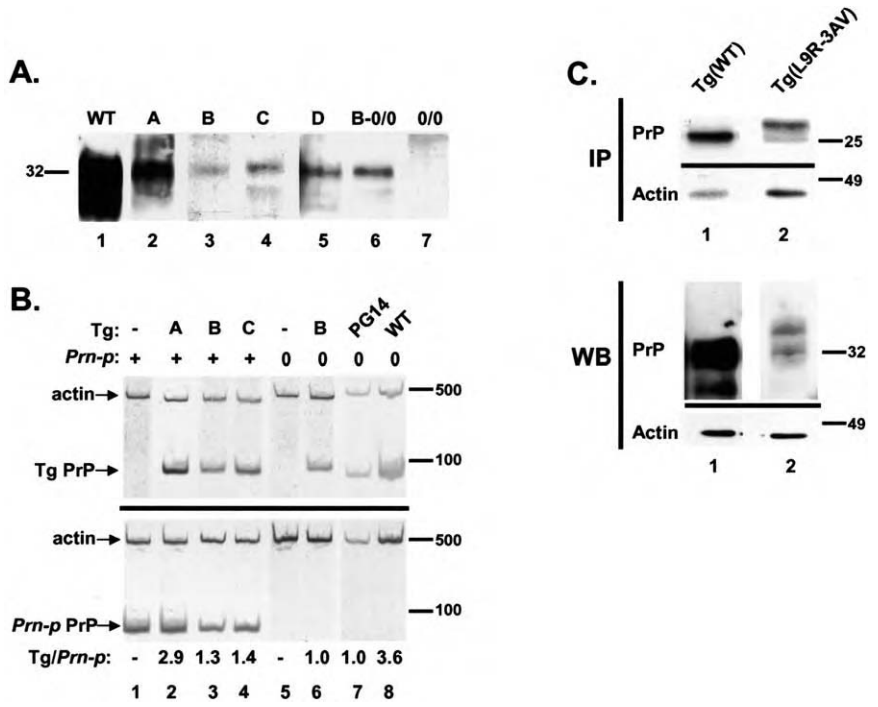

Figure 5. Expression of PrP in the brain and in cultured neurons from Tg(L9R-3AV) mice. ***A***, Brain homogenates from the following mice were analyzed by Western blotting using anti-PrP antibody 3F4: lane 1, Tg(WT); lanes 2–5, Tg(L9R-3AV $^{+/-}$)/*Prn-p*$^{+/+}$ lines A–D, respectively; lane 6, Tg(L9R-3AV $^{+/-}$)/*Prn-p*$^{0/0}$ line B; lane 7, nontransgenic *Prn-p*$^{0/0}$. Lane 1 was exposed for a shorter time than the other lanes. The molecular size marker is in kilodaltons. ***B***, RNA was extracted from the brains of mice whose transgene (Tg) and *Prn-p* status are indicated above each lane. For transgene status, A, B, and C indicate lines of Tg(L9R-3AV $^{+/-}$) mice, and a − symbol indicates that the mouse is nontransgenic. For *Prn-p* status, the + symbol indicates *Prn-p*$^{+/+}$, and the 0 symbol indicates *Prn-p*$^{0/0}$. RT-PCR was performed using primers specific for mouse β-actin and transgenically encoded PrP (top) or for mouse β-actin and endogenous (*Prn-p*-encoded) PrP (bottom). PCR products (indicated by arrows) were resolved by PAGE and stained with SYBRGreen. Tg/*Prn-p* indicates the calculated ratio of transgenically encoded to endogenous PrP. Size markers are given in nucleotides. ***C***, Duplicate cultures of cerebellar granule cells were prepared from Tg(WT) mice (lane 1) or from Tg(L9R-3AV-B $^{+/-}$)/*Prn-p*$^{0/0}$ mice (lane 2). One culture of each pair was labeled for 4 h with [^{35}S]methionine, and then PrP and actin were detected by immunoprecipitation (IP) followed by SDS-PAGE and autoradiography. The other culture of the pair was lysed, and PrP and actin were visualized by Western blotting (WB). 8H4 antibody was used to detect PrP in the experiments shown here, but similar results were obtained with 3F4 antibody (data not shown). Proteins were enzymatically deglycosylated before immunoprecipitation. In the IP experiment, the slightly slower migration of L9R-3AV PrP compared with wild-type PrP is attributable to the presence of the signal peptide on the mutant protein (Stewart and Harris, 2005).

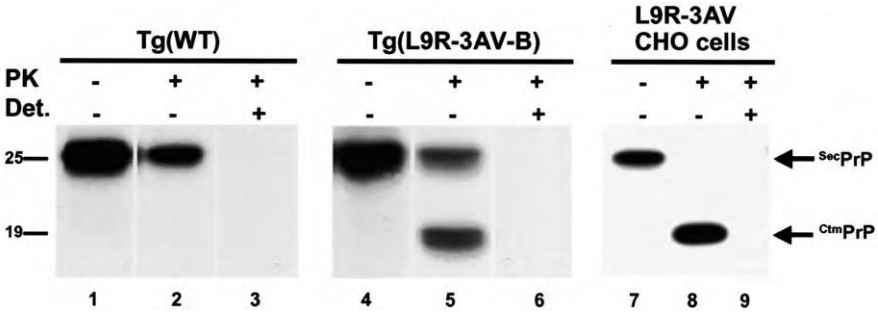

Figure 6. Neurons from Tg(L9R-3AV) mice produce both ^{Ctm}PrP and ^{Sec}PrP. CGNs cultured from Tg(WT) (lanes 1–3) or Tg(L9R-3AV-B $^{+/-}$)/*Prn-p*$^{+/+}$ (lanes 4–6) mice were labeled for 4 h with [^{35}S]methionine. CHO cells were transiently transfected with a plasmid encoding L9R-3AV PrP (lanes 7–9). Postnuclear supernatants from all cultures were then incubated with (lanes 2, 3, 5, 6, 8, 9) or without (lanes 1, 4, 7) PK in the presence (lanes 3, 6, 9) or absence (lanes 1, 2, 4, 5, 7, 8) of Triton X-100 (Det.). Proteins were then solubilized in SDS and enzymatically deglycosylated, and PrP was detected either by immunoprecipitation with 3F4 antibody (lanes 1–6) or by Western blotting with 3F4 antibody (lanes 7–9). The protease-protected forms of ^{Sec}PrP and ^{Ctm}PrP are indicated by arrows to the right of the gels.

L9R-3AV PrP does not have PrP^{Sc} properties

Previous studies have shown that ^{Ctm}PrP can cause neurodegeneration in the absence of PrP^{Sc} (Hegde et al., 1998b, 1999). We therefore tested whether PrP from Tg(L9R-3AV) mice displayed three characteristic biochemical properties of PrP^{Sc}: detergent insolubility, protease resistance, and a conformational alteration that alters antibody accessibility. As a control, we analyzed PrP from Tg(WT) and Tg(PG14) mice. Tg(PG14) mice express an insertionally mutated PrP that exhibits several PrP^{Sc}-like features (Chiesa et al., 1998). We performed these ex-

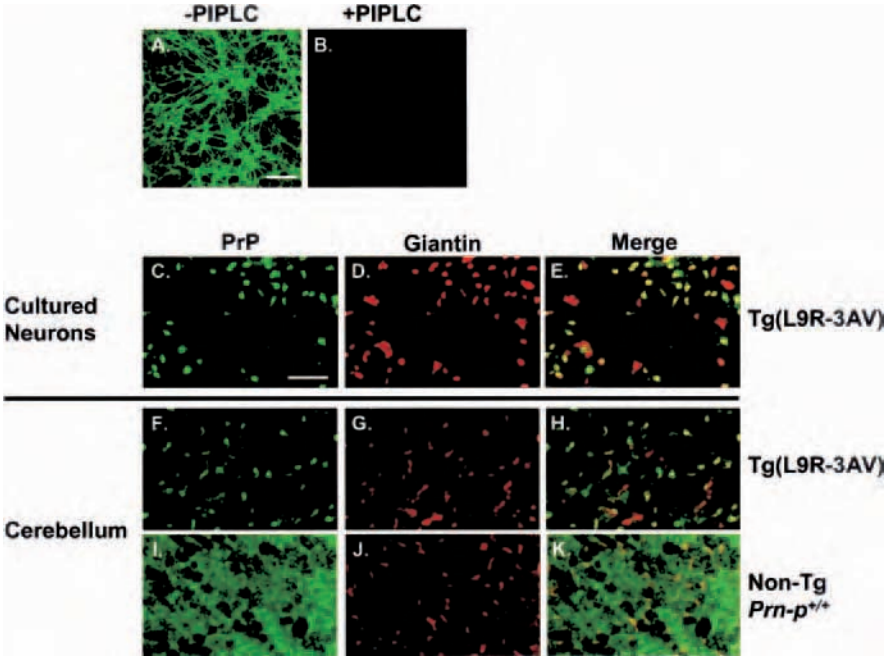

Figure 7. ^{Sec}PrP is localized to the cell surface, and ^{Ctm}PrP is localized to the Golgi apparatus. ***A***, ***B***, Cerebellar granule cells cultured from Tg(L9R-3AV-B $^{+/-}$)/*Prn-p*$^{0/0}$ mice were incubated with (***B***) or without (***A***) PIPLC and stained without permeabilization using 8H4 antibody to reveal surface PrP. ***C–E***, Cerebellar granule cells cultured from Tg(L9R-3AV-B $^{+/-}$)/*Prn-p*$^{0/0}$ mice were fixed, permeabilized with Triton X-100, and stained with anti-PrP (8B4) and anti-giantin antibodies. A green-labeled secondary antibody was used to visualize PrP (***C***), and a red-labeled secondary antibody was used to visualize giantin (***D***). ***E***, Merged image of the green and red channels demonstrating colocalization of PrP and giantin (yellow). A few cells show only red staining for giantin, presumably because they express lower levels of PrP. ***F–K***, Permeabilized vibratome sections from the cerebella of Tg(L9R-3AV-B $^{+/+}$)/*Prn-p*$^{0/0}$ (***F–H***) or nontransgenic (Non-Tg) *Prn-p*$^{+/+}$ (***I–K***) mice were stained with anti-PrP (8B4) and anti-giantin antibodies. A green-labeled secondary antibody was used to visualize PrP (***F***, ***I***) and a red-labeled secondary antibody was used to visualize giantin (***G***, ***J***). ***H***, ***K***, Merged images of the green and red channels. Images are taken from the granule cell layer of the cerebellum. Scale bars: ***A*** (for ***A***, ***B***), ***C*** (for ***C–K***), 25 μm.

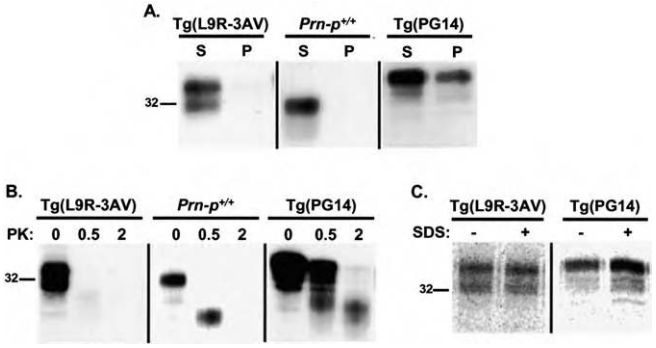

Figure 8. L9R-3AV PrP does not have PrP^{Sc} properties. ***A***, Cerebellar granule cells cultured from Tg(L9R-3AV-B $^{+/-}$)/*Prn-p*$^{+/+}$, nontransgenic *Prn-p*$^{+/+}$, or Tg(PG14) mice were labeled with [^{35}S]methionine for 4 h, and cell lysates were centrifuged at 10,000 $\times$ *g* for 10 min. The supernatant was recentrifuged at 180,000 $\times$ *g* for 45 min, and PrP in supernatant (S) and pellet (P) fractions was immunoprecipitated with 3F4 antibody [Tg(L9R-3AV), Tg(PG14)] or 8H4 antibody (*Prn-p*$^{+/+}$). ***B***, Granule cells were labeled as in ***A***. Clarified cell lysates were incubated with the indicated amounts of PK (in micrograms per milliliter) at 37°C for 20 min, after which PrP was immunoprecipitated with 3F4 antibody [Tg(L9R-3AV), Tg(PG14)] or 8H4 antibody (*Prn-p*$^{+/+}$). ***C***, Granule cells were labeled as in ***A***. PrP was immunoprecipitated from cell lysates with 3F4 antibody, either with (+) or without (−) previous denaturation in the presence of SDS.

periments by labeling cultured cerebellar neurons with [^{35}S]methionine and collecting PrP by immunoprecipitation.

In the assay for detergent insolubility (Fig. 8*A*), we found that mutant PrP in Tg(L9R-3AV) mice, like wild-type PrP in nontransgenic *Prn-p*$^{+/+}$ mice, remained in the supernatant after ultracentrifugation of a detergent lysate. In contrast, a portion of PG14 PrP was found in the pellet fraction. In the protease-resistance assay (Fig. 8*B*), we observed that L9R-3AV PrP and wild-type PrP were sensitive to digestion with low concentrations of PK under conditions in which PG14 PrP yielded a characteristic, protease-resistant fragment of 27–30 kDa. We also performed a conformation-dependent immunoassay to test the accessibility of the 3F4 epitope of PrP under native and denatured conditions (Fig. 8*C*). PrP^{Sc} and PG14 PrP, but not wild-type PrP^{C}, display a buried 3F4 epitope under native conditions (Safar et al., 1998; Chiesa et al., 2003). We found that L9R-3AV PrP (as well as wild-type PrP; data not shown) could be immunoprecipitated with 3F4 equally well in the native state and after SDS denaturation. In contrast, PG14 PrP reacted more efficiently with 3F4 after denaturation. These results indicate that L9R-3AV PrP in neurons does not display any of three biochemical signatures of PrP^{Sc}.

We also failed to detect detergent-insoluble or protease-resistant PrP when we analyzed brain homogenates from symptomatic Tg(L9R-3AV)/*Prn-p*$^{+/+}$ mice by Western blotting using either 3F4 or 8H4 antibody (data not shown). These results indicate that neither L9R-3AV PrP nor endogenous PrP is converted to a PrP^{Sc} state in clinically ill mice. We also inoculated brain homogenates from ill Tg(L9R-3AV)/*Prn-p*$^{+/+}$ mice of the B and C lines into Tga20 $^{+/0}$ indicator mice (Fischer et al., 1996) to assay for infectivity. The inoculated animals have remained healthy for >270 d, whereas Tga20 $^{+/0}$ mice inoculated with Rocky Mountain Laboratory prions become ill after 92 ± 4 d (our unpublished data). Thus, L9R-3AV PrP does not generate infectious prions.

Discussion

We have produced a neurological disorder in transgenic mice by expression of a PrP molecule that carries mutations (L9R-3AV) favoring synthesis of ^{Ctm}PrP, a transmembrane form of PrP. These mice develop severe ataxia accompanied by dramatic loss of cerebellar granule cells and hippocampal pyramidal cells. Unexpectedly, we found that development of this phenotype is strongly dependent on coexpression of endogenous, wild-type PrP. Our results provide new insights into several key issues, including the neuronal cell biology of ^{Ctm}PrP, the mechanisms of PrP-related neurotoxicity, and possible cellular activities of PrP^{C}.

Comparison of Tg(L9R-3AV) mice with other transgenic models

Hegde et al. (1998b, 1999) have previously described transgenic mice that express PrP molecules carrying mutations in the central region alone, including 3AV, that favor synthesis of ^{Ctm}PrP. These mice spontaneously develop a neurodegenerative illness characterized by ataxia and astrocytic gliosis, but without PrP^{Sc}. The mice created by Hegde et al. (1998b, 1999) differ from our Tg(L9R-3AV) mice in several important respects. First, they synthesize lower proportions of ^{Ctm}PrP (20–30%, depending on the

mutation, compared with 50% for L9R-3AV). This difference reflects the fact that mutations in the signal sequence such as L9R enhance production of ^{Ctm}PrP (Stewart and Harris, 2003). Second, the mice in the study by Hegde et al. (1998b, 1999) developed illness at much later times than our Tg(L9R-3AV) mice, when one compares lines that have an equivalent "^{Ctm}PrP index" [% ^{Ctm}PrP × Tg expression level, as defined by Hegde et al. (1999)]. We suggest that this discrepancy reflects the fact that the mice in the study by Hegde et al. (1998b, 1999) were created on the *Prn-p*$^{0/0}$ background and that introduction of the wild-type PrP allele would significantly shorten the incubation time in these animals. We hypothesize that because the mice in the study by Hegde et al. (1998b, 1999) converted proportionally more of their mutant PrP to the ^{Sec}PrP form than Tg(L9R-3AV) mice, this may be sufficient to allow disease development in the absence of endogenous, wild-type ^{Sec}PrP (see below).

Differences between transgenic neurons and transfected cells in ^{Ctm}PrP synthesis and localization

We demonstrated previously that L9R-3AV PrP is synthesized almost exclusively with the ^{Ctm}PrP topology in transiently transfected CHO, baby hamster kidney (BHK), and N2a cells (Stewart et al., 2001; Stewart and Harris, 2003). In contrast, we found that CGNs from Tg(L9R-3AV) mice express ~50% of the mutant protein as ^{Ctm}PrP and ~50% as ^{Sec}PrP. The reasons for this difference between transfected cells and granule neurons remain to be determined. One plausible explanation is that granule neurons and transformed cell lines differ in their content of protein factors that have been shown to influence the membrane topology of PrP during ER translocation (Hegde et al., 1998a; Fons et al., 2003). It is also possible that neurons possess mechanisms for selectively degrading ^{Ctm}PrP.

There is also a difference between granule neurons and transfected cells in the localization of ^{Ctm}PrP. Although most of the ^{Ctm}PrP in granule neurons from Tg(L9R-3AV) mice resides in the Golgi apparatus (this work; Stewart and Harris, 2005), most of the ^{Ctm}PrP in transfected CHO, BHK, and N2a cells expressing L9R-3AV PrP is localized to the ER (Stewart et al., 2001). We have observed that L9R-3AV PrP in fibroblasts cultured from Tg(L9R-3AV) mice is endoglycosidase H resistant (our unpublished data), arguing that the protein is trafficked to a post-ER compartment in these cells as well. Thus, factors other than cell type are likely to determine the localization of the mutant protein. It is possible that the high expression levels characteristic of transiently transfected cells cause ER retention of ^{Ctm}PrP, whereas the more physiological levels present in cells from transgenic mice allows the protein to transit further along the secretory pathway.

What is the neurotoxic species in Tg(L9R-3AV) mice, and what is its locus of action?

Tg(L9R-3AV) mice produce approximately equal proportions of mutant ^{Ctm}PrP and ^{Sec}PrP, raising the question of which of these species is responsible for the neurodegeneration seen in these animals. Two considerations argue against ^{Sec}PrP being the neurotoxic species. First, ^{Sec}PrP produced in Tg(L9R-3AV) mice behaves like wild-type PrP^{C} in terms of its cellular trafficking and biochemical properties. Second, mutations other than L9R-3AV that favor synthesis of ^{Ctm}PrP also cause neurodegeneration when expressed in transgenic mice (Hegde et al., 1998b, 1999). Thus, the L9R-3AV mutation is likely to be neurotoxic because of its effect on ^{Ctm}PrP production, rather than because of a specific alteration of the PrP amino acid sequence. It is unlikely that the neurological illness in Tg(L9R-3AV) mice is related to generation of PrP^{Sc}, because PrP from these animals does not display any of the characteristic biochemical properties of PrP^{Sc}, and the brains of these animals do not contain prion infectivity.

The localization of ^{Ctm}PrP in the Golgi apparatus raises the possibility that the neurotoxic effects of ^{Ctm}PrP may involve this organelle. The Golgi apparatus undergoes a dramatic disassembly process during apoptosis (Maag et al., 2003; Machamer, 2003). In addition, there are several caspase substrates, and at least one procaspase and a caspase inhibitor, that reside in this organelle. Thus, it is possible that ^{Ctm}PrP in the Golgi directly initiates apoptotic signals or amplifies signals that originate elsewhere in the cell.

Why is neurodegeneration in Tg(L9R-3AV) mice dependent on expression of endogenous PrP?

The most intriguing and unexpected observation to emerge from our studies is that the phenotype of Tg(L9R-3AV) mice is greatly accentuated by coexpression of endogenous, wild-type PrP. The effect of endogenous PrP is dose dependent, because Tg(L9R-3AV) mice on the *Prn-p*$^{+/0}$ background display a disease onset intermediate between that of mice on the *Prn-p*$^{0/0}$ and *Prn-p*$^{+/+}$ backgrounds. This latter result makes it unlikely that the amelioration of the phenotype associated with elimination of *Prn-p* alleles is attributable to segregation of unrelated background genes. We have ruled out several other explanations for the phenotypic disparity between mice on the *Prn-p*$^{0/0}$ and *Prn-p*$^{+/+}$ backgrounds, including differences in transgene expression level and alterations in the transgene sequence. In addition, we have confirmed that the proportion of ^{Ctm}PrP and the subcellular localization of this form are similar in CGNs of mice from both backgrounds.

Our results suggest that expression of ^{Ctm}PrP causes neurodegeneration via a process in which endogenous, wild-type PrP^{C} participates. How might this occur? Two possible models are shown in supplemental Figure 1 (available at www.jneurosci.org as supplemental material). In the simplest scheme (supplemental Fig. 1*A*, available at www.jneurosci.org as supplemental material), ^{Ctm}PrP binds to wild-type PrP^{C} (presumably in the ^{Sec}PrP form), resulting in generation of a neurotoxic signal. We also envision a second, more complex model (supplemental Fig. 1*B*, available at www.jneurosci.org as supplemental material) that takes into account a purported physiological function of PrP^{C}, namely its ability to protect neurons from various toxic insults (for review, see Roucou et al., 2004). In this scheme, PrP^{C} normally interacts with another molecule, Tr, that serves a transducer of a neuroprotective signal [supplemental Fig. 1*B* (left), available at www.jneurosci.org as supplemental material]. Because *Prn-p*$^{0/0}$ mice are phenotypically normal (Büeler et al., 1992), this neuroprotective signal would have to be nonessential under most conditions. When ^{Ctm}PrP is present along with ^{Sec}PrP, both proteins bind to Tr, causing the latter to undergo a conformational change to the Tr* state, which delivers a neurotoxic rather than a neuroprotective signal [supplemental Fig. 1*B* (right), available at www.jneurosci.org as supplemental material]. In this model, ^{Ctm}PrP is neurotoxic because it causes an inversion of the normal, neuroprotective activity of PrP^{C}. In both models, the ^{Sec}PrP component could be supplied either by endogenous, wild-type PrP or less efficiently by transgenically encoded L9R-3AV PrP if it were present in sufficient amounts. This hypothesis would explain why deleting the *Prn-p* gene ameliorated but did not completely prevent development of neurological symptoms in Tg(L9R-3AV-C$^{+/-}$)/*Prn-p*$^{0/0}$ and Tg(L9R-3AV-B$^{+/+}$)/*Prn-p*$^{0/0}$ mice. In these animals, the amount of

mutant ^{Sec}PrP may be sufficient to transmit the neurotoxic signal in the absence of endogenous ^{Sec}PrP. The fact that ^{Ctm}PrP is concentrated in the Golgi apparatus of neurons, whereas ^{Sec}PrP is found primarily on the cell surface, does not mitigate against a physical interaction of the two proteins, because ^{Sec}PrP must transit the Golgi on its way to the cell surface.

A new view of the role of ^{Ctm}PrP in prion biology

In this study, we demonstrate that ^{Ctm}PrP-associated neurodegeneration is highly dependent on the presence of wild-type PrP^{C}. This observation potentially connects the toxic activity of ^{Ctm}PrP to the normal, physiological function of PrP^{C}. There are several other situations in which expression of PrP^{C} in target neurons appears to be essential for conferring sensitivity to PrP-related neurotoxic insults (Brown et al., 1994; Brandner et al., 1996; Mallucci et al., 2003; Solforosi et al., 2004). Each of these situations could conceivably reflect the operation of a neurotoxic, PrP^{C}-dependent signaling pathway similar to the one we postulate is activated by ^{Ctm}PrP. Interestingly, the ability of PrP^{C} to accentuate the phenotype of Tg(L9R-3AV) mice appears to be the inverse of its ability to rescue the neurodegenerative phenotype of transgenic mice that ectopically express Doppel (Moore et al., 2001; Rossi et al., 2001) and N-terminally truncated PrP (Shmerling et al., 1998). It will be of great interest to determine whether these two contrasting activities of PrP^{C} are related and, if so, what molecular mechanisms account for whether PrP^{C} delivers a neurotoxic or neuroprotective signal.

References

Bolton DC, Seligman SJ, Bablanian G, Windsor D, Scala LJ, Kim KS, Chen CM, Kascsak RJ, Bendheim PE (1991) Molecular location of a species-specific epitope on the hamster scrapie agent protein. J Virol 65:3667–3675.

Borchelt DR, Davis J, Fischer M, Lee MK, Slunt HH, Ratovitsky T, Regard J, Copeland NG, Jenkins NA, Sisodia SS, Price DL (1996) A vector for expressing foreign genes in the brains and hearts of transgenic mice. Genet Anal Biomol Eng 13:159–163.

Brandner S, Isenmann S, Raeber A, Fischer M, Sailer A, Kobayashi Y, Marino S, Weissmann C, Aguzzi A (1996) Normal host prion protein necessary for scrapie-induced neurotoxicity. Nature 379:339–343.

Brown DR, Herms J, Kretzschmar HA (1994) Mouse cortical cells lacking cellular PrP survive in culture with a neurotoxic PrP fragment. NeuroReport 5:2057–2060.

Büeler H, Fischer M, Lang Y, Fluethmann H, Lipp H-P, DeArmond SJ, Prusiner SB, Aguet M, Weissmann C (1992) Normal development and behavior of mice lacking the neuronal cell-surface PrP protein. Nature 356:577–582.

Chiesa R, Harris DA (2001) Prion diseases: what is the neurotoxic molecule? Neurobiol Dis 8:743–763.

Chiesa R, Piccardo P, Ghetti B, Harris DA (1998) Neurological illness in transgenic mice expressing a prion protein with an insertional mutation. Neuron 21:1339–1351.

Chiesa R, Piccardo P, Quaglio E, Drisaldi B, Si-Hoe SL, Takao M, Ghetti B, Harris DA (2003) Molecular distinction between pathogenic and infectious properties of the prion protein. J Virol 77:7611–7622.

Drisaldi B, Stewart RS, Adles C, Stewart LR, Quaglio E, Biasini E, Fioriti L, Chiesa R, Harris DA (2003) Mutant PrP is delayed in its exit from the endoplasmic reticulum, but neither wild-type nor mutant PrP undergoes retrotranslocation prior to proteasomal degradation. J Biol Chem 278:21732–21743.

Fischer M, Rülicke T, Raeber A, Sailer A, Moser M, Oesch B, Brandner S, Aguzzi A, Weissmann C (1996) Prion protein (PrP) with amino-proximal deletions restoring susceptibility of PrP knockout mice to scrapie. EMBO J 15:1255–1264.

Fons RD, Bogert BA, Hegde RS (2003) Substrate-specific function of the translocon-associated protein complex during translocation across the ER membrane. J Cell Biol 160:529–539.

Hegde RS, Voigt S, Lingappa VR (1998a) Regulation of protein topology by *trans*-acting factors at the endoplasmic reticulum. Mol Cell 2:85–91.

Hegde RS, Mastrianni JA, Scott MR, Defea KA, Tremblay P, Torchia M, DeArmond SJ, Prusiner SB, Lingappa VR (1998b) A transmembrane form of the prion protein in neurodegenerative disease. Science 279:827–834.

Hegde RS, Tremblay P, Groth D, DeArmond SJ, Prusiner SB, Lingappa VR (1999) Transmissible and genetic prion diseases share a common pathway of neurodegeneration. Nature 402:822–826.

Hölscher C, Bach UC, Dobberstein B (2001) Prion protein contains a second endoplasmic reticulum targeting signal sequence located at its C terminus. J Biol Chem 276:13388–13394.

Kim SJ, Rahbar R, Hegde RS (2001) Combinatorial control of prion protein biogenesis by the signal sequence and transmembrane domain. J Biol Chem 276:26132–26140.

Maag RS, Hicks SW, Machamer CE (2003) Death from within: apoptosis and the secretory pathway. Curr Opin Cell Biol 15:456–461.

Machamer CE (2003) Golgi disassembly in apoptosis: cause or effect? Trends Cell Biol 13:279–281.

Mallucci G, Dickinson A, Linehan J, Klohn PC, Brandner S, Collinge J (2003) Depleting neuronal PrP in prion infection prevents disease and reverses spongiosis. Science 302:871–874.

Miller TM, Johnson Jr EM (1996) Metabolic and genetic analyses of apoptosis in potassium/serum-deprived rat cerebellar granule cells. J Neurosci 16:7487–7495.

Moore RC, Mastrangelo P, Bouzamondo E, Heinrich C, Legname G, Prusiner SB, Hood L, Westaway D, DeArmond SJ, Tremblay P (2001) Doppel-induced cerebellar degeneration in transgenic mice. Proc Natl Acad Sci USA 98:15288–15293.

Prusiner SB (1998) Prions. Proc Natl Acad Sci USA 95:13363–13383.

Rossi D, Cozzio A, Flechsig E, Klein MA, Rulicke T, Aguzzi A, Weissmann C (2001) Onset of ataxia and Purkinje cell loss in PrP null mice inversely correlated with Dpl level in brain. EMBO J 20:694–702.

Roucou X, Gains M, LeBlanc AC (2004) Neuroprotective functions of prion protein. J Neurosci Res 75:153–161.

Safar J, Wille H, Itrri V, Groth D, Serban H, Torchia M, Cohen FE, Prusiner SB (1998) Eight prion strains have PrP^{Sc} molecules with different conformations. Nat Med 4:1157–1165.

Shmerling D, Hegyi I, Fischer M, Blättler T, Brandner S, Götz J, Rülicke T, Flechsig E, Cozzio A, von Mering C, Hangartner C, Aguzzi A, Weissmann C (1998) Expression of amino-terminally truncated PrP in the mouse leading to ataxia and specific cerebellar lesions. Cell 93:203–214.

Shyng SL, Moulder KL, Lesko A, Harris DA (1995) The N-terminal domain of a glycolipid-anchored prion protein is essential for its endocytosis via clathrin-coated pits. J Biol Chem 270:14793–14800.

Solforosi L, Criado JR, McGavern DB, Wirz S, Sanchez-Alavez M, Sugama S, DeGiorgio LA, Volpe BT, Wiseman E, Abalos G, Masliah E, Gilden D, Oldstone MB, Conti B, Williamson RA (2004) Cross-linking cellular prion protein triggers neuronal apoptosis *in vivo*. Science 303:1514–1516.

Stewart RS, Harris DA (2001) Most pathogenic mutations do not alter the membrane topology of the prion protein. J Biol Chem 276:2212–2220.

Stewart RS, Harris DA (2003) Mutational analysis of topological determinants in prion protein (PrP) and measurement of transmembrane and cytosolic PrP during prion infection. J Biol Chem 278:45960–45968.

Stewart RS, Harris DA (2005) A transmembrane form of the prion protein is localized in the Golgi apparatus of neurons. J Biol Chem, in press.

Stewart RS, Drisaldi B, Harris DA (2001) A transmembrane form of the prion protein contains an uncleaved signal peptide and is retained in the endoplasmic reticulum. Mol Biol Cell 12:881–889.

Weissmann C (2004) The state of the prion. Nat Rev Microbiol 2:861–871.

Zanusso G, Liu D, Ferrari S, Hegyi I, Yin X, Aguzzi A, Hornemann S, Liemann S, Glockshuber R, Manson JC, Brown P, Petersen RB, Gambetti P, Sy MS (1998) Prion protein expression in different species: analysis with a panel of new mAbs. Proc Natl Acad Sci USA 95:8812–8816.

THE JOURNAL OF BIOLOGICAL CHEMISTRY
Vol. 280, No. 16, Issue of April 22, pp. 15855–15864, 2005
Printed in U.S.A.

A Transmembrane Form of the Prion Protein Is Localized in the Golgi Apparatus of Neurons*

Received for publication, October 29, 2004, and in revised form, January 10, 2005
Published, JBC Papers in Press, January 25, 2005, DOI 10.1074/jbc.M412298200

Richard S. Stewart and David A. Harris‡

From the Department of Cell Biology and Physiology, Washington University School of Medicine, St. Louis, Missouri 63110

^{Ctm}PrP is a transmembrane version of the prion protein that has been proposed to be a neurotoxic intermediate underlying prion-induced pathogenesis. In previous studies, we found that PrP molecules carrying mutations in the N-terminal signal peptide (L9R) and the transmembrane domain (3AV) were synthesized exclusively in the ^{Ctm}PrP form in transfected cell lines. To characterize the properties of ^{Ctm}PrP in a neuronal setting, we have utilized cerebellar granule neurons cultured from Tg(L9R–3AV) mice that developed a fatal neurodegenerative illness. We found that about half of the L9R-3AV PrP synthesized in these neurons represents ^{Ctm}PrP, with the rest being ^{Sec}PrP, the glycolipid anchored form that does not span the membrane. Both forms contained an uncleaved signal peptide, and they are differentially glycosylated. ^{Sec}PrP was localized on the surface of neuronal processes. Most surprisingly, ^{Ctm}PrP was concentrated in the Golgi apparatus, rather in the endoplasmic reticulum as it is in transfected cell lines. Our study is the first to analyze the properties of ^{Ctm}PrP in a neuronal context, and our results suggest new hypotheses about how this form may exert its neurotoxic effects.

Prion diseases are fatal neurological disorders of humans and animals characterized by ataxia and neuronal degeneration (1). Unlike other neurodegenerative diseases, they can have an infectious as well as a sporadic or familial origin. Most cases are associated with the presence of PrP^{Sc},[1] a conformationally altered isoform of PrP^{C}, a cell surface glycoprotein of uncertain function that is expressed primarily in neurons of the brain and spinal cord. PrP^{C} is monomeric, protease-sensitive, and rich in α-helical structure. In contrast, PrP^{Sc} is aggregated, protease-resistant, and rich in β-sheets. There is considerable evidence that PrP^{Sc} is an infectious protein and that conversion of PrP^{C} into PrP^{Sc} is the central event in the propagation of prions, the infectious agents in these diseases (2, 3).

Although it is clear that PrP^{Sc} accumulates in the brain during most prion diseases, there is uncertainty about the mechanisms responsible for neuronal death. Several lines of evidence suggest that PrP^{Sc} is not toxic when it is presented to neurons externally (4, 5) and that conversion of PrP^{C} to PrP^{Sc} within neurons may generate toxic intermediates or by-products. However, there is debate about the identity of these neurotoxic species (6). Several alternative forms of PrP, distinct from both PrP^{C} and PrP^{Sc}, have been proposed as key pathogenic entities based on experiments in cell culture and transgenic mice. These include transmembrane PrP (7, 8), cytosolic PrP (9), protease-sensitive PrP^{Sc} (10), and $PG14^{spon}$ PrP (11).

This report focuses on transmembrane PrP. PrP is unusual because it can exist in several different topological forms that are generated during synthesis in the endoplasmic reticulum (ER). Most molecules assume the form designated ^{Sec}PrP, in which the polypeptide chain has been fully translocated into the ER lumen with its C terminus attached to the lipid bilayer by a glycosylphosphatidylinositol (GPI) anchor (12, 13). Under certain circumstances, however, the protein can adopt either of two opposite transmembrane orientations (designated ^{Ctm}PrP and ^{Ntm}PrP) in which a highly conserved stretch of hydrophobic amino acids in the middle of the sequence integrates into the membrane (7, 14–16). In ^{Ctm}PrP, the C terminus of the protein lies in the ER lumen, whereas in ^{Ntm}PrP, the N terminus is luminal. Mutations within and adjacent to the transmembrane domain that enhance its hydrophobicity increase the proportion of ^{Ctm}PrP (from <10% to 20–30% of the total PrP) (7, 8, 17). Some of these mutations (A117V and P105L) are associated with familial prion diseases, whereas others (3AV) are not seen in human patients.

Because the brains of patients with the A117V mutation do not contain conventional PrP27–30 (the protease-resistant core of PrP^{Sc}) (18), it was proposed that ^{Ctm}PrP, rather than PrP^{Sc}, is the proximal cause of neurodegeneration in this these and possibly other cases of prion disease (7, 8). Consistent with this hypothesis, transgenic mice expressing PrP with ^{Ctm}PrP-favoring mutations develop a spontaneous neurodegenerative illness that is similar to scrapie, but without detectable PrP^{Sc} (7). Based on these and other results, it was suggested that ^{Ctm}PrP is a key neurotoxic intermediate in both familial and infectious prion diseases and that the amount of this form can be increased directly by pathogenic mutations, or indirectly by accumulation of PrP^{Sc} (8). However, uncertainties remain about the role of ^{Ctm}PrP in prion diseases because of recent reports that ^{Ctm}PrP levels do not change significantly during scrapie infection (19) or as a result of most pathogenic mutations (17).

Our laboratory has been interested in investigating further the role of ^{Ctm}PrP in prion diseases. To this end, we have identified mutations that cause PrP to be synthesized exclu-

* This work was supported by Department of Defense Grant DAMD-03-0531 (to R. S. S.) and National Institutes of Health Grant NS35496 (to D. A. H.). The costs of publication of this article were defrayed in part by the payment of page charges. This article must therefore be hereby marked "*advertisement*" in accordance with 18 U.S.C. Section 1734 solely to indicate this fact.

‡ To whom correspondence should be addressed: Dept. of Cell Biology and Physiology, Washington University School of Medicine, 660 South Euclid Ave., St. Louis, MO 63110. Tel.: 314-362-4690; Fax: 314-747-0940; E-mail: dharris@cellbiology.wustl.edu.

[1] The abbreviations used are: PrP^{Sc}, scrapie isoform of prion protein; endo H, endoglycosidase H; ER, endoplasmic reticulum; GPI, glycosylphosphatidylinositol; PIPLC, phosphatidylinositol-specific phospholipase C; PK, proteinase K; PrP, prion protein; PrP^{C}, cellular isoform of PrP; WT, wild type; CHO, Chinese hamster ovary; BHK, baby hamster kidney; Tg, transgene; PNGase, peptide:*N*-glycosidase; PBS, phosphate-buffered saline; PDI, protein-disulfide isomerase.

sively with the ^{Ctm}PrP topology, thus facilitating analysis of this form in the absence of the other topological variants. We demonstrated that ^{Ctm}PrP has an uncleaved, N-terminal signal peptide (16) and that substitution of charged residues in the hydrophobic core of the signal sequence strongly favors synthesis of ^{Ctm}PrP (19). Combining one of these mutations (L9R) with a previously studied mutation in the transmembrane domain (3AV) resulted in a protein that was expressed entirely as ^{Ctm}PrP after *in vitro* translation and transfection of cultured cells (16). The presence of the L9R-3AV mutation caused a striking change in the subcellular distribution of PrP; the protein was no longer present on the plasma membrane like wild-type PrP but was instead concentrated in the ER of transfected CHO, BHK, and N2a cells (16). This result raised the possibility that the ER could be a potential site for the neurotoxic action of ^{Ctm}PrP.

To extend our studies to an *in vivo* setting, we have recently created transgenic mice expressing L9R-3AV PrP.[2] We found that these mice develop a fatal, ataxic neurological disorder accompanied by extensive degeneration of cerebellar granule neurons and hippocampal pyramidal cells. To our surprise, we found that this phenotype was strongly dependent on coexpression of endogenous, wild-type PrP. Here we have taken advantage of the availability of Tg(L9R-3AV) mice to study the cell biology and metabolism of ^{Ctm}PrP in neurons. We find that, in contrast to transfected cell lines, cultured neurons expressing transgenically encoded L9R-3AV localize ^{Ctm}PrP to the Golgi apparatus rather than to the ER. This observation dramatically changes our view of the possible cellular pathways that may be responsible for ^{Ctm}PrP-induced neurotoxicity.

EXPERIMENTAL PROCEDURES

Transgenic Mice—Engineering of Tg(L9R-3AV) mice is described elsewhere.[2] The experiments reported here were carried out using mice from the B line, but similar results were obtained using mice from the C line (data not shown). Mice were hemizygous for the transgene array, and were maintained on both *Prn-p*$^{+/+}$ and *Prn-p*$^{0/0}$ backgrounds. Tg(WT-E1)/*Prn-p*$^{0/0}$ and Tg(PG14-A2)/*Prn-p*$^{0/0}$ mice have been described previously (20).

Cerebellar Granule Cell Culture—Primary cultures from 5-day-old pups were performed as described previously (21). Dissociated cells were resuspended in CGN medium (basal medium Eagle's, 10% dialyzed fetal bovine serum, 25 mM KCl, 2 mM glutamine, 50 μg/ml gentamycin) and plated at a density of 500,000 cells/cm^2 in polylysine-coated plastic plates or 8-well glass chamber slides. Cells were used after 4–5 days in culture. Based on staining with cell type-specific marker proteins, these cultures typically contained >95% granule neurons, with the remainder of cells being fibroblasts and astrocytes.

Antibodies—The following anti-PrP antibodies were used for immunoprecipitation, immunofluorescence staining, or Western blotting: 8H4 and 8B4 (22); 3F4 (23); anti-SP (19); P45-66 (12).

Metabolic Labeling of Cultured Cells and Immunoprecipitation of PrP—Cerebellar granule cells were labeled with 100–500 μCi/ml of ^{35}S-Promix (Amersham Biosciences) in CGN medium lacking methionine, cysteine, and bovine serum and containing B27 vitamin supplement (Invitrogen). In some experiments, cells were chased in complete medium lacking radioactive methionine and cysteine, with or without PIPLC (1 unit/ml; purified from *Bacillus thuringiensis* as described by Shyng *et al.* (24)). Pulse-chase labeling of CHO cells was carried out as described previously (25).

Cells were lysed in 0.5% SDS, 50 mM Tris-HCl (pH 7.5), and immunoprecipitation of PrP was carried out as described previously (25). To treat PrP with glycosidases, protein was eluted from protein A-Sepharose beads by heating at 95 °C for 5 min in 0.1% SDS, 50 mM Tris-HCl (pH 6.7). The eluate was incubated for 1 h at 37 °C with endo H, neuraminidase, or PNGase F (all from New England Biolabs, Beverly, MA) according to the manufacturer's directions. Immunoprecipitated PrP was analyzed by SDS-PAGE and autoradiography.

PrP Membrane Topology Assay—Cerebellar granule cells were metabolically labeled for 4–6 h as described above. Cells were then scraped into PBS, spun at 2,000 × *g* for 5 min, and resuspended in ice-cold homogenization buffer (250 mM sucrose, 5 mM KCl, 5 mM $MgCl_2$, 50 mM Tris-HCl (pH 7.5)). Cells were lysed by 12 passages through silastic tubing (0.3-mm inner diameter) connecting two syringes with 27-gauge needles, and nuclei were removed by centrifugation at 5,000 × *g* for 10 min. Aliquots of the postnuclear supernatant were diluted into 50 mM Tris-HCl (pH 7.5) and incubated for 60 min at 4 °C with 250 μg/ml PK in the presence or absence of 0.5% Triton X-100. Digestion was terminated by addition of phenylmethylsulfonyl fluoride (5 mM final concentration), and PrP was then immunoprecipitated and deglycosylated by treatment with PNGase F.

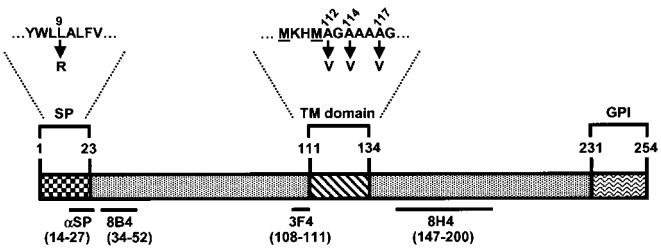

FIG. 1. **Schematic structure of mouse PrP.** *SP*, signal peptide; *TM*, transmembrane; *GPI*, glycosylphosphatidylinositol anchor addition sequence. The numbers *above* the drawing are the amino acid positions that define the ends of each domain. The *horizontal lines below* the drawing indicate the locations of epitopes recognized by antibodies used in this study, with the amino acid positions of each epitope given in *parentheses.* The amino acid sequence surrounding the L9R and 3AV mutations are shown *above* the signal peptide and transmembrane domains, respectively. 3AV is the designation for the triple mutation A112V/A114V/A117V. The *two underlined* methionine residues at positions 108 and 111 were introduced to create an epitope for 3F4 antibody, which allows discrimination of transgenically encoded and endogenous PrP.

Western Blotting—Brain tissue was homogenized using a Teflon pestle in 10 volumes of PBS containing protease inhibitors (phenylmethylsulfonyl fluoride, 20 μg/ml; leupeptin and pepstatin, 10 μg/ml). Homogenates were clarified by centrifugation at 2,000 × *g* for 5 min. Cultured neurons were lysed in 0.5% SDS, 50 mM Tris-HCl (pH 7.5), and the lysates were heated at 95 °C for 10 min. Protein was quantified using a BCA Assay (Pierce). Samples were analyzed by SDS-PAGE followed by immunoblotting with anti-PrP antibodies. In some cases, samples were treated with endo H or PNGase F, and proteins were recovered by methanol precipitation prior to SDS-PAGE.

Immunocytochemistry—Cerebellar granules cells were grown in 8-well chamber slides. For surface staining, cells were transferred to B27 medium (Dulbecco's modified Eagle's medium containing B27 vitamin supplement) and stained with anti-PrP antibodies (1:500 dilution) for 10 min at 37 °C. After rinsing in PBS, cells were fixed for 10 min at room temperature in 4% paraformaldehyde, 5% sucrose in PBS, blocked for 10 min in PBS, 2% goat serum, and stained with Alexa 488-conjugated goat anti-mouse IgG (Molecular Probes, Eugene, OR). Cells were mounted in 50% glycerol/PBS. In some cases, cells were incubated at 37 °C for 2 h with PIPLC (1 unit/ml) in B27 medium prior to fixation.

For visualization of intracellular PrP, cells were first fixed for 10 min at 4 °C in 4% paraformaldehyde, 5% sucrose in PBS and were then incubated for 10 min at 4 °C, either in 0.2% Triton X-100 in PBS (to permeabilize all membranes) or in 10 μg/ml digitonin in digitonin buffer (10% sucrose, 100 mM KOAc, 2.5 mM $MgCl_2$, 1 mM EDTA, 10 mM HEPES-HCl, pH 7.0) (to selectively permeabilize the plasma membrane) (26–28). After treatment with blocking solution, cells were stained with antibodies against PrP, giantin (Covance, Berkeley, CA), or PDI (StressGen, Victoria, British Columbia, Canada). Cells were then incubated with secondary antibodies (Alexa 488-conjugated goat anti-mouse IgG and Alexa 546-conjugated goat anti-rabbit IgG). In some experiments, cells were treated for 4 h with 10 μg/ml brefeldin A (Sigma) prior to staining. Cells were viewed with a Zeiss LSM 510 confocal microscope equipped with an Axiovert 200 laser scanning system.

RESULTS

The L9R-3AV mutation is illustrated in Fig. 1. We have generated and characterized two lines of transgenic mice that express PrP carrying this mutation.[2] These Tg(L9R-3AV) mice

[2] Stewart, R. S., Piccardo, P., Ghetti, B., and Harris, D. A. (2005) *J. Neurosci.*, in press.

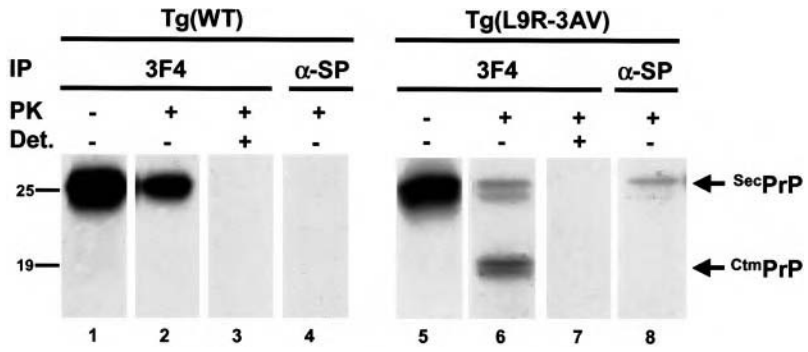

FIG. 2. **Neurons from Tg(L9R-3AV) mice produce both ^{Ctm}PrP and ^{Sec}PrP.** Cerebellar granule neurons cultured from Tg(WT) mice (*lanes 1–4*) or from Tg(L9R-3AV-B)/*Prn-p*$^{0/0}$ mice (*lanes 5–8*) were labeled for 4 h with [^{35}S]methionine. Postnuclear supernatants from all cultures were then incubated with (*lanes 2–4* and *6–8*) or without (*lanes 1* and *5*) PK in the presence (*lanes 3* and *7*) or absence (*lanes 1*, *2*, *4*, *5*, *6*, and *8*) of Triton X-100 (*Det.*). Proteins were then solubilized in SDS and enzymatically deglycosylated, and PrP was detected either by immunoprecipitation (*IP*) with either 3F4 antibody (*lanes 1–3* and *5–7*) or anti-SP antibody (*lanes 4* and *8*). The protease-protected forms of ^{Sec}PrP and ^{Ctm}PrP are indicated by *arrows to the right* of the gels. The protected bands appear as doublets in some samples due to nibbling of the polypeptide chain by PK. Molecular size markers are in kilodaltons.

develop a spontaneous neurological disorder characterized by ataxia and by loss of cerebellar granule cells and hippocampal pyramidal neurons. We utilized primary cultures of granule cells prepared from the cerebella of Tg(L9R-3AV) mice at postnatal day 5 to characterize the cell biology and metabolism of the mutant PrP in a neuronal setting.

Cultured Neurons from Tg(L9R-3AV) Mice Produce Both ^{Ctm}PrP and ^{Sec}PrP—We first used a protease protection assay to analyze the topology of L9R-3AV PrP in microsomes from granule neurons. Microsomes in a postnuclear supernatant prepared from [^{35}S]methionine-labeled neurons were subjected to digestion with proteinase K (PK), and PrP was then immunoprecipitated with 3F4 antibody after enzymatic deglycosylation (Fig. 2). We observed the following two protease-protected forms of PrP in approximately equal amounts (Fig. 2, *lane 6*): a 27-kDa band representing ^{Sec}PrP molecules that were fully protected from digestion because of their localization in the microsome lumen, and a 19-kDa fragment representing the luminal and transmembrane domains of ^{Ctm}PrP with the exposed cytoplasmic domain removed. We did not detect a 15-kDa fragment indicative of ^{Ntm}PrP. As expected, inclusion of Triton X-100 during protease treatment in order to disrupt microsomal membranes resulted in complete digestion of PrP (Fig. 2, *lane 7*). When the same analysis was carried out on microsomes from Tg(WT) neurons, only a fully protected 25-kDa band corresponding to ^{Sec}PrP was observed (Fig. 2, *lane 2*). Thus, granule neurons produce approximately equal proportions of ^{Sec}PrP and ^{Ctm}PrP from PrP carrying the L9R-3AV mutation. For both wild-type and mutant proteins, there was a decrease in the total amount of protected PrP after PK treatment, an effect that we attribute to the presence of some inside-out and damaged microsomes and not to the presence of cytoplasmic PrP.

Biosynthesis and Turnover of Mutant PrP—We used pulse-chase labeling with [^{35}S]methionine to analyze the biosynthetic maturation and degradation of L9R-3AV PrP in cerebellar granule neurons (Fig. 3*A*). A portion of each cell lysate was incubated with endoglycosidase H (endo H) prior to immunoprecipitation of PrP in order to test whether the *N*-linked glycans had matured to an endo H-resistant state, a step that occurs as proteins transit the mid-Golgi apparatus. At the end of the 20-min pulse-labeling period, a single species of PrP with a molecular mass of 32 kDa was observed. This form was shifted to 27 kDa, the size of unglycosylated PrP, by treatment with endo H, indicating the presence of immature glycan chains. The 32-kDa species was converted into two glycoforms of 32 and 35 kDa over the next 20 min of chase. Both of these mature forms contained glycans that were endo H-resistant. The 32- and 35-kDa glycoforms both decayed with a half-life of ~2.5 h, similar to the half-life of wild-type PrP in granule neurons (25). These data suggest the existence of a single metabolic pool of L9R-3AV PrP in neurons, implying that the ^{Ctm}PrP and ^{Sec}PrP in these cells do not have markedly different kinetic properties.

For comparison, we also analyzed the biosynthesis of L9R-3AV PrP in transiently transfected CHO cells (Fig. 3*B*). In CHO cells, the mutant protein was initially synthesized as two species of 32 and 27 kDa. The 27-kDa form was not glycosylated, and the 32-kDa form was core-glycosylated, because it is sensitive to endo H. However, the 32-kDa form in CHO cells remained endo H-sensitive throughout the entire chase period, unlike the case for the glycosylated forms of L9R-3AV in granule neurons. These results indicate that, whereas the mutant protein is retained in a pre-Golgi compartment in CHO cells, it transits beyond the mid-Golgi in granule neurons. Despite these differences in glycosylation and cellular trafficking, L9R-3AV PrP in CHO cells decayed with a half-life (~2.5 h) that was similar to the one observed for this mutant in neurons (see above) and for wild-type PrP in CHO cells (25).

L9R-3AV PrP Retains an Uncleaved Signal Peptide—We demonstrated previously that ^{Ctm}PrP synthesized by *in vitro* translation or by expression in CHO cells contains an uncleaved N-terminal signal peptide (16). To determine whether L9R-3AV PrP in cerebellar granule neurons also has the same feature, we immunoprecipitated PrP from [^{35}S]methionine-labeled cultures using anti-SP, an antibody that specifically recognizes PrP molecules containing an intact signal peptide (19). Parallel samples were immunoprecipitated with 3F4 or 8H4 antibodies, which recognize PrP molecules regardless of the presence of the signal peptide (see Fig. 1 for the location of antibody epitopes). As an additional way of discriminating molecules with and without the signal peptide, proteins were enzymatically deglycosylated to permit detection of the small size difference between the two species (27 and 25 kDa for signal peptide bearing, and signal peptide-cleaved forms, respectively).

When cultures from Tg(L9R-3AV)/*Prn-p*$^{+/+}$ mice were analyzed, two bands (25 and 27 kDa) of approximately equal intensity could be resolved after immunoprecipitation with 8H4 antibody (Fig. 4, *lane 1*). However, only the larger band was recognized by 3F4 and anti-SP antibodies (Fig. 4, *lanes 2* and *3*). This result demonstrates that the 27-kDa form represents transgenically encoded PrP that contains the 3F4 epitope and has an intact signal peptide, whereas the 25-kDa form represents endogenous mouse PrP that lacks the 3F4 epitope and has a cleaved signal peptide. Because >90% of the PrP recog-

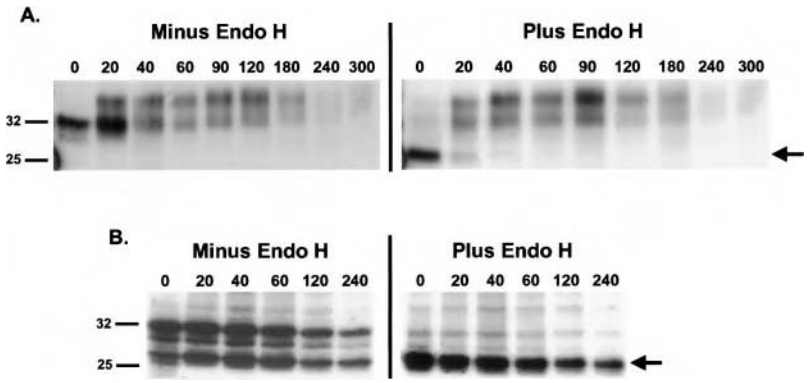

FIG. 3. **L9R-3AV PrP matures into an endo H-resistant form in cerebellar granule neurons but not in CHO cells.** *A*, cerebellar granule cells cultured from Tg(L9R-3AV-B)/*Prn-p*$^{+/+}$ mice were pulse-labeled with [^{35}S]methionine for 20 min and then chased for the indicated times (in min) in medium containing nonradioactive methionine. Cells were then lysed, and PrP was isolated by immunoprecipitation with 3F4 antibody. Half of the immunoprecipitated PrP was treated with endo H (gels on the *right*), and half was left untreated (gels on the *left*) prior to analysis by SDS-PAGE and autoradiography. The *arrow* at the *right* indicates the position of unglycosylated PrP. *B*, the same experiment as in *A* was performed on CHO cells transiently transfected with a plasmid encoding L9R-3AV PrP.

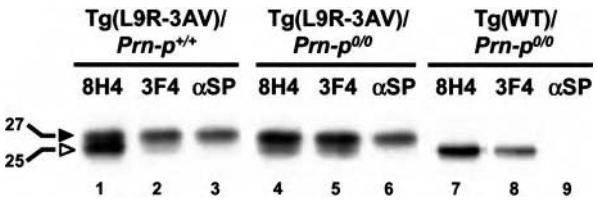

FIG. 4. **L9R-3AV PrP in neurons has an uncleaved signal peptide.** Cerebellar granule neurons from Tg(L9R-3AV-B)/*Prn-p*$^{+/+}$ mice (*lanes 1–3*), Tg(L9R-3AV-B)/*Prn-p*$^{0/0}$ mice (*lanes 4–6*), or Tg(WT)/*Prn-p*$^{0/0}$ mice (*lanes 7–9*) were labeled with [^{35}S]methionine for 4 h. PrP was then immunoprecipitated from cell lysates using either 8H4 (*lanes 1*, *4*, and *7*), 3F4 (*lanes 2*, *5*, and *8*), or anti-SP (*lanes 3*, *6*, and *9*) antibodies. Immunoprecipitated PrP was enzymatically deglycosylated with PNGase F prior to analysis by SDS-PAGE. The *filled* and *open arrowheads* to the *left* of *lane 1* indicate the signal peptide-bearing (27 kDa) and the signal peptide-cleaved (25 kDa) forms of PrP, respectively.

nized by 3F4 migrated at 27 kDa (*lane 2*), we infer that the majority of the L9R-3AV PrP in granule neurons, comprising both ^{Sec}PrP and ^{Ctm}PrP, retained an intact signal peptide. This conclusion was confirmed when we analyzed neurons from Tg(L9R-3AV)/*Prn-p*$^{0/0}$ mice. In this case, ~90% of the PrP immunoprecipitated by 3F4 migrated at 27 kDa, with the rest migrating at 25 kDa (Fig. 4, *lane 5*). A similar ratio of the two forms was observed with 8H4, the expected result because the neurons contain no endogenous PrP that would be recognized by this antibody (Fig. 4, *lane 4*). Again, only the 27-kDa form was immunoprecipitated by anti-SP (Fig. 4, *lane 6*). The amount of 25-kDa PrP in Tg(L9R-3AV) neurons varied somewhat in different experiments, possibly due to artifactual proteolysis after cell lysis, but it never exceeded ~20% of the total. As anticipated, Tg(WT) neurons produced only a 25-kDa form of PrP that was immunoprecipitated by 8H4 and 3F4 but not by anti-SP (Fig. 4*, lanes 7–9*).

Further evidence that ^{Sec}PrP contains an uncleaved signal peptide was provided by immunoprecipitation of PrP from PK-treated microsomes using anti-SP antibody (Fig. 2). The fully protected 27-kDa species in Tg(L9R-3AV) neurons reacted with anti-SP (Fig. 2, *lane 8*), whereas the corresponding 25-kDa band from Tg(WT) neurons did not (*lane 4*), implying that ^{Sec}PrP in the former cells contains an uncleaved signal peptide. As expected, the 19-kDa ^{Ctm}PrP fragment in Tg(L9R-3AV) neurons was not recognized by anti-SP (compare Fig. 2, *lanes 6* and *8*), because the N terminus of ^{Ctm}PrP lies on the cytoplasmic side of the membrane, and so its uncleaved signal peptide would be accessible to protease digestion.

^{Sec}PrP but Not ^{Ctm}PrP Is Present on the Neuronal Surface—In a previous study, we found by immunofluorescence staining that L9R-3AV PrP was absent from the surface of transfected CHO and BHK cells and was completely retained in the ER (16). This result was in accord with the observed endo H sensitivity of the protein in these cells. Our observation (Fig. 3) that L9R-3AV PrP in granule neurons matures to an endo H-resistant form suggested that localization of the mutant protein in these cells was likely to be different from CHO and BHK cells. We therefore analyzed the distribution of L9R-3AV PrP in granule neurons by using immunofluorescence microscopy.

In our first set of experiments, neurons from Tg(L9R-3AV)/*Prn-p*$^{0/0}$ mice were stained in the living state without permeabilization to selectively recognize PrP on the cell surface. As shown in Fig. 5, *A–C*, we observed positive staining with antibodies directed against three different epitopes distributed along the length of the PrP molecule (Fig. 1), including 8B4 (residues 34–52), 3F4 (residues 108–111), and 8H4 (residues 147–200). Staining was distributed along neuronal processes, which formed an extensive network throughout the culture. Because the epitopes for antibodies 8B4 and 3F4 are extracellular in ^{Sec}PrP but not in ^{Ctm}PrP, the accessibility of these epitopes to externally applied antibodies implied that at least some of the L9R-3AV PrP on the surface of the neurons must be in the ^{Sec}PrP form. Control experiments demonstrated that endogenous, wild-type PrP on neurons from *Prn-p*$^{+/0}$ mice stained with 8B4 and 8H4, but not with 3F4 (because endogenous PrP lacks the 3F4 epitope) (Fig. 5, *D–F*), and that none of the antibodies stained neurons from *Prn-p*$^{0/0}$ mice (not shown). In addition, neurons were not stained with an antibody directed against a cytoplasmic epitope of the Golgi protein, giantin, confirming the integrity of the surface membrane (not shown).

To further demonstrate the presence of ^{Sec}PrP on the cell surface, we treated living neurons with PIPLC, a bacterial enzyme which cleaves the C-terminal GPI anchor. PIPLC is predicted to release ^{Sec}PrP, but not ^{Ctm}PrP, from the cell surface, because the latter has a transmembrane segment that would maintain attachment to the plasma membrane even after the GPI anchor was cleaved. We found that PIPLC treatment eliminated virtually all surface staining for PrP, assayed by using 8H4 antibody, implying that most of the protein on the surface represented ^{Sec}PrP (Fig. 6, *A* and *D*). Any residual ^{Ctm}PrP should have reacted with 8H4, because the epitope recognized by this antibody is extracellular. As expected, wild-type PrP was also completely released by PIPLC from the surface of nontransgenic, *Prn-p*$^{+/+}$ neurons (Fig. 6, *B* and *E*). As an additional control, we demonstrated that neurons from Tg(PG14) mice did display residual PrP staining after PIPLC

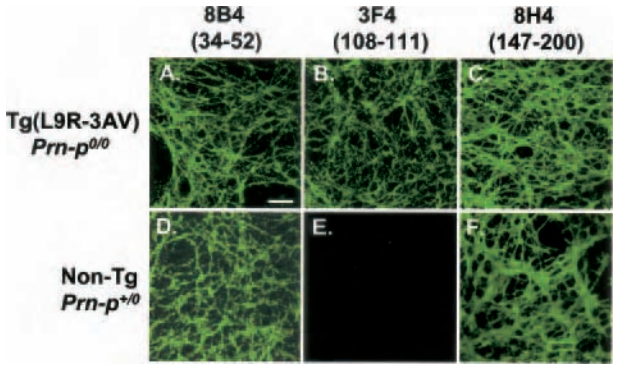

FIG. 5. **L9R-3AV PrP on the cell surface is accessible to antibodies recognizing epitopes distributed along the length of the molecule.** Cerebellar granule neurons cultured from Tg(L9R-3AV-B)/*Prn-p*$^{0/0}$ mice (*A–C*) or nontransgenic *Prn-p*$^{+/0}$ mice (*D–F*) were stained without permeabilization using antibodies 8B4 (*A* and *D*), 3F4 (*B* and *E*), or 8H4 (*C* and *F*) to reveal surface PrP. The epitopes recognized by each antibody are given in *parentheses*. The *scale bar* in *A* (applicable to all panels) is 25 μm.

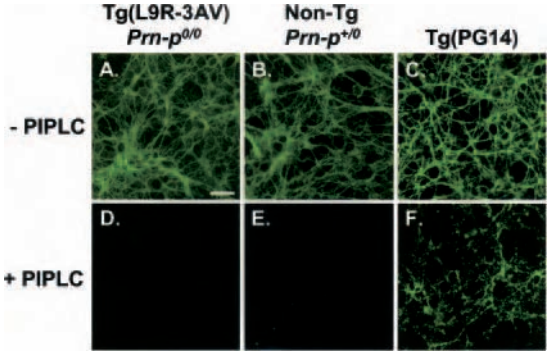

FIG. 6. **L9R-3AV PrP on the cell surface is releasable with PIPLC.** Cerebellar granule cells cultured from Tg(L9R-3AV-B)/*Prn-p*$^{0/0}$ mice (*A* and *D*), nontransgenic *Prn-p*$^{+/0}$ mice (*B* and *E*), or Tg(PG14) mice (*C* and *F*) were incubated with (*D–F*) or without (*A–C*) PIPLC and were then stained without permeabilization using anti-PrP antibodies. 8H4 antibody was used for *A*, *B*, *D*, and *E*; and 3F4 antibody was used for *C* and *F*. The *scale bar* in *A* (applicable to all panels) is 25 μm.

treatment, consistent with the partial resistance of the PG14 protein to GPI anchor cleavage (20) (Fig. 6, *C* and *F*). This control rules out the possibility that protease contamination in the PIPLC preparation degraded surface PrP. Taken together, our results indicate that there is little ^{Ctm}PrP on the cell surface and that most of the protein in this location represents ^{Sec}PrP.

^{Ctm}PrP Is Localized to the Golgi Apparatus—Because about half of the L9R-3AV PrP present in granule neurons represents ^{Ctm}PrP (Fig. 2), and because little of this form is present on the cell surface (Fig. 6), our results suggested that ^{Ctm}PrP was likely to be localized in an intracellular compartment. To visualize the intracellular distribution of the mutant protein, we stained neurons that had been permeabilized with Triton X-100. In control experiments with *Prn-p*$^{+/0}$ neurons, wild-type PrP was found to be localized primarily along neuronal processes (Fig. 7*A*), corresponding to the surface PrP visualized on these cells by staining without permeabilization (Fig. 5, *D* and *F*). The distribution of PrP in neurons from Tg(L9R-3AV) mice, on both *Prn-p*$^{0/0}$ and *Prn-p*$^{+/+}$ backgrounds, was markedly different. The mutant protein was concentrated in discrete, perinuclear structures in the soma that colocalized with the Golgi marker protein, giantin (Fig. 7, *D–F*). Staining of neuronal processes was less prominent in these permeabilized neurons than in unpermeabilized ones (compare Figs. 5*A* and 7*D*),

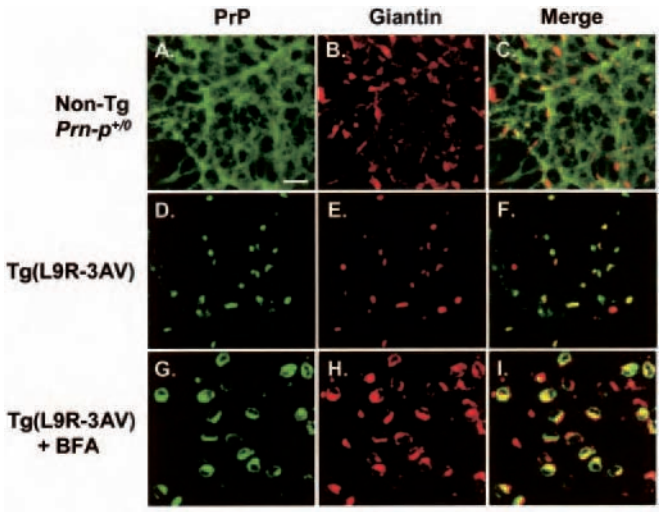

FIG. 7. **L9R-3AV PrP inside neurons is localized to the Golgi apparatus and is redistributed by brefeldin A (*BFA*).** Cerebellar granule cells cultured from nontransgenic *Prn-p*$^{+/0}$ mice (*A–C*) or from Tg(L9R-3AV-B)/*Prn-p*$^{0/0}$ mice (*D–I*) were fixed, permeabilized with Triton X-100, and then stained with anti-PrP and anti-giantin antibodies. Prior to fixation, one set of cultures (*G–I*) was treated with brefeldin A (10 μg/ml) for 4 h at 37 °C. A *green*-labeled secondary antibody was used to visualize PrP (*A*, *D*, and *G*), and a *red*-labeled secondary antibody was used to visualize giantin (*B*, *E*, and *H*). *C*, *F*, and *I* show a merged image of the green and red channels, demonstrating colocalization of PrP and giantin (*yellow*) in neurons from Tg(L9R-3AV) but not nontransgenic mice. Brefeldin A causes a redistribution of both PrP and giantin in Tg(L9R-3AV) neurons. 8H4 was used to stain PrP in *A* and 8B4 in *D* and *G*, but equivalent results were obtained regardless of which of these two antibodies was used (not shown). The *scale bar* in *A* (applicable to all panels) is 25 μm.

which reflects partial extraction of plasma membrane PrP as well as enhanced reactivity of cytoplasmic epitopes of Golgi-resident PrP after Triton X-100 treatment.[3] To confirm the Golgi localization of L9R-3AV PrP, we treated neurons with brefeldin A, which causes fusion of the ER and Golgi compartments. This treatment resulted in a redistribution of both PrP and giantin to a more diffuse pattern, consistent with the conclusion that the two proteins reside in the same structures (Fig. 7, *G–I*). We conclude from these results, and from the results with unpermeabilized cells (Figs. 5 and 6), that L9R-3AV PrP in neurons is present in the Golgi apparatus as well as on the plasma membrane.

We performed a series of experiments to directly probe the membrane topology of L9R-3AV PrP *in situ* by immunofluorescence staining. Treatment of cells with digitonin, a cholesterol-binding detergent, permeabilizes only the plasma membrane but not internal membranes such as those of the Golgi and ER, because the latter have a lower content of cholesterol (26–28). In contrast, Triton X-100 permeabilizes all membranes. We found that antibody 8B4, which is directed against an N-terminal epitope (Fig. 1, *34–52*), produced prominent Golgi staining in neurons permeabilized with either digitonin or Triton (Fig. 8, *A* and *E*). A similar result was seen with another N-terminally directed antibody, P45-66, which recognizes residues 45–66 within the octapeptide repeat region (not shown). In contrast, antibody 8H4, which reacts with a C-terminal region (Fig. 1, *147–200*), stained PrP in the Golgi only after Triton treatment (Fig. 8, *F–H*); in digitonin-treated neurons, staining was visible exclusively on neuronal processes, representing cell surface PrP molecules (Fig. 8, *B–D*). The observation that N-terminal epitopes of L9R-3AV PrP are accessible without permeabilization of Golgi membranes, whereas C-ter-

[3] R. S. Stewart and D. A. Harris, unpublished observations.

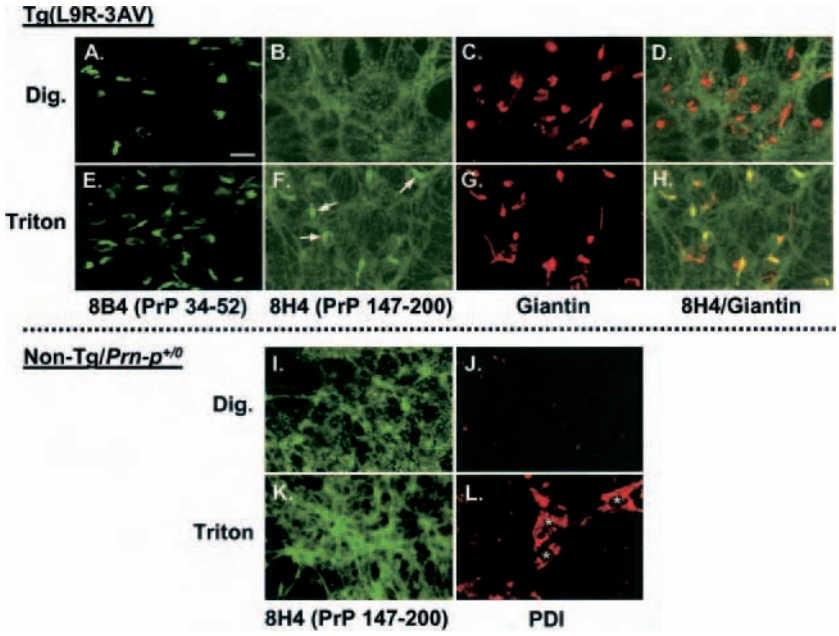

FIG. 8. **L9R-3AV PrP in the Golgi apparatus has the ^{Ctm}PrP topology.** Cerebellar granule cells cultured from Tg(L9R-3AV-B)/*Prn-p*$^{0/0}$ mice (*A–H*) or nontransgenic *Prn-p*$^{+/0}$ mice (*I–L*) were fixed and permeabilized with either digitonin (*Dig.*) (*A–D*, *I*, and *J*) or Triton X-100 (*E–H*, *K*, and *L*). Cells were then stained for PrP using either 8B4 (*A* and *E*) or 8H4 (*B*, *F*, *I*, and *K*) in conjunction with a green-labeled secondary antibody. Cells were simultaneously stained for a cytoplasmic epitope of giantin (*C* and *G*) or for PDI (*J* and *L*) in conjunction with a red-labeled secondary antibody. *D* and *H* show a merged image of the red and green channels. The *arrows* in *F* indicate spots of PrP staining that become apparent only after Triton permeabilization and that colocalize with giantin (*yellow* color in *H*). The *asterisks* in *L* indicate the location of fibroblasts in which PDI is visualized only after Triton permeabilization. The *scale bar* in *A* (applicable to all panels) is 25 μm.

minal epitopes are not, indicates that mutant protein in the Golgi has the ^{Ctm}PrP topology. When we performed the same experiment on neurons from nontransgenic *Prn-p*$^{+/0}$ mice, neurite staining was observed with both 8B4 and 8H4, regardless of the method of permeabilization (Fig. 8, *I* and *K*). This result reflects the fact that most wild-type PrP is found on the surface of neuronal processes, where it is present in the form of ^{Sec}PrP.

Two control experiments demonstrated the selectivity of the permeabilization procedures. Protein-disulfide isomerase (PDI), a luminal ER protein, was accessible to staining in Triton-treated but not digitonin-treated cultures, proving that digitonin did not permeabilize internal membranes. This result was most easily appreciated in the small number of fibroblasts present in the cultures, which have higher PDI levels than the neurons (Fig. 8, *J* and *L*). In contrast, an antibody to a cytoplasmic epitope of giantin stained the Golgi apparatus of neurons treated with either digitonin or Triton, demonstrating permeabilization of the plasma membrane by both detergents (Fig. 8, *C* and *G*).

Taken together, our immunofluorescence localization studies of intact and permeabilized neurons indicate that the ^{Ctm}PrP form L9R-3AV PrP is concentrated in the Golgi apparatus, whereas the ^{Sec}PrP form is present on the surface of neuronal processes like wild-type PrP.

^{Sec}PrP and ^{Ctm}PrP Are Differentially Glycosylated—We wondered whether the 32- and 35-kDa glycoforms of L9R-3AV PrP seen in pulse-labeling experiments (Fig. 3) might correspond to the two different topological forms of the protein, one being ^{Sec}PrP and the other, ^{Ctm}PrP. To answer this question, we treated [^{35}S]methionine-labeled neurons with PIPLC in order to release ^{Sec}PrP from the cell surface. We found that only the 32-kDa band was released into the medium by PIPLC, implying that this glycoform represents ^{Sec}PrP (Fig. 9*A*, *upper panels*). At least some of the 35-kDa glycoform that remained cell-associated after PIPLC treatment must therefore represent ^{Ctm}PrP. However, our results do not rule out the possibility that the 35-kDa band might also include molecules of ^{Sec}PrP that reside in intracellular compartments not accessible to externally applied PIPLC. In control experiments, wild-type PrP was completely released into the medium by PIPLC treatment, consistent with localization of virtually all of the protein on the cell surface (Fig. 9*A*, *lower panels*). In addition, both the 32- and 35-kDa glycoforms of L9R-3AV PrP underwent a characteristic decrease in gel mobility when detergent lysates were treated with PIPLC (Fig. 9*B*). Thus, lack of release of the 35-kDa form was due to its residence in an intracellular compartment, rather than to the presence of a phospholipase-resistant anchor structure.

To further analyze the glycoform profile of L9R-3AV in neurons, we tested the sensitivity of the oligosaccharide chains to neuraminidase, which cleaves sialic acid residues that are added in the trans cisterna of the Golgi. We found that both the 32- and 35-kDa forms of mutant PrP were shifted by neuraminidase treatment, although the shift was larger for the latter form (Fig. 9*C*, *lanes 2* and *3*). As observed previously, neither form was sensitive to endo H (Fig. 9*C*, *lane 4*). In contrast, both forms were shifted to 27 kDa, the size of unglycosylated PrP, by treatment with PNGase F, which cleaves all *N*-linked glycans regardless of structure (Fig. 9*C*, *lane 5*). These results indicate that both the 32- and 35-kDa forms of L9R-3AV PrP transit the trans cisterna of the Golgi in neurons but that the latter form is more heavily modified by sialic acid residues in that compartment. Consistent with an unusual oligosaccharide composition of the 35-kDa species is the fact that it has a higher M_r than mature, doubly glycosylated, wild-type PrP from cultured neurons, which migrates at 32 kDa (Fig. 9*C*, compare *lanes 1* and *2*).

Because our previous experiments were carried out on isolated cerebellar granule neurons, we also analyzed the glycosylation pattern of L9R-3AV PrP in whole brain by Western blotting. We found that the mutant protein in brain, as in cultured neurons, was composed of 32- and 35-kDa glycoforms, both of which were endo H-resistant and PNGase-sensitive

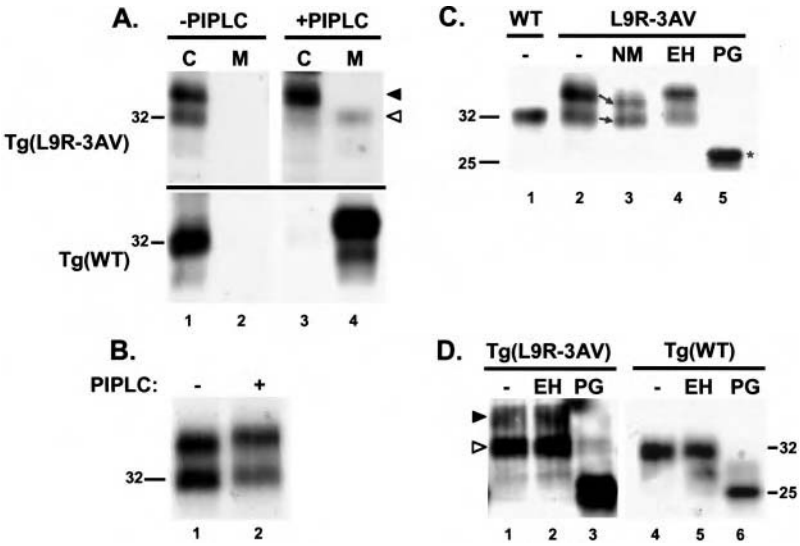

FIG. 9. **^{Sec}PrP and ^{Ctm}PrP are differentially glycosylated.** *A*, cerebellar granule cells cultured from Tg(L9R-3AV-B)/*Prn-p*$^{+/+}$ mice (*upper panels*) or from Tg(WT) mice (*lower panels*) were labeled for 3 h with [^{35}S]methionine and were then chased for 1.5 h in nonradioactive medium containing (*lanes 3* and *4*) or lacking (*lanes 1* and *2*) PIPLC. PrP in cells (*C*, *lanes 1* and *3*) and medium (*M*, *lanes 2* and *4*) was then immunoprecipitated with 3F4. Only the 32-kDa glycoform of L9R-3AV PrP (*open arrowhead*) is released into the medium by PIPLC, whereas the 35-kDa glycoform (*filled arrowhead*) remains cell-associated. Wild-type PrP is quantitatively released by PIPLC (*lower panel*, *lane 4*). *B*, cerebellar granule cells cultured from Tg(L9R-3AV-B)/*Prn-p*$^{+/+}$ mice were labeled and chased as in *A*. Cell lysates were incubated with (*lane 2*) or without (*lane 1*) PIPLC, and PrP was immunoprecipitated with 3F4. Note that both glycoforms undergo a small decrease in gel mobility. *C*, cerebellar granule cells cultured from Tg(WT) mice (*lane 1*) or from Tg(L9R-3AV-B)/*Prn-p*$^{+/+}$ mice (*lanes 2–5*) were labeled for 4 h with [^{35}S]methionine, and PrP was then immunoprecipitated from cell lysates using 3F4. Immunoprecipitated PrP was incubated without enzyme (*lanes 1* and *2*) or was treated with neuraminidase (*lane 3*), endo H (*lane 4*), or PNGase F (*lane 5*) prior to analysis by SDS-PAGE. The *arrows* between *lanes 2* and *3* indicate a shift in migration of the two glycoforms of L9R-3AV PrP following neuraminidase treatment. This shift is larger for the 35-kDa glycoform than for the 32-kDa glycoform (1.5 *versus* 1 kDa, respectively). The *asterisk* to the *right* of *lane 5* indicates the position of unglycosylated PrP. *WT*, wild type; *NM*, neuraminidase; *EH*, endo H; *PG*, PNGase F. *D,* homogenates of Tg(L9R-3AV) brain (*lanes 1–3*) or Tg(WT) brain (*lanes 4–6*) were Western-blotted by using 3F4 antibody. Samples were either left untreated (*lanes 1* and *4*) or were treated with endo H (*lanes 2* and *5*) or PNGase F (*lanes 3* and *6*). The *open* and *filled arrowheads* to the *left* of *lane 1* indicate the positions, respectively, of the 32- and 35-kDa glycoforms of L9R-3AV PrP.

(Fig. 9*D*, *lanes 1–3*). The proportion of the 35-kDa glycoform appeared to be lower in brain than in cultured neurons, but it was difficult to draw quantitative conclusions concerning the ratio of the two forms because of the weak reactivity of L9R-3AV PrP on Western blots.[2] In comparison, wild-type PrP in transgenic brain migrated as a major species of 32 kDa (Fig. 9*D*, *lane 4–6*). These results suggest that the post-translational processing of L9R-3AV PrP by isolated cerebellar granule neurons may be qualitatively similar to its processing by neurons *in situ* within transgenic brain.

DISCUSSION

We report here our analysis of PrP synthesized in cerebellar granule neurons cultured from Tg(L9R-3AV) mice. The PrP molecules in these cells carry an L9R-3AV mutation that strongly favors synthesis of ^{Ctm}PrP (16). Tg(L9R-3AV) mice develop a fatal neurological illness accompanied by extensive degeneration of several populations of neurons in the brain, including cerebellar granule cells.[2] Our results demonstrate that, in cerebellar granule neurons, ^{Ctm}PrP is concentrated in the Golgi apparatus, rather than in the ER as it is in transfected cells. Our study is the first to analyze the synthesis and subcellular localization of ^{Ctm}PrP in a neuronal context, and our results suggest new hypotheses about the mechanism by which this form may exert its neurotoxic effects.

Regulation of PrP Topology in Neurons—We found that granule neurons from Tg(L9R-3AV) mice express about 50% of the mutant protein as ^{Ctm}PrP and about 50% as ^{Sec}PrP. In contrast, we demonstrated previously that L9R-3AV PrP is synthesized almost exclusively with the ^{Ctm}PrP topology in transiently transfected CHO, BHK, and N2a cells (16). This difference between granule neurons and transfected cells may reflect the action of important regulatory mechanisms. The membrane topology of PrP is determined by sequence determinants in the polypeptide chain as well as by trans-acting factors that operate at the translocon during the translocation process (15, 29–31). ^{Ctm}PrP is the default topology of PrP synthesized in translocation reactions reconstituted from minimal components (Sec61p complex and SRP receptor) (31). Inclusion of an additional protein complex known as TRAP (translocon-associated protein) allows synthesis of ^{Sec}PrP as well as ^{Ctm}PrP in these reactions (32). One plausible explanation for our results is that the amount or activity of the TRAP complex, or of some other accessory factors, is different in granule neurons compared with transformed cell lines. It is also possible that, in conjunction with decreased capability for synthesis of ^{Ctm}PrP, neurons possess mechanisms for selectively degrading this form. This latter process may be important if neurons are particularly susceptible to a toxic effect of ^{Ctm}PrP.

^{Ctm}PrP and ^{Sec}PrP Are Differentially Localized—Our data demonstrate that ^{Sec}PrP is present on the plasma membrane, primarily on neuronal processes, whereas ^{Ctm}PrP is found in the Golgi apparatus in the cell body. This conclusion is based on immunofluorescence staining of cultured granule neurons and is consistent with the observed endo H resistance of L9R-3AV PrP in lysates of granule neurons and brain. We have also observed Golgi localization of L9R-3AV PrP in neurons by immunocytochemical staining of vibratome sections cut from the cerebellum, hippocampus, and cerebral cortex of Tg(L9R-3AV) mice, confirming the results reported here on granule neurons in culture.[2] Our data suggest the following model for the cellular trafficking of ^{Ctm}PrP and ^{Sec}PrP in neurons (Fig. 10). Both ^{Ctm}PrP and ^{Sec}PrP are initially synthesized in the ER and are then transported to the Golgi. ^{Ctm}PrP remains trapped

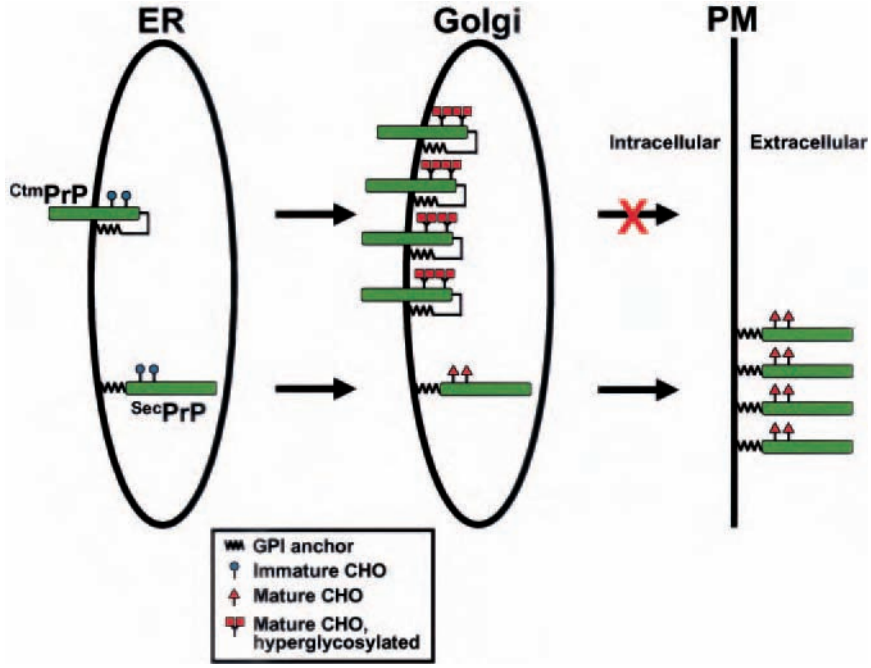

FIG. 10. **Model for the trafficking and glycosylation of ^{Ctm}PrP and ^{Sec}PrP in neurons based on analysis of L9R-3AV PrP.** *CHO*, *N*-linked oligosaccharide chain; *ER*, endoplasmic reticulum; *PM*, plasma membrane. Both ^{Ctm}PrP and ^{Sec}PrP are synthesized in the endoplasmic reticulum with immature (endo H-sensitive) oligosaccharide chains. Both forms are then transported to the Golgi where the oligosaccharide chains mature to an endo H-resistant form. ^{Ctm}PrP is retained in the Golgi where it becomes hyperglycosylated (35 kDa), and ^{Sec}PrP (32 kDa) continues along the secretory pathway to the plasma membrane.

in the Golgi, whereas ^{Sec}PrP continues its transit to the plasma membrane where it is eventually distributed along neuronal processes.

The explanation for the differential trafficking of ^{Ctm}PrP and ^{Sec}PrP remains to be determined. One possibility is that ^{Ctm}PrP contains a Golgi retention or retrieval signal that is absent in ^{Sec}PrP. The transmembrane domain of ^{Ctm}PrP is a likely candidate for such a retention signal, because a number of other Golgi resident proteins utilize membrane-embedded segments as retention signals (33). The L9R-3AV mutation itself does not seem to impair delivery of ^{Sec}PrP molecules to the cell surface, implying that this mutation does not result in gross misfolding of the protein.

The subcellular localization of L9R-3AV PrP in granule neurons is dramatically different from its localization in transiently transfected CHO, BHK, and N2a cells. In these transfected cells, the mutant protein is retained in the ER and remains endo H-sensitive throughout its metabolic lifetime (this paper and see Ref. 16). We have observed that L9R-3AV PrP is endo H-resistant in fibroblasts cultured from Tg(L9R-3AV) mice,[3] arguing that factors other than cell type determine the localization of the mutant protein. It is possible that the high expression levels characteristic of transiently transfected cells cause ER retention of ^{Ctm}PrP, whereas the more physiological levels present in cells from transgenic mice allow the protein to transit further along the secretory pathway.

Post-translational Processing of ^{Ctm}PrP and ^{Sec}PrP—Our pulse-chase labeling experiments indicate that L9R-3AV PrP is synthesized in the ER as an endo H-sensitive precursor that subsequently matures to two endo H-resistant glycoforms as the protein transits the Golgi. Our analysis indicates that these two glycoforms of 32 and 35 kDa correspond to ^{Sec}PrP and ^{Ctm}PrP, respectively. The 35-kDa form is larger than the mature, doubly glycosylated wild-type PrP (~32 kDa), and it undergoes a larger shift in gel mobility after treatment with neuraminidase. These observations suggest that ^{Ctm}PrP is hyperglycosylated, possibly due to its protracted residence in the Golgi apparatus, where sialic acids are added in the trans cisterna. Because the two glycoforms of mutant PrP migrate with different mobilities even after neuraminidase treatment, ^{Ctm}PrP must be distinguished from ^{Sec}PrP by post-translational modifications in addition to sialic acid residues. These conclusions regarding the maturation and glycosylation of ^{Ctm}PrP and ^{Sec}PrP have been incorporated into the model shown in Fig. 10.

Despite the difference in their subcellular localization and glycosylation, ^{Ctm}PrP and ^{Sec}PrP appear to decay with a similar metabolic half-life (~2.5 h). The mechanisms responsible for degradation of L9R-3AV in neurons and other cells remain to be determined. In a previous report, we showed by Western blotting that L9R-3AV PrP accumulated in transiently transfected BHK cells treated for 16 h with a proteasome inhibitor (16). This observation suggested that ^{Ctm}PrP may be a substrate for proteasomal degradation following retrotranslocation from the ER. However, we subsequently discovered that long term treatment of cells with proteasome inhibitors causes an artifactual increase in PrP mRNA levels when expression is driven from a strong viral promoter (25). When we tested shorter inhibitor treatments in pulse-chase labeling experiments, we found that the inhibitors had no effect on the maturation or turnover of L9R-3AV PrP in either cerebellar granule neurons or transfected cells.[3] We thus conclude that the proteasome does not play a prominent role in the metabolism of L9R-3AV PrP in these cell types.

The signal sequence of ^{Sec}PrP, like that of other secreted glycoproteins, is normally cleaved by a signal peptidase that acts in the lumen of the ER. In contrast, ^{Ctm}PrP contains an uncleaved signal sequence (16), reflecting the fact that the N terminus of this form remains in the cytoplasm and does not enter the ER lumen. We report here that, in neurons, both the Ctm and Sec forms of L9R-3AV PrP contain an uncleaved signal sequence, even though the latter molecules have been completely translocated into the ER lumen. One explanation for this phenomenon is that the L9R mutation itself interferes with the action of signal peptidase. Alternatively, signal peptidase may be less active, or the topogenesis of ^{Sec}PrP may be different, in neurons compared with non-neuronal systems. Analysis of L9R PrP expressed in neurons would help resolve this issue.

The presence of an uncleaved signal peptide does not seem to interfere with trafficking of mutant ^{Sec}PrP to the neuronal cell surface. Moreover, ^{Sec}PrP could be released from the cell surface by PIPLC, suggesting that the hydrophobic signal peptide does not integrate into the lipid bilayer. In pulse-chase exper-

iments (not shown), we found that L9R-3AV PrP molecules recognized by anti-SP antibody were present throughout the chase period and appeared to decay with a half-life similar to that of molecules recognized by 3F4 antibody. These results indicate that the mutant PrP in neurons is synthesized with an intact signal peptide and that the signal peptide is not selectively cleaved during maturation and turnover of the protein.

All of the experiments reported here have been carried out on cerebellar granule neurons cultured from Tg(L9R-3AV) mice. Of course, it is possible that other types of neurons may handle the mutant PrP differently. However, we find that Western blots of brain lysates from Tg(L9R-3AV) mice display the same endo H-resistant PrP glycoforms of 32 and 35 kDa that are seen in cultured granule neurons, albeit in different relative amounts. This result is consistent with the possibility that the post-translational processing and subcellular localization of mutant protein are qualitatively similar in many types of neurons in Tg(L9R-3AV) brain. This conclusion is also consistent with our observation that L9R-3AV PrP is concentrated in the Golgi of neurons from a number of brain regions, based on immunocytochemical staining of brain sections.[2]

Comparison with Other Studies—Ours is the first published study to examine the localization and metabolism of ^{Ctm}PrP in cultured neurons. Hegde *et al.* (7) have reported that PrP carrying either of two ^{Ctm}PrP-favoring mutations (3AV or K109I/H110I) is endo H-resistant in brain lysates from transgenic mice. This result implies that ^{Ctm}PrP induced by these mutations has also transited the mid-Golgi, although immunocytochemical localization studies would be necessary to confirm its precise localization.

Singh and colleagues have reported increased surface expression of a C-terminal fragment of ^{Ctm}PrP in neuroblastoma cells that have been treated with the synthetic peptide PrP106–126 (34), or that have been transfected to express another PrP mutant (P101L) (35). However, the fact that this fragment is releasable by treatment of cells with PIPLC calls into question its relationship to ^{Ctm}PrP.

Clues to the Neurotoxicity of ^{Ctm}PrP—Cerebellar granule neurons, as well as hippocampal pyramidal cells, undergo massive degeneration in the brains of Tg(L9R-3AV) mice. The localization of ^{Ctm}PrP in the Golgi apparatus of cerebellar granule neurons in culture raises the possibility that the toxic effects of ^{Ctm}PrP on this cell type *in vivo* may involve this organelle. Although apoptotic pathways are known to be triggered in the ER as a result of protein misfolding, the role of the Golgi in programmed cell death is less clear. The Golgi apparatus undergoes a dramatic disassembly process during apoptosis (36, 37). In addition, there are several caspase substrates and at least one procaspase and a caspase inhibitor that reside in this organelle. Thus, it is possible that ^{Ctm}PrP in the Golgi directly initiates apoptotic signals or amplifies signals that originate elsewhere in the cell. On the cell surface, PrP^{C} is known to be localized to lipid rafts that contain other GPI-anchored proteins (38, 39) and that have been implicated in several kinds of signaling pathways (40, 41). Because ^{Ctm}PrP contains a GPI anchor (16, 17), it is conceivable that this form is incorporated into lipid rafts that begin to assemble in the Golgi (40) and that this localization plays a role in neurotoxic signaling. Because the N-terminal half of the ^{Ctm}PrP molecule is cytoplasmic, interaction with pro-apoptotic proteins in the cytoplasm could play a role in the neurotoxic effects of ^{Ctm}PrP regardless of where along the secretory pathway this form is localized.

Most unexpectedly, we have found that the neurodegenerative phenotype in Tg(L9R-3AV) mice is strongly dependent on coexpression of endogenous, wild-type PrP.[2] For example, Tg(L9R–3AV-B$^{+/-}$)/*Prn-p*$^{+/+}$ mice develop neurological symptoms at ~170 days of age and die with extensive loss of cerebellar and hippocampal neurons at ~390 days of age. In contrast, mice from the same line on the *Prn-p*$^{0/0}$ background never develop symptoms and have histologically normal brains. These results imply that wild-type PrP^{C} influences the transmission of a toxic signal from ^{Ctm}PrP. We have shown in this study that the *Prn-p* status of the mice from which granule neurons are cultured has no effect on the topology ratio, subcellular localization, or post-translational processing of L9R-3AV PrP. Thus, endogenous PrP^{C} most likely influences the phenotype of the mice by altering the functional activity of ^{Ctm}PrP, rather than by changing its amount or distribution. We have postulated that wild-type ^{Sec}PrP normally mediates a neuroprotective signal that is converted to a toxic signal upon physical interaction with ^{Ctm}PrP.[2] This interaction may occur as ^{Sec}PrP transits the Golgi on its way to the cell surface. An important goal now will be the identification of the signaling pathways of which ^{Sec}PrP and ^{Ctm}PrP may be components. Neurons cultured from Tg(L9R-3AV) mice may prove crucial in these investigations.

Acknowledgments—We thank Richard Kascsak for 3F4 antibody, and Man-Sun Sy for 8H4 and 8B4 antibodies. We are grateful to Cheryl Adles and Michelle Kim for mouse colony maintenance and genotyping and to Leanne Stewart for assistance with neuronal culture techniques. We also thank Mike Green for a critical reading of the manuscript.

REFERENCES

1. Prusiner, S. B. (ed) (2004) *Prion Biology and Diseases*, 2nd Ed., Cold Spring Harbor Laboratory Press, Cold Spring Harbor, NY
2. Prusiner, S. B. (1998) *Proc. Natl. Acad. Sci. U. S. A.* **95,** 13363–13383
3. Weissmann, C. (2004) *Nat. Rev. Microbiol.* **2,** 861–871
4. Brandner, S., Isenmann, S., Raeber, A., Fischer, M., Sailer, A., Kobayashi, Y., Marino, S., Weissmann, C., and Aguzzi, A. (1996) *Nature* **379,** 339–343
5. Mallucci, G., Dickinson, A., Linehan, J., Klohn, P. C., Brandner, S., and Collinge, J. (2003) *Science* **302,** 871–874
6. Chiesa, R., and Harris, D. A. (2001) *Neurobiol. Dis.* **8,** 743–763
7. Hegde, R. S., Mastrianni, J. A., Scott, M. R., Defea, K. A., Tremblay, P., Torchia, M., DeArmond, S. J., Prusiner, S. B., and Lingappa, V. R. (1998) *Science* **279,** 827–834
8. Hegde, R. S., Tremblay, P., Groth, D., DeArmond, S. J., Prusiner, S. B., and Lingappa, V. R. (1999) *Nature* **402,** 822–826
9. Ma, J., Wollmann, R., and Lindquist, S. (2002) *Science* **298,** 1781–1785
10. Tremblay, P., Ball, H. L., Kaneko, K., Groth, D., Hegde, R. S., Cohen, F. E., DeArmond, S. J., Prusiner, S. B., and Safar, J. G. (2004) *J. Virol.* **78,** 2088–2099
11. Chiesa, R., Piccardo, P., Quaglio, E., Drisaldi, B., Si-Hoe, S. L., Takao, M., Ghetti, B., and Harris, D. A. (2003) *J. Virol.* **77,** 7611–7622
12. Lehmann, S., and Harris, D. A. (1995) *J. Biol. Chem.* **270,** 24589–24597
13. Stahl, N., Borchelt, D. R., and Prusiner, S. B. (1990) *Biochemistry* **29,** 5405–5412
14. Hölscher, C., Bach, U. C., and Dobberstein, B. (2001) *J. Biol. Chem.* **276,** 13388–13394
15. Kim, S. J., Rahbar, R., and Hegde, R. S. (2001) *J. Biol. Chem.* **276,** 26132–26140
16. Stewart, R. S., Drisaldi, B., and Harris, D. A. (2001) *Mol. Biol. Cell* **12,** 881–889
17. Stewart, R. S., and Harris, D. A. (2001) *J. Biol. Chem.* **276,** 2212–2220
18. Tateishi, J., Kitamoto, T., Doh-ura, K., Sakaki, Y., Steinmetz, G., Tranchant, C., Warter, J. M., and Heldt, N. (1990) *Neurology* **40,** 1578–1581
19. Stewart, R. S., and Harris, D. A. (2003) *J. Biol. Chem.* **278,** 45960–45968
20. Chiesa, R., Piccardo, P., Ghetti, B., and Harris, D. A. (1998) *Neuron* **21,** 1339–1351
21. Miller, T. M., and Johnson, E. M., Jr. (1996) *J. Neurosci.* **16,** 7487–7495
22. Zanusso, G., Liu, D., Ferrari, S., Hegyi, I., Yin, X., Aguzzi, A., Hornemann, S., Liemann, S., Glockshuber, R., Manson, J. C., Brown, P., Petersen, R. B., Gambetti, P., and Sy, M. S. (1998) *Proc. Natl. Acad. Sci. U. S. A.* **95,** 8812–8816
23. Bolton, D. C., Seligman, S. J., Bablanian, G., Windsor, D., Scala, L. J., Kim, K. S., Chen, C. M., Kascsak, R. J., and Bendheim, P. E. (1991) *J. Virol.* **65,** 3667–3675
24. Shyng, S. L., Moulder, K. L., Lesko, A., and Harris, D. A. (1995) *J. Biol. Chem.* **270,** 14793–14800
25. Drisaldi, B., Stewart, R. S., Adles, C., Stewart, L. R., Quaglio, E., Biasini, E., Fioriti, L., Chiesa, R., and Harris, D. A. (2003) *J. Biol. Chem.* **278,** 21732–21743
26. Otto, J. C., and Smith, W. L. (1994) *J. Biol. Chem.* **269,** 19868–19875
27. Kuroda, R., Kinoshita, J., Honsho, M., Mitoma, J., and Ito, A. (1996) *J. Biochem.* (*Tokyo*) **120,** 828–833
28. Eckhardt, M., Gotza, B., and Gerardy-Schahn, R. (1999) *J. Biol. Chem.* **274,** 8779–8787
29. Rutkowski, D. T., Lingappa, V. R., and Hegde, R. S. (2001) *Proc. Natl. Acad.*

Sci. U. S. A. **98,** 7823–7828
30. Kim, S. J., and Hegde, R. S. (2002) *Mol. Biol. Cell* **13,** 3775–3786
31. Hegde, R. S., Voigt, S., and Lingappa, V. R. (1998) *Mol. Cell* **2,** 85–91
32. Fons, R. D., Bogert, B. A., and Hegde, R. S. (2003) *J. Cell Biol.* **160,** 529–539
33. Colley, K. J. (1997) *Glycobiology* **7,** 1–13
34. Gu, Y., Fujioka, H., Mishra, R. S., Li, R., and Singh, N. (2002) *J. Biol. Chem.* **277,** 2275–2286
35. Mishra, R. S., Gu, Y., Bose, S., Verghese, S., Kalepu, S., and Singh, N. (2002) *J. Biol. Chem.* **277,** 24554–24561
36. Machamer, C. E. (2003) *Trends Cell Biol.* **13,** 279–281
37. Maag, R. S., Hicks, S. W., and Machamer, C. E. (2003) *Curr. Opin. Cell Biol.* **15,** 456–461
38. Vey, M., Pilkuhn, S., Wille, H., Nixon, R., DeArmond, S. J., Smart, E. J., Anderson, R. G. W., Taraboulos, A., and Prusiner, S. B. (1996) *Proc. Natl. Acad. Sci. U. S. A.* **93,** 14945–14949
39. Gorodinsky, A., and Harris, D. A. (1995) *J. Cell Biol.* **129,** 619–627
40. Brown, D. A., and London, E. (1998) *Annu. Rev. Cell Dev. Biol.* **14,** 111–136
41. Mouillet-Richard, S., Ermonval, M., Chebassier, C., Laplanche, J. L., Lehmann, S., Launay, J. M., and Kellermann, O. (2000) *Science* **289,** 1925–1928